Volume 10, Number 1
December 2016
ISSN (Print) 1818-2518
ISSN (Online) 2542-2537

Journal of Hydrology and Meteorology

Society of Hydrologists and Meteorologists - Nepal
SOHAM-Nepal

JOURNAL OF HYDROLOGY AND METEOROLOGY

AIMS AND SCOPE

Research and studies related to weather, climate and water are vital in understanding the behavior of earth-atmosphere system and its various aspects. The research and studies in Himalayan region, where the interaction of weather with its topography is an unique one, has become a great challenging task to the scientific communities.

With the view of helping to understand the vagaries of the natural phenomena related to hydrology and meteorology, to interact and to disseminate the results, this journal came into its existence. This journal hopes to act as a forum in publishing peer-reviewed papers in the field of meteorology and hydrology and it in turn helping to disseminate the result of the studies and research. Though the main focus of the journal is the weather and water related issues in the Himalayan region, it also intends to include relevant areas like climate change, atmospheric and water pollution, floods, droughts, desertification, glaciology and many others.

The understanding of these phenomena will help a step forward in mitigating the harmful effects of high-impact on weather and climate events. We hope that this journal will be of some help to the society in addressing these challenges and move ahead in complementing the current scientific and technical development with cross-disciplinary and integrated approach.

Global weather and climate patterns are interdependent and not even a single nation can be entirely self-sufficient in the provision of all of its meteorological, hydrological and related environmental services. It is the main reason of having a broad scope of this journal so as to be an integral part, may be in a smaller way to the global concerted effort in understanding the ever challenging aspects of weather, climate and water.

The authors are solely responsible for their statements and opinions expressed in their contributions published in "Journal of Hydrology and Meteorology". The Editor does not hold himself responsible for any such statements and opinions expressed by the authors in their papers.

Web : www.soham.org.np, Email : info@soham.org.np

EXECUTIVE COMMITTEE

JOURNAL OF HYDROLOGY AND METEOROLOGY

Society of Hydrologists and Meteorologists-Nepal
P.O.Box 11444, New Baneshwor, Kathmandu, Nepal
Email: info@soham.org.np
Web: www.soham.org.np

Price
Nepal : Individual NRs. 150.00, Institution NRs. 250.00
SAARC Countries : US$ 10.00
Other Countries : US$ 15.00

Impact of Climate Change in the Karnali Basin, Nepal

Harshana Shrestha[1*], Utsav Bhattarai[1], Khada Nanda Dulal[1], Shrijwal Adhikari[1], Suresh Marahatta[2], Laxmi Prasad Devkota[3]

[1] *Water Modeling Solutions Pvt. Ltd., Gwarko, Lalitpur*
[2] *RECHAM Consult Pvt. Ltd, Putalisadak, Kathmandu*
[3] *Nepal Development Research Institute (NDRI), Pulchowk, Lalitpur*
[*] *Corresponding author: harshanashrestha@gmail.com*

ABSTRACT

This study highlights the impacts of climate change (CC) in the Karnali Basin of Nepal assessing precipitation as the climatic variable. Long term trend analysis of precipitation was performed by RClimDex using historical time series data from 14 stations owned and administered by Department of Hydrology and Meteorology (DHM). The analyses included observing decadal trends for a period of 30 years (1981-2010). The latest projections for CC scenarios prescribed by the Fifth Assessment report of Intergovernmental Panel for Climate Change (IPCC) AR5 were used for the analysis. CC projection data from Canadian Earth System Model (CanESM2) is used for generating future climate data which was downscaled using Statistical Downscaling Model (SDSM) for Representative Concentration Pathways (RCP) 2.6, 4.5 and 8.5 representing low, average and high radiative forcing scenarios respectively. Analysis of future CC was carried out for three time windows, namely, near-future (2011-2040), mid-future (2041-2070) and far-future (2071-2100). Trend analysis of past precipitation data did not show any distinct pattern or trend towards any particular direction, although natural climatic variability was clearly observed. Further, comparison of the annual mean precipitation for the future (2011-2100) with the baseline period (1981-2010) showed increasing pattern in all the stations for the 2.6, 4.5 and 8.5 RCPs for all the time windows.

Key words: *Precipitation, RClimDex, SDSM, Climate Change, Downscaling, Karnali*

1. Introduction

Nepal receives an annual average precipitation varying from 1500mm to 2500mm out of which 80% occurs during the monsoon period from June to September (WECS, 2011). Almost the entire country has surplus water to unmanageable limits during these four months while the remaining eight months are water deficit. As precipitation is the major source of water for springs, streams and rivers, the water shortage during the dry period affects drinking water, irrigation, hydropower and overall livelihood of the people. In some river basins of

Nepal, acute shortage of water seen particularly during the pre-monsoon period (March to May). Generally, the eastern part receives more precipitation declining towards the western part of the country (Marahatta et al., 2009).

Climate change (CC) has recently got considerable attention at different spatial scales; globally to locally. Different global circulation models (GCMs) have varying results on the direction as well as magnitude of CC impacts for the region. Researchers studying Nepal have come up with different results regarding CC in the regional and national levels. For example, some studies show a significant warming trend in recent decades (Devkota et al., 2014; Lohani, 2007). Similarly, CC scenarios for Nepal across multiple GCMs convergence on the projection that continuous warming will be felt, with average mean temperature increases of 1.2°C and 3°C by 2050 and 2100 respectively (World Bank, 2009). Miller et al. (2012) states that the impacts of glacier melt changes are minimal for the Ganges whereas change in rainfall amount, mainly increasing rainfall may lead to increased flows. Another study predicts that average annual discharge and seasonal discharges would increase with rise in temperature in the Kali Gandaki basin as a result of future climate (Manandhar et al., 2013). Similarly, Immerzeel et al. (2013) report that precipitation and temperature are projected to increase in the Ganges basin until the end of this century and consequently increasing future runoff in the Langtang watershed. A study by Bharati et al. (2014) for Koshi River basin articulated that, impact of CC is very much scale dependent – both temporally and spatially.

Palazzoli et al. (2014) carried out a study to investigate the effect of the prospective CC on hydrology and productivity of rain fed crops in Indrawati river basin, Nepal making use of the recent IPCC prescribed Representative Concentration Pathways (RCP) scenarios. The study foresees considerable changes in hydrology along with reduction in crop yields. Lutz et al (2014) has studied the impact of CC on future water availability in five river basins namely, Indus, Ganges, Brahmaputra, Salween and Mekong using latest ensemble of climate models analyzing different RCPs. The study projected an increase in runoff at least until 2050 mainly by increase in precipitation in Upper Ganges, Bramhaputra, Salween and Mekong basins and from accelerated melt in the Upper Indus Basin.

With this background, this study was devised in order to identify how global CC has affected the Karnali Basin considering precipitation as the climatic variable and making use of the latest climate datasets and models. In the first part, long term trend analysis of precipitation was performed by RClimdDex using historical time series data from Department of Hydrology and Meteorology (DHM) stations. The analyses included observing decadal trends for a period of 30 years (1981-2010). The second part consisted of generating future CC datasets for the scenarios prescribed by the Fifth Assessment Report (AR5) of IPCC. Statistical Downscaling model (SDSM) was used to downscale projected precipitation data to the local scale for three scenarios namely; RCPs 2.6, 4.5 and 8.5 representing low, average and high radiative forcing cases respectively.

Study Area

The Karnali Basin is located on the western part of Nepal between 28° 19' N to 30° 27' N

latitudes and 80° 33' N to 83° 42' N longitudes encompassing 21 districts, some wholly and some partly (Figure 1). Karnali is a perennial trans-boundary river originating from the Himalayas on the Tibetan plateau. The Karnali River flows from north to south through one of the most remote and least explored areas of Nepal.

Figure 1: Location map of the Karnali Basin showing district boundaries

The Karnali River Basin starts from the high mountains and carries snow fed flows where it integrates most of the river systems covering small to medium scale rivers. The headwaters of Karnali River lies about 230 km North from Chisapani (mainstream Karnali River length) covering mountainous ranges. Figure 2 shows the elevation variation of the Karnali Basin generated using the Shuttle Radar Mission (SRTM)[1] based Digital Elevation Model (DEM) which is approximately 90 m x 90 m raster dataset. Figure 2 shows, the headwaters of Karnali river originates from the altitude in an around 5000m above sea level and more. The total drainage area of Karnali at Chisapani is approximately 44,000 km2 (WECS, 2011) and is roughly in a shape of rectangle with length 230 km and width 200 km (NDRI, 2009). Its main tributaries are Humla Karnali, Mugu Karnali, Tila, West Seti and Thuli Bheri along with a number of minor ones (Dulal and Bhattarai, 2014). A major portion of the basin, especially the upper areas have 15° to 45° slope. Some steep areas in the basin have slopes greater than 60°. However, the low lying areas in the Terai have a slope of below 15°. According to the nature of soil in the region, Karnali River with its tributaries carry huge amount of sediment load during the rainy season in the form of sands, coarse gravels, cobbles and boulders (GEOCE, 2004).

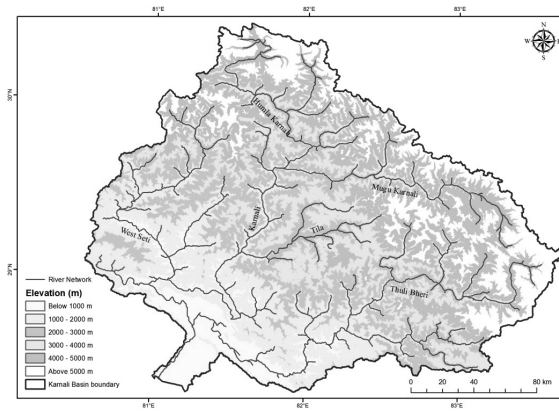

Figure 2: Elevation Variation of Karnali Basin with major tributaries

The Karnali Basin has four distinct seasons. Spring, from March to May is warm and dusty with rain showers. Summer, from June to August, is the monsoon season. Autumn, from September to November, is cool with clear skies. Mean summer temperatures range from 27 to 30 ºC in the Terai, to about 3 to 6 ºC in the hilly region of the country. In winter, mean temperatures in the Terai range from 15 to 18 ºC while the mid-hills experience chilly between 0 to 6 ºC. Much colder temperatures prevail at

[1] (http://srtm.csi.cgiar.org/index.asp)

high mountains reaching a mean value below -3ºC.

Mool et al. (2001) has studied the glaciers in the Nepal Himalaya and mentions that the Karnali River basin consists of 1,361 glaciers with an area of 1,740.2 km^2 and an ice reserve of 127.72 km^3. All the lakes at elevations higher than 3,500 msl are considered to be glacial lakes and it is estimated that the Karnali Basin contains 907 such lakes. WECS (2003) has quantified the reach length of the Karnali River to be 507 km with a total drainage area of 44,000 km^2 out of which 41,890 km^2 is in Nepal. It is estimated that the runoff from this basin is 1441 m^3/s out of which 1371 m^3/s flows from the Nepalese part of the basin. The report further mentions that about 20% of the total available surface water of Nepal is within the Karnali Basin while only 9% of the total national population resides within this basin. Thus, it has tremendous potential as a source of irrigation and hydropower development due to its water availability throughout the year. Further, it has been estimated that the Karnali Chisapani hydropower project will have an installed capacity of 10,800 MW and its cost will be USD 7,666 million (WECS, 2003). World Bank (2009) further highlights that the annual stream flow volume of the Bheri River is 14,149 MCM out of which 597 MCM is the glacier melt contribution. The water balance of the Karnali River is surplus even during the dry periods of the year; however CC could lead to high degrees of fluctuation in the water balance (WECS, 2011).

2. Data and Methods

The current study is based on analysis of secondary data. Daily time-series precipitation data of the stations lying within the study basin was acquired from DHM (Figure 3). It can be seen that the distribution of the stations is very sparse especially in the upper parts of the study basin.

The methodology consisted of two parts: 1) analysis of historical data and 2) analysis of future climate change data.

Analysis of historical data

A total of 36 DHM precipitation stations from 1981 to 2010 (30 years) were taken for this study. However, due to a lot of missing data only 14 stations having relatively reliable data and of good quality were used for the trend analysis. The selected 14 stations have less than 5% missing values. These data gaps were filled using weighted averaging methods.

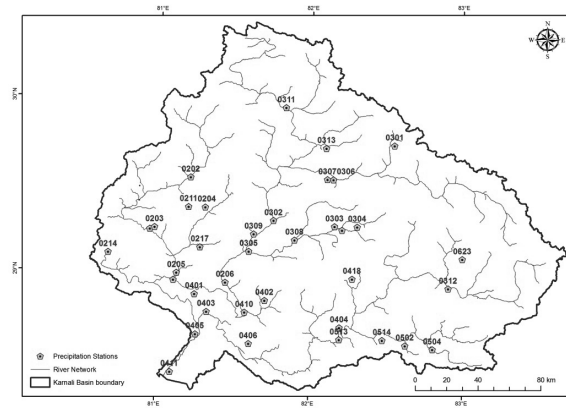

Figure 3: DHM precipitation stations with river network of Karnali Basin

Daily precipitation data from these selected stations were taken and decadal trend analysis was carried out in RClimDex for the baseline period (1981-2010). RClimDex is a software-package designed to provide a user friendly interface to calculate indices of climate extremes for monitoring and detecting CC (Zhang and Yang, 2004). RClimDex computes all 27

core indices recommended by the (Climate Change Levy/ Climate and Ocean: Variability, Predictability and Change CCl/CLIVAR) Expert Team for Climate Change Detection Monitoring and Indices (ETCCDMI) as well as some other temperature and precipitation indices with user defined thresholds. Table 1 shows the precipitation indices that were considered for the analysis along with their short description. Many recent studies (Bastakoti et al., 2016; Devkota and Bhattarai, 2015; Manandhar et al., 2013; Malla, 2013 ;) have successfully made use of RClimDex to quantify and analyze the impacts of CC in Nepalese river basins.

Table 1: Precipitation indices considered for the trend analysis

ID	Index Name	Description	Units
Rx1day	One day precipitation	Maximum 1 day precipitation amount	mm
CDD	Consecutive dry days	Maximum number of consecutive days with daily rainfall < 1 mm	Days
CWD	Consecutive wet days	Maximum number of consecutive days with daily rainfall >= 1 mm	Days
R95p	Very wet days	Annual total precipitation when RR>95th percentile	Days
R99p	Extremely wet days	Annual total precipitation when RR>99th percentile	Days
PRCPTOT	Annual total precipitation	Annual total precipitation in wet days when daily rainfall >= 1 mm	Mm

Adapted from Zhang and Yang (2004)

Analysis of Future Climate Change Data

The Fifth assessment report of IPCC has now published new sets of climate data with different climate forcing. It relies heavily on the Coupled Model Inter-comparison Project, Phase 5 (CMIP5), and a collaborative climate modeling process coordinated by the World Climate Research Programme (WCRP). There has been a fundamental change from AR4 to AR5 in the way that the IPCC is dealing with climate change scenarios (Moss et al., 2008). Unlike the sequential form of scenario development in AR4, the AR5 provides better integration, consistency and consideration of feedback with the new parallel approach. RCPs are newly developed greenhouse gas emission scenarios and adopted in the IPCC's AR5 report (IPCC, 2013).The scenario set containing emission, concentration and land-use trajectories is composed of four RCPS; RCP2.6, RCP4.5, RCP6 and RCP8.5 representing radiation forcing values respectively, +2.6, +4.5, +6 and +8.5 W/m^2 in the year 2100. RCP 2.6, RCP 4.5 and RCP 8.5 are respectively lowest, medium and highest forcing scenarios.

The selection of GCM depends on its availability and applicability with a desired method of downscaling. This study has used a single GCM from second generation Canadian Earth System Model (CanESM2) developed by Canadian Centre for Climate Modeling and Analysis (CCCma) of Environment Canada. It is the only GCM that made daily predictor variables available to be directly fed into SDSM. In the model, large scale atmospheric variables from National Centers for Environmental Prediction

(NCEP)/ National Center for Atmospheric Research (NCAR) reanalysis project are available that were used for establishing a statistical relationship with observed station data. The CanESM2 outputs were downloaded at the study station locations, for three different climate scenarios viz., RCPs 2.6, 4.5 and 8.5. Both the CanESM2 output and NCEP/NCAR reanalysis project data are available in Canadian Climate Data and Scenarios website, which can be downloaded for the study location at a spatial resolution of 2.8° * 2.8°. Both of these are provided with 26 predictors (Table 2).

Statistical Down Scaling Model (SDSM)

SDSM (Wilby et al., 2002) is a hybrid model of multiple regression and stochastic weather generator techniques for long term data generation. SDSM is widely applied with its performance favorably for precipitation downscaling and can produce characteristics of observed data (Khan et al., 2006a). As this method highly depend on long term past data, it requires good quality of data to produce a reliable result.

SDSM has been widely used in many basins globally to study the impacts due to climate change. Babel et. al. (2013) has studied the potential hydrological impact of future climate in the Bagmati River basin, Nepal, making use of SDSM to downscale temperature and precipitation outputs from Hadley Center Coupled model, HadCM3. Similarly, Shrestha et al. (2013) has studied spatial and temporal impacts of CC on rice, wheat cropping systems, focusing on irrigation water requirement in the Bagmati river basin of Nepal in which SDSM was used for downscaling. Hu et al. (2013) investigated the possible changes in mean and extreme temperature indices and their elevation dependency over the Yellow River. It presents SDSM performs better result for maximum temperature indices then the minimum temperature indices. Pervez and Henebry, (2014) report that model accuracy for reproducing precipitation using SDSM at the monthly scale was acceptable, but less accurate at the daily scale to simulate some daily extreme precipitation events. Khan et al. (2006a) studied uncertainty of statistical downscaling methods among three downscaling models namely SDSM, Long Ashton Research Station Weather Generator (LARS-WG) model and Artificial Neural Network (ANN). Their results indicate that SDSM is the most capable of reproducing various statistical characteristics of observed data in its downscaled results with 95% confidence level; the ANN is the least capable in this respect.

Screening of Predictors

The major and important step in this method is screening of predictor variables. There are altogether 26 predictor variables and screening is performed to get the best set of predictors that produce a good correlation with the predict and (Wilby and Dawson 2007). It was considered that at least one predictor should significantly correlate with the predictant variable for each of the months. The significance level was taken to as 5%. Firstly the predictors are screened for the high correlation coefficient (r), and then among them predictors are selected on the basis of significance level (P). The association of each selected predictor variable with predictant is visualized using scatter plot to select most appropriate predictors. Studies from Wilby et al. (2002); and Mahmood and Babel (2013) studies suggest few variables are enough to capture the variation of a predictant during calibration.

Table 2 List of Predictors Variables in SDSM

Predictor code	Description	Predictor code	Description
p500	500 h Pa Geopotential height	p_th	1000 h Pa Wind direction
p8_v	850 h Pa Meridional velocity	p5_f	500 h Pa Wind speed
s500	500 h Pa Specific humidity	p5_z	500 h Pa Vorticity
shum	1000 h Pa Specific humidity	p8_f	850 h Pa Wind speed
p5_u	500 h Pa Zonal velocity	p5zh	500 h Pa Divergence
p_u	1000 h Pa Zonal velocity	p8_z	85 0 h Pa Vorticity
p5_v	500 h Pa Meridional velocity	p_f	1000 h Pa Wind speed
s850	850 h Pa Specific humidity	temp	Screen (2 m) air temperature
p–v	1000 h Pa Meridional velocity	p8zh	850 h Pa Divergence
p8_u	850 h Pa Zonal velocity	p__z	1000 h Pa Vorticity
mslp	Mean sea level pressure	p8th	850 h Pa Wind direction
p850	850 h Pa Geopotential height	p_zh	1000 h Pa Divergence
p5th	500 h Pa Wind direction	Precp	Precipitation

Model Calibration and Validation

After rigorous screening and selection of predictor variables, the model is calibrated and validated using daily precipitation from 1980 to 2010. The ordinary least squares optimizing model has been used for monthly calibration. The study aimed to conduct bias correction separately for the generated results, so the bias correction is set for no bias in the model. The next step was to generate the ensembles of synthetic daily weather data for the desired period with the help of parameter file prepared during calibration and large scale predictor variables from NCEP/NCAR reanalysis datasets. The number of ensembles can be obtained as per the requirements. 20 ensembles of daily weather data series were generated for calibration period of 1980 to 2010. In order to compare the observed and simulated data, summary statistics function is used from SDSM that summarizes the results. This helps in rapid assessment of simulated data against observed data visually. Need for re-calibration and finally validation is dependent on this step until satisfactory results are obtained.

Scenario generation

After successful calibration and validation, the final step was to obtain future datasets through the calibrated model. Using this operation, twenty ensembles of synthetic daily data were generated for the three emission scenarios represented by RCPs 2.6, 4.5 and 8.5 for the period of 2006 to 2100 for all the stations.

Bias correction

In this study, bias correction (BC) is also applied to the downscaled data obtained from the SDSMs using CanESM2 predictors, to obtain more realistic and unbiased data of downscaled future climate. In this method, the biases are obtained by dividing the long term observed monthly mean data with simulated control data. The biases are then adjusted with future downscaled daily time series according to their respective months. Mahmood and Babel, (2012) has applied this method to downscaled

simulated precipitation. The following equation is used to de-bias daily precipitation:

$$\text{Pdeb} = P_{SCEN} * \left(\frac{\text{long term average } P_{obs}}{\text{long term average } P_{CONT}}\right)$$

Where, P_{dab} is the de-biased (corrected) daily time series of precipitation for the future periods. SCEN represents the scenario data downscaled by SDSM for future periods, CONT represents downscaled data by SDSM for the present period. is the daily time series of precipitation generated by SDSM for future period. "long term average " is the long term mean monthly values for observed precipitation and "long term average " is the long term mean monthly values for precipitation for the controlled simulated by SDSM.

Precipitation variability is affected mainly by frequency and intensity of precipitation (Sharma et. al., 2007). This bias correction method is to correct the precipitation amount but not the frequency. In addition to this, it also removes any systematic errors belonging to SDSM during downscaling (Mahmood and Babel, 2012). It is assumed that, SDSM simulates frequency much accurately.

3. Results and Discussion

Results have been elaborated in two parts; one for the historical trend analysis results and the other for downscaling of future precipitation results.

Historical trend analysis

The annual precipitation in the Karnali Basin averaged over the study period (1980-2010) varies from 636 mm (station 0302) to 2249 mm (station 0405). Table 3 shows only five stations (0302, 0303, 0308, 0311 and 0312) of the basin receives lower precipitation (below 1000 mm) compared to the remaining stations that about 2000 mm in an average annually. Analysis of daily precipitation data for 30 year period (Table 3) shows that Rx1day has an increasing trend in eight stations with rates varying from 0.07 mm (station 0404) to 2.33 mm (station 0214) per year. Rx1day shows decreasing trend in the other six stations with values ranging from 0.19 mm (station 0303) to 2.43 mm (station 0312). The values were statistically significant at 5% for three stations and at 10% for five stations. Similarly, CDD showed increasing trends in all 14 stations with rates in between 0.33 mm (station 0303) and 11.57 mm (station 0311) per year. These rates were statistically significant at 5% for 7 stations and at 10% for 11 stations. Analysis of CWD shows that nine stations reported decreasing trends with values up to 0.64 days per year (station 0403). The remaining five stations showed increasing trends in CWD, mostly gentle, with the highest rate of increase being 0.99 days per year for station 0312, the results being statistically significant at 5% in two stations and at 10% in five stations. R95p showed decreasing trends in ten stations with the highest value being 19.46 mm per year (station 0418). The remaining four stations showed increasing trends in R95p with gentle rates varying from 0.08 mm (station 0308) to 8.73 mm (station 0214) annually. The results were statistically significant at 5% for four stations. R99p showed decreasing trends in nine stations with the highest magnitude of change being 4.96 mm per year (station 0312). The remaining five stations showed increasing trends in R99p mostly with gentle slopes and the highest value being 8.1 mm per year for station 0214. The results were statistically significant at 5% for three stations. Similarly, PRCPTOT

showed decreasing trends in ten stations with the highest rate of 42.51 mm per year (station 0403). The other four stations showed increasing trends with gentle slopes in most of the stations. The increasing trend was the highest in station 0214 with a magnitude of 3.35 mm per year. These results were found to be statistically significant at 5% for six stations.

Table 3: Trend analysis results of precipitation indices of Karnali Basin (1980-2010)

St. No.	Annual Precipitation (mm)	RX1day			CDD			CWD			R95p			R99p			PRCPTOT		
		Slope	SD	p-value	Slope	SD	p-value	Slope	SD	p-value	Slope	SD	p-value	Slope	SD	p-value	Slope	SD	p-value
0204	2019	0.31	0.58	0.60	***1.32***	0.59	0.03	-0.38	0.27	0.17	2.92	6.17	0.64	5.24	3.71	0.17	-18.19	12.31	0.15
0205	1838	-0.54	1.08	0.62	***1.36***	0.50	0.01	-0.13	0.08	0.14	-0.19	5.20	0.97	1.76	2.95	0.56	3.18	8.98	0.73
0214	1979	2.33	1.41	0.11	*0.80*	0.44	0.08	*-0.27*	0.14	0.06	8.73	6.86	0.21	8.10	5.70	0.17	3.35	7.39	0.65
0302	636	0.33	0.43	0.45	***1.08***	0.52	0.05	-0.03	0.09	0.74	-0.53	1.96	0.79	-0.39	1.25	0.76	-2.87	3.28	0.39
0303	824	-0.19	0.31	0.54	0.33	0.41	0.42	-0.04	0.10	0.67	-1.12	1.52	0.47	-0.18	1.12	0.88	*-4.10*	2.02	0.05
0308	785	0.23	0.37	0.54	0.55	0.44	0.23	0.08	0.10	0.45	0.08	1.95	0.97	-0.11	0.94	0.91	0.13	2.97	0.97
0311	832	***-0.97***	0.40	0.02	*11.57*	5.81	0.06	*-0.28*	0.15	0.08	***-11.55***	3.46	0.00	-2.21	1.45	0.14	***-22.83***	6.78	0.00
0312	647	***-2.43***	0.56	0.00	***4.20***	0.89	0.00	***0.99***	0.40	0.02	***-11.21***	5.14	0.04	***-4.96***	1.85	0.01	***-26.02***	9.46	0.01
0403	1158	*1.03*	0.53	0.06	***3.50***	1.23	0.01	***-0.64***	0.16	0.00	***-8.21***	3.43	0.02	***4.82***	1.65	0.01	***-42.51***	8.95	0.00
0404	1911	0.07	0.77	0.92	0.71	0.57	0.22	-0.06	0.19	0.76	-1.71	4.09	0.68	-0.30	2.75	0.91	***-19.38***	8.15	0.02
0405	2249	0.56	1.23	0.65	***1.17***	0.56	0.05	0.08	0.13	0.53	7.36	6.50	0.27	1.82	4.53	0.69	1.65	8.60	0.85
0406	1668	*-1.64*	0.93	0.09	***2.75***	1.10	0.02	-0.08	0.15	0.59	-4.04	3.31	0.23	-4.03	2.81	0.16	-10.11	7.33	0.18
0418	2018	***-1.83***	0.58	0.00	*1.63*	0.91	0.08	*0.50*	0.26	0.06	***-19.46***	4.03	0.00	***-5.30***	2.12	0.02	***-25.90***	11.50	0.03
0504	1711	0.59	0.94	0.53	*0.86*	0.46	0.07	0.08	0.14	0.54	-5.91	3.84	0.14	-1.45	2.32	0.54	-10.12	7.90	0.21

Slope: Annual rate of change of the index; SD: standard deviation of the slope; p-value: statistical significance value; Bold faced correspond to the values of indices with p-value < 0.05; Italicized correspond to the values of indices with p-value < 0.1

Trend analysis result of the PRCPTOT variable for station 0308 has been plotted in Figure 4 for the purpose of illustration. It is interesting to note although an increasing trend is visible, the rate is very gentle (0.13 mm per year). Moreover, the results are not statistically significant for this station (p-value = 0.97).

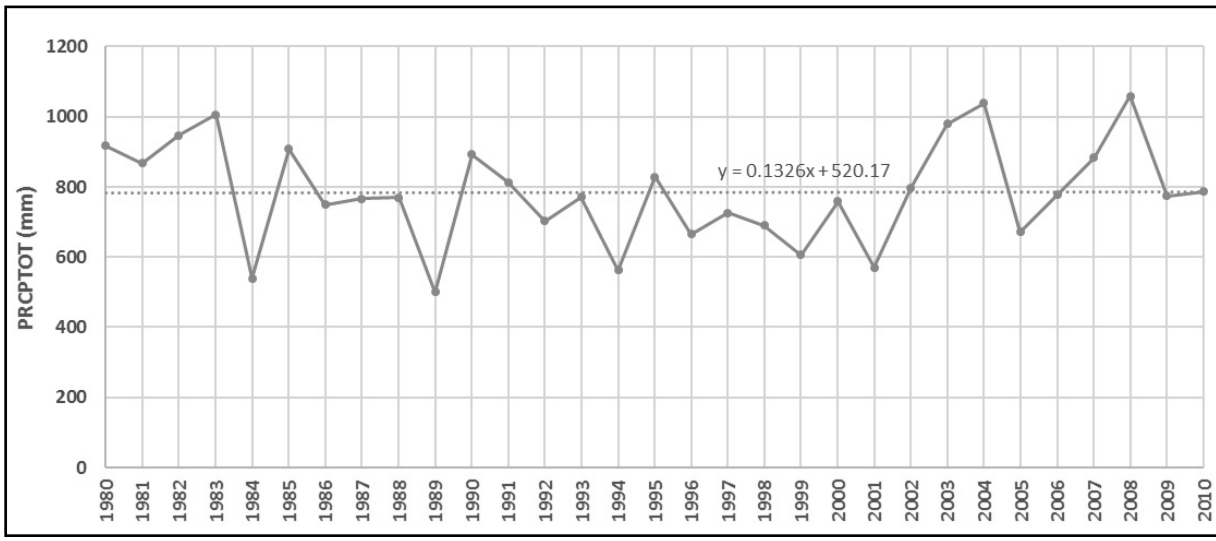

Note: Solid lines represent actual annual values while the dotted line is the linear trend line

Figure 4: Trend trend analysis results of total annual precipitation (PRCPTOT) for station 0308

Climate downscaling using SDSM

As stated in above section, SDSM is used for the downscaling purpose of precipitation in the station that lies in Karnali basin. It is also stated in the previous section that only 14 stations were selected on the basis of its quality for historical trend analysis. Here, for the precipitation downscaling purpose, eight stations area selected on the basis of representative location that covers the entire basin. As the grid size of CanESM2 is 2.8 degree *2.8 degree, more than one precipitation station lies in the same grid. Thus, with this basis, precipitation is downscaled for eight stations that can represent overall area of Karnali basin. The selected eight stations numbers are; 0204, 0214, 0303, 0308, 0311, 0312, 0406 and 0504.

Selected predictor variables

The predictor variables were selected through screening of NCEP/NCAR reanalysis predictors by preliminary analysis of explained variance and later calculating correlation coefficient (partial r). The final set of predictor variables were selected after analyzing the correlation coefficient, and visualizing its association with predictant using scatter plot.

Performance Evaluation of SDSM

Based on available observed data sets, two daily datasets, 1980 to 2000 and 2001 to 2010 were selected for precipitation calibration and validation respectively. In the present study SDSM using monthly sub model, was developed NCEP/NCAR predictor variables that were selected during the screening process at each stations. Percentage of explained

variance (R-Squared value) and Standard Error were used as performance indicators during the calibration of SDSM.

The mean percentage explained variance and mean standard error obtained as the result of the calibration at each station are given in Table 4. The highest (27.4%) and lowest (18.6%) explained variances were found at station 406 and 214 respectively. The standard error has been ranges from 0.28 to 0.38.

Table 4: Explained variance and Standard Error during calibration

Station	Precipitation	
	Explained variance (E%)	Standard Error (SE)
204	25.0	0.3
214	18.6	0.32
303	25.4	0.308
308	26.3	0.287
311	22.0	0.288
312	20.1	0.38
406	27.4	0.330
508	22.0	0.289

The performance indicators, the coefficient of determination (R^2), the root mean square error (RMSE) and mean bias (MB) were used for monthly calibration and validation of the model. Table 5 presents the performances at different stations during calibration and validation period for mean monthly precipitation. The best and lowest RMSE of 0.340mm/month is obtained in station 311 whereas the highest, the worst RMSE of 5.677mm/month obtained in station 204. R^2 ranges from 0.855 to 0.991 showing well representation of mean monthly simulated precipitation with observed precipitation. Mean bias varies from -0.132 to 0.990 mm/month. In the daily precipitation plot between observes and simulated, peaks are not well match but it is trying to match for mean monthly precipitation plot. SDSM is a regression-based model, and a regression-based method can often explain only a fraction of the observed variability in the provided calibration dataset; therefore, simulating extreme precipitation events using regression methods is problematic because extreme events tend to lie at the margins or beyond the range of the variability captured by the regression (Wilby et al., 2002). SDSM may not be the most efficient tool while downscaling future extreme precipitation events at a daily scale, but it is an efficient tool for providing future downscaled precipitation at a monthly time scale.

Table 5: The performance evaluation of SDSM during calibration and validation for Precipitation

	Calibration, 1980-2005			Validation, 2006-2010		
Stations	R^2	RMSE	MB	R^2	RMSE	MB
204	0.959	3.318	0.990	0.926	5.677	0.950
214	0.971	0.982	0.213	0.977	5.658	-0.915
303	0.963	1.016	-0.132	0.954	1.717	0.264
308	0.922	0.383	0.012	0.913	2.011	-0.271
311	0.936	0.330	0.261	0.911	1.184	-0.500
312	0.978	1.477	-0.191	0.870	1.182	0.819

406	0.979	3.245	-0.182	0.855	4.304	-0.456
504	0.991	3.216	-0.357	0.964	2.647	0.651

Figures 5 (a to d) show the calibration and validation graphs for a station 214. Figure 5a and 5b shows the observed and simulated daily precipitation for calibration and validation respectively, Figure 5c shows observed and simulated mean monthly precipitation for calibration and validation period and Figure 5d shows the scatter plot for mean monthly precipitation for calibration and validation period respectively.

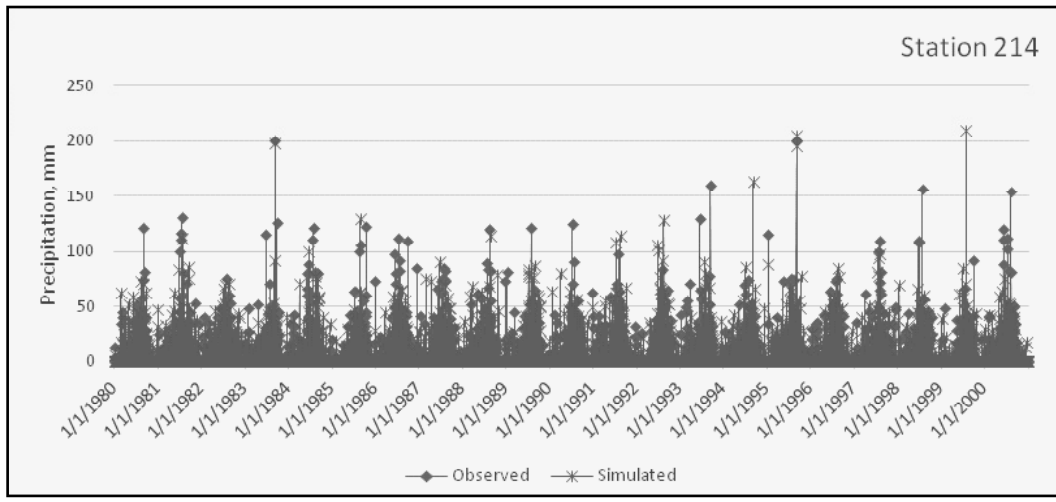

Figure 5a: Observed and Simulated Daily Precipitation for Calibration period

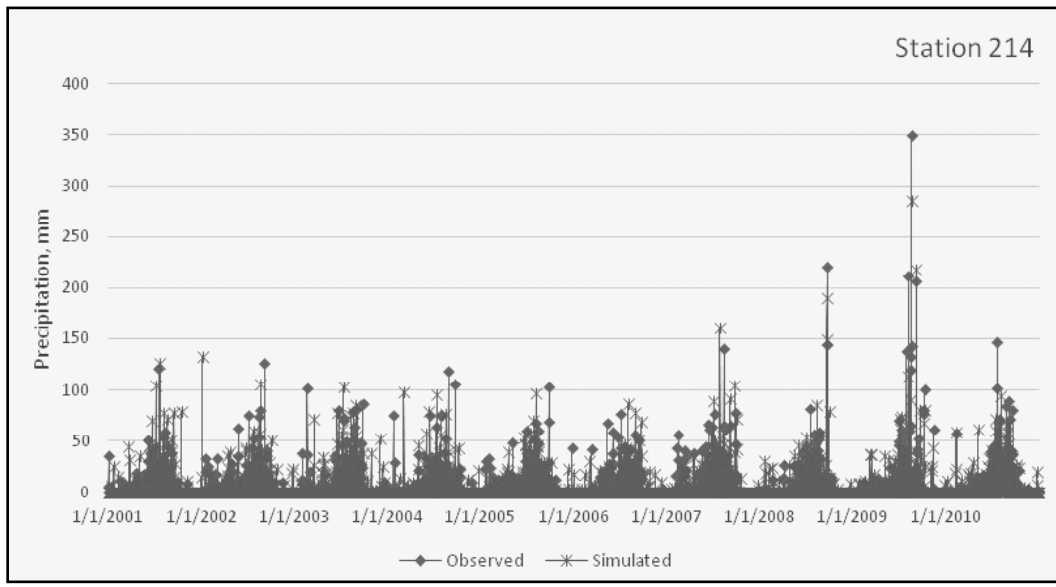

Figure 5b: Observed and Simulated Daily Precipitation for Validation period

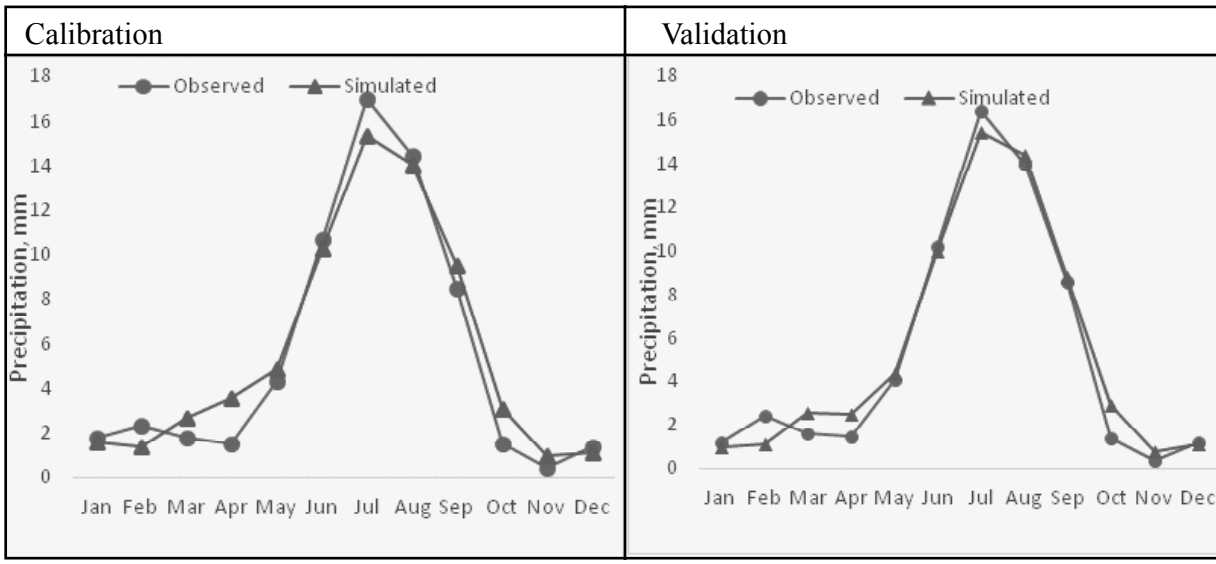

Figure 5c: Observed and simulated monthly precipitation during calibration and validation

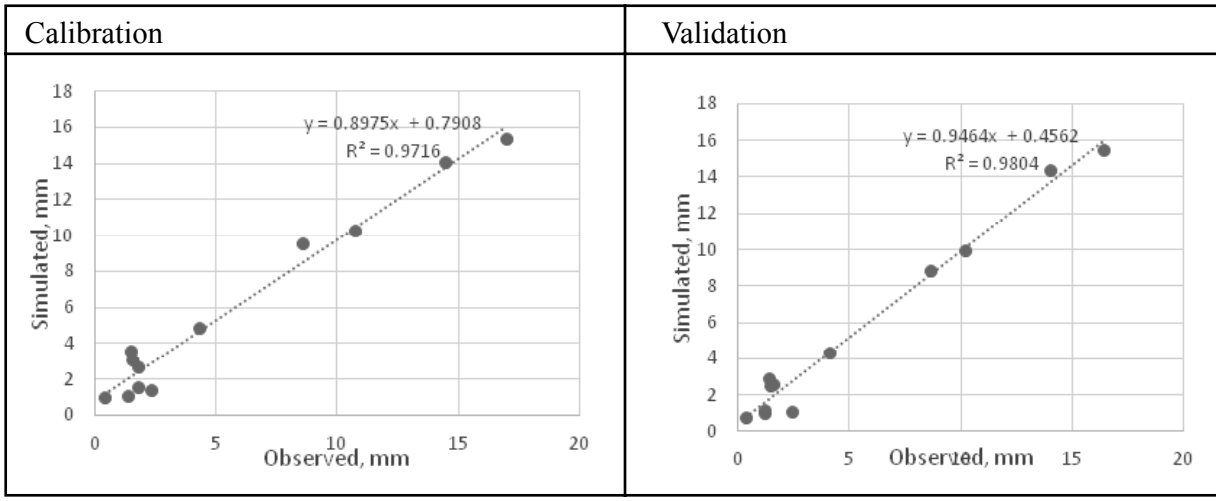

Figure 5d: Scatter plot between observed and simulated monthly precipitation

Bias Correction

The long term mean monthly precipitation values are obtained from observed as well as control simulation for the period of 1980 to 2000. Bias correction was first applied to the simulation precipitation of 2001 to 2005 and validated with the observed precipitation of the same time period on daily time series. After successful validation, bias correction was applied to the future downscaled data by CanESM2. Bias values were calculated for each station using the long term mean monthly observed and simulated precipitation with NCEP/NCAR predictors for the period of 1980 to 2000. Figure 6 shows the observed precipitation with simulated precipitation with bias correction and without bias correction for two stations 214 (Figure 6, left hand side) and 308 (Figure 6, right hand side). This process is carried out

for all stations to check the performance of bias in each station. In these figures, NCEP_WBC and NCEP_WOBC are simulated results through NCEP predictors with bias correction and simulated results through NCEP predictor without bias correction respectively.

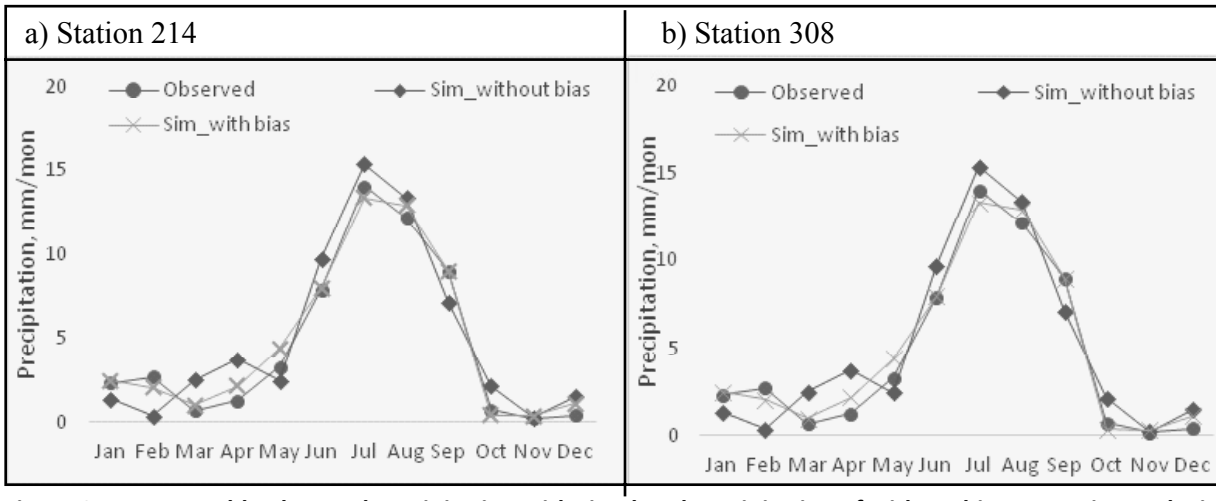

Figure 6 Mean monthly observed precipitation with simulated precipitation of without bias correction and with bias correction

Downscaled future Precipitation (with Bias correction)

As the final step of analysis, downscaling of future precipitation for scenarios RCPs 2.6, 4.5 and 8.5 was carried out. Calibrated model for each station was used to generate future precipitation. With the successful validation of bias correction in previous section, it is then applied in future downscaled precipitation from 2011 to 2100. Figures 7 (a to c) shows the station wise annual precipitation for all three scenarios for the three time windows: Near future (2011-2040), Mid-term future (2041-2071) and long-term future (2072-2100) due to scenarios RCP 2.6, 4.5 and 8.5.

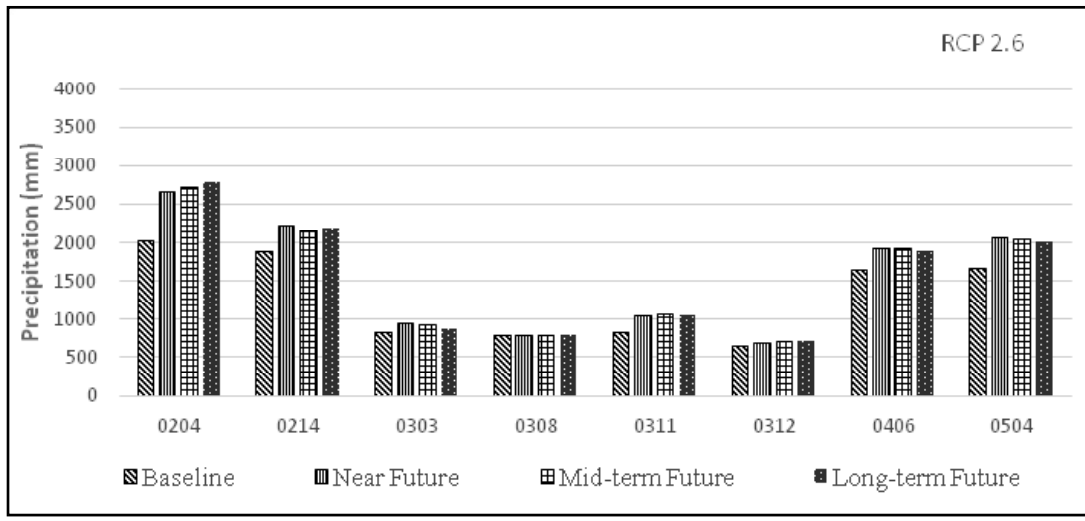

Figure 7a: Baseline and future projected annual mean precipitation at stations for RCP 2.6

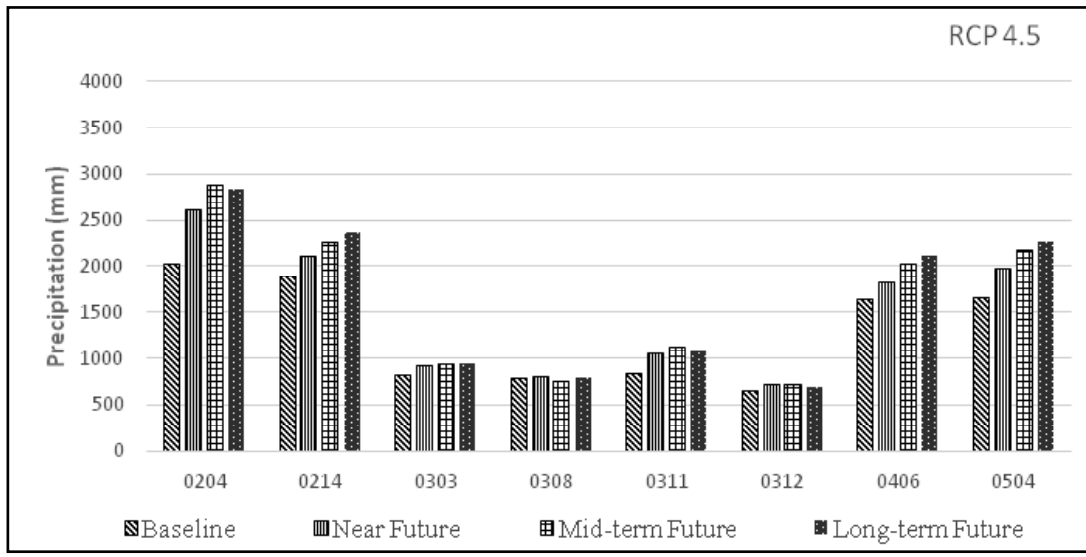

Figure 7b: Baseline and future projected annual mean precipitation at stations for RCP 4.5

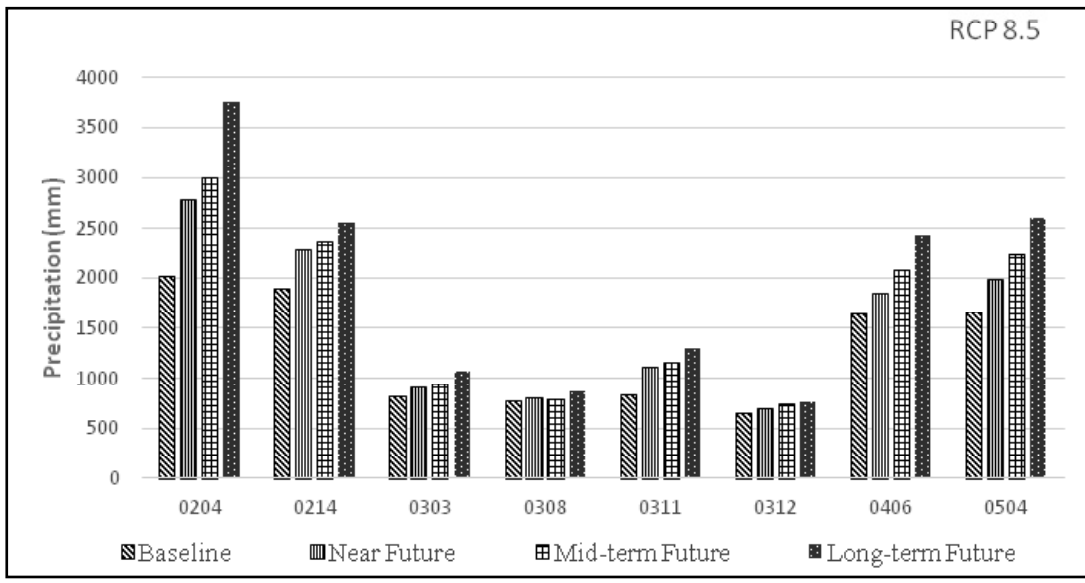

Figure 7c: Baseline and future projected annual mean precipitation at stations for RCP 8.5

Average annual precipitations with respect to baseline were shown in the above figures. These results provides, around 1% to 38% percentage increase in average annual precipitation is expected for the whole analysis period due to RCP 2.6 while comparing to the baseline period. Similarly, around 3% to 43% increase in precipitation is expected due to RCP 4.5 for the whole analysis period whereas, around 3% to 85% is expected due to RCP 8.5 with respect to baseline period. With these same results, it is expected that around 3% to 37% average annual precipitation increase in Near Future, whereas it is around 1% to 48% in Mid-term future and 1% to 86% in Long term future with respect to baseline period.

4. Conclusion

From this study, it was found that only a limited number of DHM precipitation stations in the Karnali Basin had data of sufficient length and of good quality. Trend analysis of historical precipitation data depict that all the stations do not agree on the magnitude and direction of change observed in the last 31 years. Most of the indices in the study basin have a very gentle rate of change (increase or decrease). Thus, we cannot strongly conclude that the observed changes are true representations of CC. Nevertheless, we summarize that as with other basins of Nepal, the natural variability in precipitation is prevalent. The magnitudes of the increase in the future projected precipitation were found to be varying with station. Station 0308 shows only 1% to 12% increment for the whole analysis period of 2010 to 2100 with all three scenarios. Whereas, station 0204 resulted increment starts from least 29% to the most 86% for the whole analysis period covering all scenarios. Thus, the projected precipitation varies from 1% to 86% in overall Karnali basin. Some climate change studies have also presented a wide range of projected precipitation. Climate change study in Koshi basin by Bharati, et.al. (2014) presents the projected precipitation ranges from +2% to +214%. Similarly, a study by Shrestha, et.al. (2016) presented projected precipitation ranges from -8% to +24.8% based on climate change study in Upper Tamakoshi hydropower project.

Although downscaling and bias corrections were carried out satisfactorily, the results are based on the analysis of a single GCM data. Therefore, it is recommended that similar study be carried out using at least three other GCM datasets for the study basin to better predict the impacts of climate change in the future and also to minimize the uncertainties.

Acknowledgement

The study being a part of research conducted with the Department of Hydrology and Meteorology (DHM), Nepal, authors wish to thank DHM for their technical and financial assistance to carry out this study.

References

Babel, M. S., Bhusal, S. P., Wahid, S. M., Agarwal, A., 2013. Climate Change and Water Resources in the Bagmati River Basin, Nepal.

Bastakoti, R. C., Bharati, L., Bhattarai, U., Wahid, S. M., 2016. Agriculture under changing climate conditions and adaptation options in the Koshi Basin. Climate and Development. http://dx.doi.org/10.1080/17565529.2016.1223594.

Bharati, L., Gurung, P., Jayakody, P., Smakhtin, V., Bhattarai, U., 2014. The Projected Impact of Climate Change on Water Availability and Development in the Koshi Basin, Nepal. Mountain Research and Development. Vol 34 No 2.

Bharati, L., Gurung, P., Maharjan, L., and Bhattarai U., 2015. Past and future variability in the hydrological regime of the Koshi Basin, Nepal.

Chu, J., Xia, J., Xu, CY., Singh, V., 2010. Statistical Downscaling Of Daily Mean Temperature, Panevaporation And Precipitation For Climate Change Scenarios in Haihe River,China. Theor.Appl.Climatol. 99(1),149–161. http://dx.doi.org/ 10.1007/s00704-009-0129-6.

Devkota, L. P., Gyawali, D. R., 2014. Impacts of Climate Change on Hydrological Regime and Water Resources Management of the Koshi River Basin, Nepal, Journal of Hydrology: Regional Studies.

Devkota, R. P., and Bhattarai, U., 2015. Assessment of climate change impact on floods from a techno-social perspective. DOI: 10.1111/jfr3.12192.

Dulal, K. N., and Bhattarai, U., 2014. Report on Scoping and Feasibility Study to Identify a Suitable Hydrological Model for Karnali Basin. Technical Report submitted to Practical Action Consulting, Kathmandu, Nepal.

GEOCE (2004). Karnali River Training Works Final Report. GEOCE Consultants (P) Ltd.

Hu, Y., Maskey, S., Uhlenbrook, S., 2013. Expected changes in future temperature extremes and their elevation dependency over the Yellow River source region. Hydrology and Earth System Sciences. 17(7), 2501-2514. DOI: 10.5194/hess-17-2501-2013.

Immerzeel, W. W., Pellicciotti, F., Bierkens, M.F.P., 2013. Rising river flows throughout the twenty-first century in two Himalayan glacierized watersheds. Nature Geoscience, Vol 6. DOI: 10.1038/NGEO189.

IPCC (2013). Summary for policymakers. Stocker, T.F., Qin, D., Plattner, G.-K., Tignor, M., Allen, S.K., Boschung, J., et al. (Eds.), Climate Change 2013: The Physical Science Basis. Contribution of Working Group I to the Fifth Assessment Report of the Intergovernmental Panel on Climate Change. Cambridge University Press, Cambridge, United Kingdom and New York.

Khan, M. S., Coulibaly, P., Dibike. Y., 2006a. Uncertainty analysis of statistical downscaling methods. J Hydrol 319(1–4): 357–382.

Lohani, S. N., 2007. Climate change in Nepal: Shall we wait until bitter consequences? Agriculture and Environment. Vol. 8, pp. 38-45.

Lutz, A. F., Immerzeel, W. W., Shrestha, A. B., Bierkens, M.F.P., 2014 Consistent increase in High Asia's runoff due to increasing glacier melt and precipitation. Nature Climate Change 4(7): 587–592

Mahmood, R., and Babel, M. S., 2013. Evaluation of SDSM developed by annual and monthly sub-models for downscaling temperature and precipitation in the Jhelum basin, Pakistan and India. Theoretical and Applied Climatology, 113(1-2), 27–44. http://doi.org/10.1007/s00704-012-0765-0.

Malla, R., 2013. Climate change impacts and adaptation options for Indrawati sub-basin. Research report submitted to World Wide Fund for Nature (WWF) Nepal.

Manandhar, S., Pandey, V.P., Ishidaira, H., Kazama, F., 2013. Pertubation study of climate change impacts in a snow-fed river basin. Hydrol Process. Vol. 27, pp.3461-3474. DOI: 10.1002/hyp.9446.

Marahatta, S., Dongol, B. and Gurung, G. (2009) Temporal and Spatial Variability of Climate Change over Nepal (1976-2005). Practical Action, Kathmandu.

Miller, J. D., Immerzeel, W.W., Rees, G., 2012. Climate Change Impacts on Glacier Hydrology and River Discharge in the Hindu Kush-Himalayas. Mountain Research and Development, 32(4):461-467. DOI: http://dx.doi.org/10.1659/MRD-JOURNAL-D-12-00027.1.

Mool, P. K., Bajracharya, S. R., Joshi, S. P., 2001. Inventory of Glaciers, Glacial Lakes and Glacial Lake Outburst Floods Monitoring and Early Warning Systems in the Hindu Kush Himalayan Region, Nepal. ICIMOD. Kathmandu, pp. 36.

Moss, R., Babiker, M., Brinkman, S., and Calvo, E., 2008, Towards new scenarios for analysis of emissions, climate change, impacts, and response strategies, Noordwijkerhout, The Netherlands.

NDRI (2009) Identification of Sub-basin of the Karnali River. Final Report Submitted to Concern World Wide Nepal.

Palazzoli, I., Maskey, S., Uhlenbrook, S., Nana, E., & Bocchiola, D., 2014. Impact of prospective climate change on water resources and crop yields in the Indrawati basin, Nepal.

Pervez, S. M., and Henebry, G. M., 2014. Projections of the Ganges-Brahmaputra precipitation: downscaled from GCM predictors, Journal of Hydrology, DOI: 10.1016/j.jhydrol.2014.05.016.

Sharma, D., Gupta, A. D., Babel, M, S., 2007. Spatial disaggregation of bias-corrected GCM precipitation for improved hydrologic simulation: Ping River Basin, Thailand. Hydrology and Earth System Sciences. 4:35–74.

Shrestha, B., Babel, M. S., Maskey, S., van Griensven, A., Uhlenbrook, S., Green, A., Akkharath, I. 2013. Impact of climate change on sediment yield in the Mekong River basin: a case study of the Nam Ou basin, Lao PDR. Hydrol. Earth Syst. Sci. 17, pp. 1-20.

Shrestha, K. L., Shrestha, M. L., Shakya, N. M., Ghimire, M. L., Sapkota, B. K., Climate Change and Water Resources in Nepal. Climate Change and Water Resources in South Asia, Proceedings of Year-end workshop, Kathmandu, 7-9 January, 2003.

Shrestha, S., Gyawali, B., and Bhattarai, U., 2013. Impacts of climate change on irrigation water requirements for rice-wheat cultivation in Bagmati River Basin, Nepal, Journal of Water and Climate Change, 04.4, DOI:10.2166/wcc.2013.050.

Shrestha, S., Bajracharya, A. R., Babel, M. S., Climate Risk Management (2016), Vol.14: 27–41 http://dx.doi.org/10.1016/j.crm.2016.08.002-.

Wang, X. Y., Yang, T., Shao, Q. X., Acharya, K., Wang, W. G., Yu, Z. B., 2012. Statistical downscaling of extremes of precipitation and temperature and construction of their future scenarios in an elevated and cold zone. Stoch. Environ. Res. Risk A 26 (3), pp. 405–418.

WECS (2003) Water Resources Strategy Nepal. Water and Energy Commission Secretariat, Government of Nepal, Kathmandu, Nepal.

WECS (2011) Water Resources of Nepal in the Context of Climate Change. Water and Energy Commission Secretariat, Government of Nepal, Kathmandu, Nepal.

Wilby, R. L., Dawson, C. W., Barrow, E. M., 2002. SDSM—A Decision Support Tool For The Assessment Of Regional Climate Change Impacts. Environ Model Softw 17(2), pp. 145–157.

Wilby, R. L., and Dawson, C. W., 2007. SDSM 4.2-A decision support tool for the assessment of regional climate change impacts, Version 4.2 User Manual. Lancaster University: Lancaster/Environment Agency of England and Wales, pp. 1–94.

World Bank (2009) Glacier Retreat in the Nepal Himalaya: An Assessment of the Role of Glaciers in the Hydrologic Regime of the Nepal Himalaya. Prepared for the South Asia Sustainable Development (SASDN) Office, Environment and Water Resources Unit.

Zhang, X., Yang, F., 2004. RClimDex (1.0) User Guide. Climate Research Branch Environment Canada: Downsview, Ontario, Canada.

Drought Analysis in Western, Central and Eastern Development Regions of Nepal using Reconnaissance Drought Index

Hemu Kharel Kafle
Nepal Academy of Science and Technology, Khumaltar, Lalitpur, GPO Box: 3323, Kathmandu, Nepal
Email: hemukafle@gmail.com

ABSTRACT

Recent and potential future increases in global temperatures are likely to be associated with impacts on the hydrologic cycle, including changes to precipitation and increases in extreme events such as droughts. This study has investigated the spatial and temporal changes in drought occurrence in western, eastern and central development regions of Nepal with the help of Standardized Reconnaissance Drought Index (RDI_{st}) Quantification of the severity and frequency of drought within different ecological zones is based on 30 years of monthly precipitation and temperature datasets from 46 meteorological stations. Among 173 drought events, 68 drought events occurred in west, 62 in central and 43 in eastern region of Nepal. It has been revealed that all the three kinds, moderate, severe and extreme events of droughts occurred in all three development regions. Highest number of extreme events was observed in eastern region and lowest number in central region. These events occurred when precipitation recorded its lowest range. Over the study period, the year 1989, 1992, 1994, 2005, 2006, 2010 and 2011 were the worst widespread droughts in all three development regions.

Keywords: *Drought, temperature, Precipitation, Nepal reconnaissance drought index (RDI)*

1. INTRODUCTION

Drought is a naturally occurring phenomenon, its basic cause being the lack of precipitation over a time period. Precipitation is the primary factor controlling the formation and persistence of drought conditions. Other climatic factors such as high temperature, high wind, and low relative humidity are often associated with it in many regions of the world and can significantly aggravate its severity (Kundzewicz, 1997). A combination of droughts or sequences of droughts have serious impacts on human and environmental welfare (Sheffield & Wood, 2008). Of all the natural disasters, the economic and environmental consequences of drought are among the highest, due primarily to the longevity and widespread spatial and extent of many droughts (Wilhite, 2000). With the increase in extreme climatic events, droughts are projected to become more frequent and severe with global warming (Trenberth et al.,2014), in particular, during the warmest decade of the twenty-first century (2001-2012), 17–35 % of

global land area experienced moderate droughts, 7–15 % experienced severe droughts, and 2–6 % experienced extreme droughts (Kogan et al.,2013). Therefore, it is essential for droughts to be accurately and persistently monitored for mitigating its adverse effects on national and regional scales.

Nepal is a land-locked country situated in the middle belt of the Himalayas, having an area of 147181 km^2 and a population of approx 28.7 million. The climate varies from tropical in the southern plain to temperate in the central part, and from arctic in the higher Himalayas to arid in the Trans Himalayas (Manandhar et al, 2011). Since Nepal is located at the northern-most edge of the South Asian monsoon system, the wet season is relatively short (Saha, 2010) lasting from mid-June to August / September in contrast to the Indian subcontinent monsoon while the dry season persists somewhat longer (Shrestha, 2000). Nepal is divided into five development regions - eastern, western, central, mid-western and far-western. As the monsoon comes from the east it first strikes eastern Nepal and then it slowly proceeds to the west.

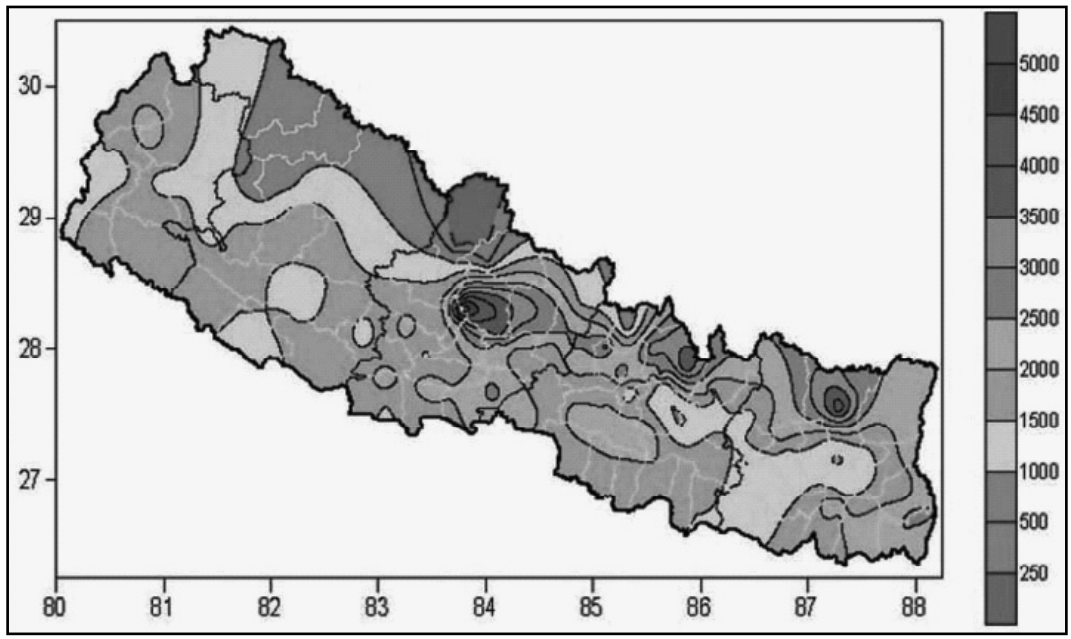

Figure.1:Annual mean rainfall pattern (mm) over Nepal (Source: Practical Action Nepal Office, 2009).

It takes nearly more than a week for the monsoon to reach the western border of Nepal (Gautam & Regmi, 2014). Likewise, the westerlies move from west to east. In both of these cases the intensity of rainfall varies in space and time (DIHM, 1974). During monsoon the amount of rainfall is much higher in the eastern region and substantially decreases from the east to west. The western half, especially the northern parts of mid-western development region is generally drier as compared to the eastern half as shown in Figure 1.

Moreover, temperature is directly related to season and altitude of the location. The hottest part of the country is the southern Terai belt and the coldest part lies in the high Himalaya in the north (Figure 2).

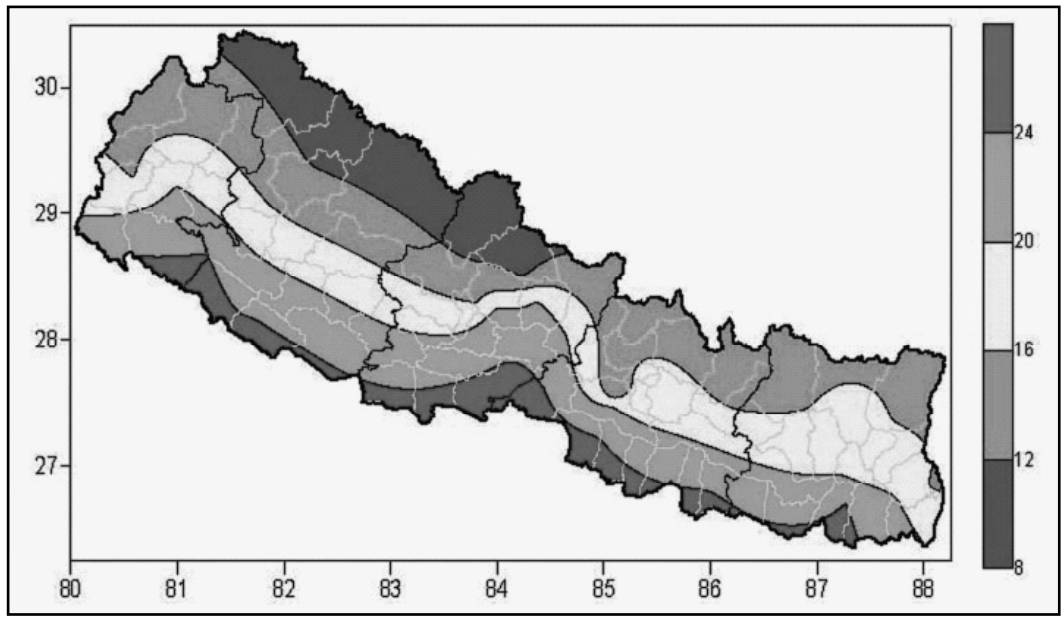

Figure 2: Spatial variation of mean temperature (°C) (Source: Practical Action Nepal Office 2009).

In Nepal, temperature is lowest during winter (December - February) and increases as spring advances due to increase in solar insolation. However, the arrival of monsoon rain checks the increase in temperature making generally May or early June the hottest months. The temperature starts decreasing from October and reaches the minimum in January/February.

Very few studies on drought have been reported in Nepal although there is a need for extensive study on drought assessments and its impact in rural livelihood. Some scientific study on drought observation (Sigdel & Ikeda, 2010; Shakya and Yamaguchi, 2010; Wang et al., 2013; Kafle, 2014; Dahal et al., 2016) and its impact (Bhatt et al., 2014; Shrestha et al., 2014; Devkota et al., 2015) have been recorded so far. Recent studies on drought analysis in far and mid western development region indicate that there has been a tendency toward more frequent and intense droughts during the dry season over the past decades (Kafle, 2014; Wang et al., 2013). Western part of Nepal has experienced consecutive and worsening winter droughts since 2000, culminating with especially severe drought between 2008 and 2009 (Wang et al., 2013). In recent years this situation has been deteriorating with increased drought frequency, severely affecting agricultural production (Bhatt et al., 2014). In some cases traditionally surplus production areas have fallen into deficit.

Although it is not possible to avoid droughts they can be predicted, monitored, (www.drought.gov), and their adverse impacts can be alleviated by regular monitoring of potential regions at high risk of drought. Careful monitoring as well as early warning for dryness is a big challenge for drought management in Nepal (GWP, 2014). A detailed study on drought occurrence and its severity in western, central and eastern development region using the standardized reconnaissance drought index (RDI) has been presented in this article. This index used both precipitation and temperature data as input parameters, which are suitable for quantifying the variations in severity and duration of drought.

2. STUDY AREA

Three development regions (western, central and eastern) among five development regions (far western, mid western, western, central and eastern) of Nepal has been chosen for this study. The study is based on monthly precipitation and temperature datasets. Monthly datasets for 31 years (1982-2012) of altogether 46 meteorological stations obtained from Department of Hydrology and Meteorology (DHM), Government of Nepal were used for this study. Twenty-two climatological stations from western, seventeen from central and fifteen from eastern development regions were selected based on percentage of missing records less than 10%.

Table 1: Studied meteorological stations of three development regions of Nepal

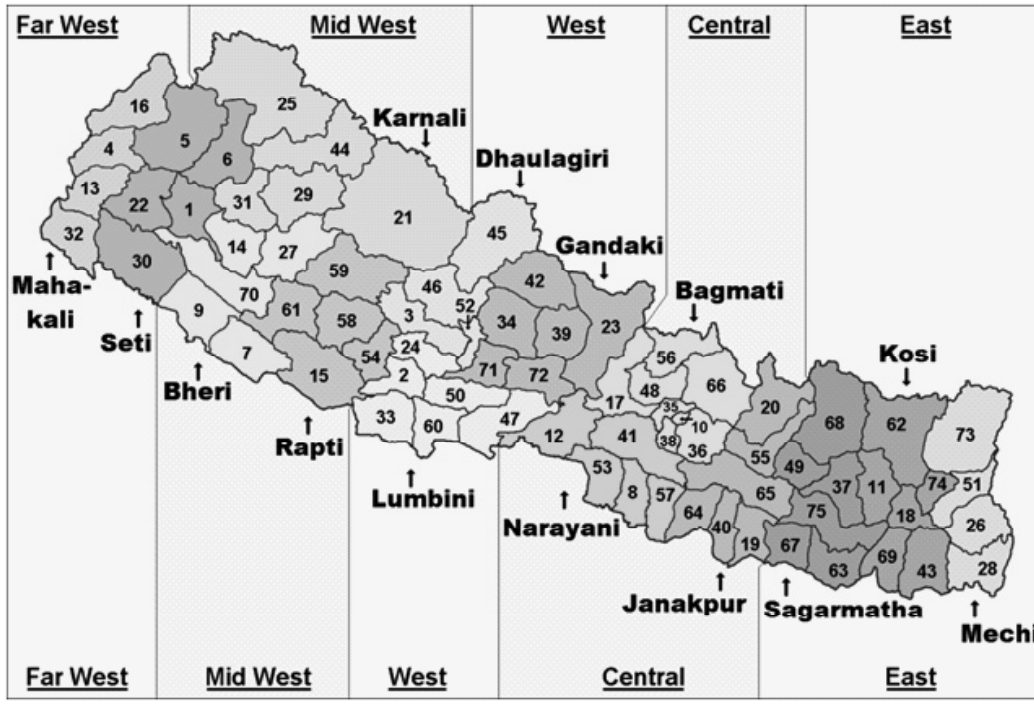

Figure 3: Map of Nepal showing study area (West, Central and East) (Source: https://en.wikipedia.org/wiki/Development_regions_of_Nepal).

Table 1: Studied meteorological stations of three development regions of Nepal

Station Name	Period	Agro-Eco zones
Jomsom	1982-2012	High hill
Baglung	1982-2012	middle hill
Lete	1998-2011	High hill
Benibazar	1989-2012	middle hill
Kushma	1989-2012	middle hill
Gurjakhani	2008-2011	High hill
Tansen	1988-2012	middle hill
Bhairahawa airport	1988-2011	Terai
Dumkauli	1982-2012	Terai
Kanchikot	1987-2012	middle hill
Taulihawa	1988-2012	Terai
Tamghas	1988-2012	middle hill
Khudi bazar	1987-2012	middle hill
Pokhara airport	1982-2011	middle hill
Syanjha	1988-2011	middle hill
Gorkha	1987-2011	middle hill

Chapkot	1988-2011	Terai
Malepatan (Pokhara)	1988-2011	middle hill
Lumle	1982-2011	middle hill
Khairinitar	1987-2011	Terai
Chame	1988-2011	High hill
Rampur	1982-2010	Terai
Daman	1982-2010	High hill
Hetauda	1982-2009	Terai
Simara airport	1982-2010	Terai
Parwanipur	1982-2010	Terai
Nuwakot	1984-2010	Middle hill
Kakani	1987-2012	High hill
Dhulikhel	1987-2011	Middle hill
Khumaltar	1987-2012	Middle hill
Kathmandu airport	1982-2011	Middle hill
Panchkhal	1982-2011	Middle hill
Dhunibesi	1982-2010	Middle hill
Nagarkot	1982-2011	High hill
Dhunche	1989-2010	High hill
Jiri	1982-2010	High hill
Sindhuligadi	1989-2010	Middle hill
Janakpur airport	1982-2010	Terai
Manusmara	1987-2008	Terai
Taplejung	1982-2011	Mid hill
Okhakdhunga	1982-2011	Mid hill
Pakhribas	1987-2012	Mid hill
Kanyam tea estate	1987-2011	Mid hill
Tehrathum	1989-2011	Mid hill
Chainpur	1987-2011	Mid hill
Ilam tea estate	1987-2009	Mid hill
Dhankuta	1987-2011	Mid hill
Phidim	1989-2011	Mid hill
Udyapurgadhi	1989-2011	Mid hill
Dharan Bazar	1998-2011	Terai
Lahan	1984-2011	Terai
Fatepur	1982-2011	Terai
Rajbiraj	1984-2011	Terai
Biratnagar airport	1982-2011	Terai

3. METHODOLOGY

3.1. DROUGHT INDICES

Drought indices are important elements of drought monitoring and assessment since they simplify complex interrelationships between many climate and climate-related parameters. Along the various indices proposed for characterization of meteorological drought, two widely accepted and used are the Palmer's drought severity Index (PDSI) (Palmer, 1965, Guttman *et al.,* 1992) and the standardized precipitation Index (SPI) (McKee, 1995, Agnew, 2000). The Palmer Index uses precipitation, evapotranspiration and soil moisture conditions as the key determinants, which are not recorded in all meteorological stations, therefore it is difficult to use for spatial analysis. On the other hand SPI index uses only one meteorological parameter, precipitation, for describing the water deficit. However meteorological drought conceived as a water deficit should be approached by a sort of balance between input and output (Tsakiris & Vangelis, 2005). A step forward could be to consider the balance between two major meteorological parameters such as precipitation (P) (input) and potential evapotranspiration (PET) (output).

3.2. RECONNAISSANCE DROUGHT INDEX

Reconnaissance drought index (RDI) is based on the ratio between two aggregated quantities of precipitation and potential evapotranspiration (Tsakiris & Vangelis, 2005). The initial value of the index for a certain period, indicated by a certain month (k) during a year, is calculated by the following equation:

$$ak=\frac{\sum_{j=1}^{j=k} P_j}{\sum_{j=1}^{j=k} PET_j} \quad (1)$$

In which P_j and PET_j are the precipitation and potential evapotranspiration of the j^{th} month of the hydrological year (Kafle, 2014). PET is calculated with the Thronthwaite formulas and adjusted to Penman with a correction factor, according to the United Nations Convention to Combat Desertification (UNEP, 1992). Thronthwaite method of calculating Aridity Index is well known and has been used for classifying the climate of USA (Thronthwaite, 1931), as well as for the classification of the climates of earth and others (Thronthwaite, 1933, 1948, 1957; Kafle, 2009). The hydrological year for the studied region starts in January, hence for January k=1. Equation 1 may be calculated for any period of the year. It can be also written starting from any month of the year. For real world applications if a_k is calculated as a general indicator of meteorological drought, it is advisable to use periods of 3, 6, 9 and 12 months. In this case 12 month period is selected. The two expressions of the new index are the Normalized RDI and the Standardized RDI. The Normalized RDI *(RDI_n)* is computed using the following equation:

$$RDI_n(k)=\frac{a_k}{\bar{a}_k}-1 \qquad (2)$$

Finally, the Standardized RDI *(RDI_{st})* is computed as follows: $RDI_{st}(k)=\frac{y_k-\tilde{y}_k}{\delta_k}$ (3)

In which y_k is the $\log a_k$, $\tilde{y}_k$ is its arithmetic mean and $\grave{\sigma}_k$ is its standard deviation.

Table 2: Classification of drought categories based on RDI

RDI	Category
Less than -1.0	Moderate drought
Less than -1.5	Severe drought
Less than -2.0	Extreme drought

Regarding equation 3, the standardization was achieved by assuming that follows a lognormal distribution. The standardized RDI (RDI_{st}), behave in a generally similar way to the SPI, and therefore the interpretation of the results is similar since the same thresholds as SPI can be used as shown in Table 2. .Hazard assessment of drought was evaluated in terms of frequency and severity.

4. RESULTS AND DISCUSSION

4.1. DROUGHT ANALYSIS USING INDEX FOR WESTERN REGION

Time Series analysis of three meteorological stations of western region representing all three eco-zones- high hill (Jomsom), mid hill (Baglung) and Terai (Dumkauli) is shown in Figure 4. There was not any kind of similarity in drought occurrence year in three eco-regions. Within twenty two studied stations of western region, highest number of drought occurred at Dumkauli in 1983, 1989, 1992, 1997, 2008 and 2009. and least number of drought year, was recorded in Gurjakhani. It should be noted that the study period of Gurjakhani is from 2008-2011. Moreover, continuous droughts for two year period were recorded in Jomsom, Benibazar, Dumkauli, Taulihawa, Khudibazar Synjgha, Chapkot, and Khairinitar . Occurrences of extreme drought events were observed at Baglung, Jomsom , Tansen, Taulihawa, Gorkha, Chapkot and Chame independent of the eco-regions.

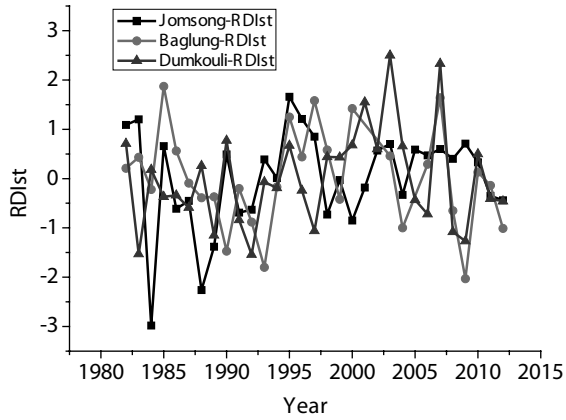

Figure 4: Time series of RDI index in Jomsom, Baglung and Dumkauli stations of Western region

In the year of 1992, 2002, 2006 and 2009 we observed occurrence of drought in most of the meteorological stations of western region.

4.2. DROUGHT ANALYSIS USING INDEX FOR CENTRAL REGION

Within central development region, highest number of drought occurred in Parwanipur and lowest number of drought occurred in Panchkhal and Dhunibesi. Parwanipur is in Terai region whereas Panchkhal and Dhunibesi lies in mid hill eco-region (see Table 1).

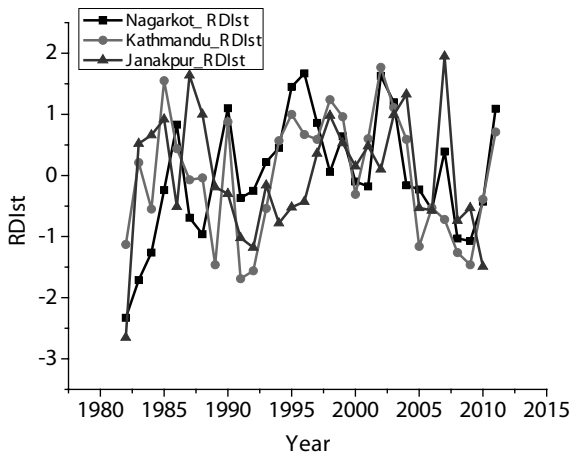

Figure 5: Time series of RDI index in Nagarkot, Kathmandu airport and Janakpur airport of Central region

Time Series analysis of three meteorological stations of central region representing all three eco-zones- high hill (Nagarkot), mid hill (Kathmandu airport) and Terai (Janakpur airport) is shown in Figure 5. No similar trend has been observed among these three eco zones for RDI analysis. Four continuous drought years were obtained in Daman, Nagarkot, Hetauda, Parwanipur, Nuwakot, Dhulikhel, Khumaltar, Janakpur airport and Manusmara. Extreme drought was seen in five meteorological stations of central region- Daman, Nuwakot, Panchkhal, Nagarkot and Janakpur airport.

Among seventeen studied stations, Nuwakot experienced highest number of extreme drought events. Calculated drought year in most of the stations of central region were found to occur in 1991, 1992 and 2009. Therefore, the year 1991, 1992 and 2009 were found to be rainfall deficient years which coincided with the results of Dahal et al., 2016.

4.3. DROUGHT ANALYSIS USING INDEX FOR EASTERN REGION

Within fifteen studied stations of eastern region, highest number of drought occurred at Rajbiraj, and Okhaldhunga. Similarly, least number of drought year was recorded in Udyapurgadhi and Kanyam tea estate. Occurrence of extreme drought events were observed at Fatepur, Tehrathum, Lahan, Chainpur, Pharkibas, Dharanbazar, Biratnagar airport, Ilam tea estate and Kanyam tea estate. Time Series analysis of two meteorological stations of eastern region representing two eco-zones- mid hill (Taplejung) and Terai (Biratnagar airport) is shown in Figure 6.

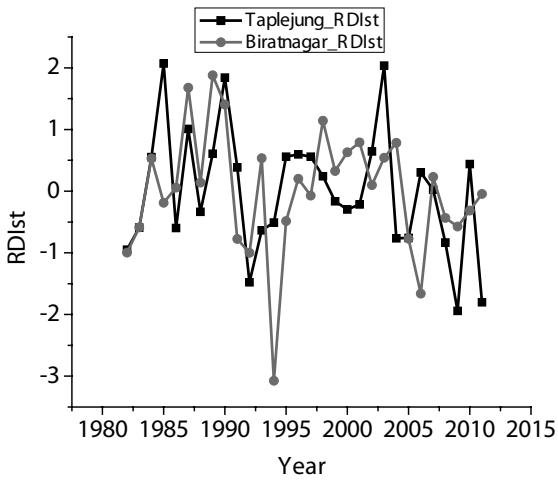

Figure 6: Time series of RDI index in Taplejung and Biratnagar airport of Eastern region

Moreover, continuous droughts were recorded in five stations of eastern region, Okhaldhunga, Fatepur, Rajbiraj, Chainpur and Dhankuta. No similarity was noticed in the time period of occurrence of drought of each meteorological stations in eastern region. Most stations experienced drought in the year 1992, 1994 and 2009.

5. CONCLUSION

The present study has been conducted to analyze the occurrence of drought, its frequency and severity in western, central and eastern development region of Nepal. It has been found that all the three kinds, moderate, severe and extreme events of drought occurred in all three development regions of Nepal with the number of 112, 39 and 22 respectively. Among 173 drought events, 68 drought events occurred in west, 62 in central and 43 in eastern region of Nepal. Highest numbers of extreme events were observed in eastern region and lowest number, in central region of Nepal. That means western region experienced more drought events whereas eastern region experienced more extreme events. Frequency of continuous drought events was higher in central region of Nepal. Drought analysis in three agro eco-zones revealed that the frequency of drought occurrence was higher in low altitude region, i.e. in Terai zone and lowest in high-hill zones. Similarly, extreme events were found to occur mostly in higher altitude region. These events occurred when precipitation recorded its lowest range. Maximum numbers of drought events were recorded in the year 1991, 1992, 1994, 2002, 2006, and 2009 in all three development regions. However, 1992 and 2009 were the only time period when drought occurred in whole Nepal. Besides 1992 and 2009 all other drought years were found to be independent of eco-regions and development regions. There were no similarities of drought events within eco-regions. That means occurrence of drought in Nepal is not always influenced by the monsoonal conditions of Nepal. Local geography as well as anthropogenic effects must be the causes of drought conditions in Nepal.

ACKNOWLEDGEMENTS

The author acknowledges Nepal Academy of Science and Technology for giving an opportunity to carry out this research and for providing necessary meteorological datasets.

REFERENCES

Agnew, C. 2000. Using the SPI to identify drought. *Drought Network News***12**(1): 6-12.

Bhatt, D., S. Maskey, M.S. Babel, S. Uhlenbrook, K.C. Prasad 2014. Climate trends and impacts on crop production in the Koshi river basin of Nepal. Reg Environ Change 14:1291-1301.

Dahal, P., N. S. Shrestha, M. L Shrestha, N. Y. Krakauer, J. Panthi, S. M. Pradhanang, A. Jha, T. Lakhankar 2016.Drought risk assessment in central Nepal: temporaland spatial analysis. *Nat Hazards* 80:1913–1932.

Devkota L.P. and D. R. Gyawali, 2015.Impacts of climate change on hydrological regime and water resources management of the Koshi River Basin, Nepal. *Journal of Hydrology: Regional Studies*4: 502–515.

DIHM. 2004. *Climatological and surface water records from 1965 to 1973*. Department of Irrigation, Hydrology and Meteorology. HMG Nepal.

Gautam, D.K. and S.K. Regmi 2014. Recent trends in the onset and withdrawal of summer monsoon over Nepal. *ECOPERSIA* **1**(4):353-367**.**

Guttman, N., J. Wallis and J. Hosking. 1992. Spatial comparability of the Palmer drought severity index. *Water Resources Bulletin* **28**(6): 1111-1119.

GWP_SA_Summary_Report_Need_Assessment_Survey_2014.

https://en.wikipedia.org/wiki/Development_regions_of_Nepal

Kafle, H. K. and H. J. Bruins 2009.Climatic trends in Israel 1970- 2002: warmer and increasing aridity in land. *Journal of Climatic Change* 29: 63–77.

Kafle, H.K. 2014. Study of Drought in Far and Mid Western region of Nepal: Time Series Analysis 1982-2012. Nepal Journal of Science and Technology, 15 (2), 65-76.

Kogan, F., T., Adamenko., and W., Guo 2013. Global and regional drought dynamics in the climate warming era. *Remote Sensing Letters* 4(4):364–372.

Kundzewicz, Z. W. 1997.Water resources for sustainable development. *Hydrol. Sci. J.* **42**(4): 467-480.

Manandhar Sujata, D.S.Vogt, S.R.Perret,F. Kazama 2011.Adaptating cropping systems to climate chnagein Nepal: a cross-regional study of farmers' perception and practices. *Reg Environ Change* 11: 335-348.

McKee, T., N. Doesken and J. Kleist. 1995. Drought monitoring with multiple time scales. In: *9th Conference on Applied Climatology*, 15-20 Jan., 1995, Dallas, USA, pp.233-236.

Palmer, W. 1965. *Meteorological drought*. Research paper 45, US Weather Bureau, Washington, D.C.

Practical Action Nepal Office. 2009. *Temporal and spatial variability of climate change over Nepal (1976-2005).* ISBN: 978-9937-8135-2-5, http://practicalaction.org/file/region_nepal/Climate Change 1976-2005.pdf (accessed on 10/27/2014).

Saha, K. 2010. Monsoon over Southern Asia. *Tropical Circulation Systems and Monsoons*. Springer, pp 89-122.

Shakya, N. and Y., Yamaguchi 2010. Vegetation, water and thermal stress index for study of drought in Nepal and central northeastern India. *International Journal of Remote Sensing* **31**(4): 903-912.

Sheffield,J. and E. F. Wood. 2008.Projected changes in drought occurrence under future global warming from multi-model, multi-scenario, IPCC AR4simulations. *Clim. Dyn.***31**:79–105.

Shrestha, M.L. 2000. Interannual variation of summer monsson rainfall over Nepal and its relation to Southern Oscillation Index. *Journal of Meteorology and Atmospheric Physics***75**(1-2):21-28.

Shrestha, S., M. Khatiwada, M. S. Babel and K. Parajuli, 2014. Impact of Climate Change on River Flow and Hydropower Production in Kulekhani Hydropower Project of Nepal. *Environ. Process* 1:231–250.

Sigdel M. and M. Ikeda, 2010. Spatial and temporal analysis of drought in Nepal using standardized precipitation index and its relationship with climate indices. *Journal of Hydrology and Meteorology* **7**(1): 59-74.

Thronthwaite, C.W. 1931. The climates of North America: According to a new classification. *Geographical Review* **21**(4): 633-655.

Thronthwaite, C.W. 1933. The climates of earth. *Geographical Review***23**: 433-440.

Thronthwaite, C.W. 1948. An approach towards a rational classification of climate. *Geographical Review***38**: 55-94.

Thronthwaite, C.W.1957. Instructions and tables for computing potential evapotranspiration and the water balance. *Publications in Climatology*X (3): 185-243.

Trenberth, K.E., A. Dai, G. V..Schrier, P. D. Jones, J. Barichivich, K.R.Briffa, J. Sheffield 2014. Global warming and changes in drought. *Nature Clim. Change* 4(1):17–22.

Tsakiris, G. and H. Vangelis 2005. Establishing a drought index incorporating evapotranspiration. *European Water* **9/10**:3-11.

UNEP. 1992. World atlas of desertification. Edward Arnold, London.

Wang, S., Yoon, J.H, Gillies, R.R and Cho, C. 2013. What caused the winter drought in western Nepal during recent years? *Journal of Climate.*

Wilhite, D.A. 2000. Drought as natural hazards: concepts and definitions. In: *Drought: a global assessment*, vol.1 (Ed.D. Whilhite).Routledge Publishers, London. pp 3-18.

www.lgcdp.gov.np/home/map-center.php

www.drought.gov

Spatial and Temporal Variation in Rainfall in Panchase Mountain Ecological Region of Nepal

Shobha Kumari Yadav
Institute for Social and Environment Transition-Nepal (ISET-N), Manasi Marga, Kathmandu Municipality-4, Chandol, Kathmandu
shobhas.yadav@gmail.com

Abstract

Time series statistical tests were applied to examine the spatial and temporal rainfall annual trends and four seasons (Pre-monsoon; Monsoon; Post-Monsoon and Winter Monsoon) during the period 1972–2013 in Panchase region of Western Nepal. Pre-monsoon, Monsoon and Post-monsoon rainfall was observed to follow positive trends where as the winter rainfall depicts negative trend. The non-parametric Mann-Kendall and Spearman's rho (SR) statistical tests were used to determine positive or negative trend in data with statistical significance. The test, applied on a seasonal basis to the precipitation revealed no statistically significant trends over the past 41 years. The results highlighted a mix of positive (increasing) and negative (decreasing) trends in monthly, seasonal, and annual precipitation. The rainfall coefficients of variation have been calculated to measure the spatial variations in rainfall in the study area. The study provides major evidences that rainfall is highly variable within local settings. This understanding benefits climate and hydrological studies, and water resources management. The findings were used in resilience planning at local level in which the community members envisioned future scenario. The scenarios emphasised in proposing adaptation measures in Panchase Region (PR). The findings are further helpful for planning and efficient use of water for agriculture.

Keywords: *Panchase, Nepal, rainfall trend, Mann-Kendall, Spearman's rho coefficient*

1. Introduction

Nepal's climate is a result of the Asian monsoon and the interaction with the extreme topography of the country including an enormous range of altitude within such a short south-north distance. Monsoon precipitation plays a dominant role in the country's hydrological regime contributing to 80% of rainfall from June to September. Precipitation, however, differs from place to place. Precipitation is higher in eastern part of the country compared to the west. Only fewer studies (Shrestha, 2000; Lang and Barros, 2002; Barros and Lang, 2003; Barros and Lang, 2003; Chalise et al. 2003; Kansakar et al., 2004; and Alison et al., 2006) have examined the spatial and temporal variability of precipitation across Nepal. But, results from such studies are not sufficient to generalize wider spatial patterns across mountainous relief. This study investigated spatial distributions of annual and seasonal and monthly precipitation and long-term trends to improve understanding of rainfall

variability in Panchase Region (PR) of Nepal.

The Panchase Region is a unique and rich ecosystem located in Nepal's Mid Hill region. With enchanting landscapes that offer spectacular views of Himalayan peaks including Annapurna, Dhaulagiri and Machhapuchhre, it is a home of diverse range of human cultures. Agriculture is the main livelihood which is primarily dependent on rainfall. The annual cycle of rainfall is similar to the rest of Nepal and is dominated by the South Asian monsoon system. However, the marked differences in elevation over short distances greatly affect daily, seasonal and annual temperatures and rainfall. Because of this, rainfall may vary considerably over short horizontal distances with sharp changes in the elevation. Hence, a deeper understanding of the characteristics and distribution of rainfall patterns is imperative to support water management, agricultural development and disaster risk management and planning. Therefore, this paper discusses monthly, seasonal and annual rainfall series for the Panchase to explore the variability of rainfall both spatially and temporally.

The study applied both parametric and non-parametric factors to analyze the spatial and temporal rainfall variability. Mann-Kendall test, Spearmen rank test, trend analysis has been performed to determine trend and variability. Emphasis was given to explore significant change in the rainfall time series records over the years. The study provides major evidence that rainfall is highly variable within local settings. The results contribute to improve the general understanding of the rainfall variability and trends over PR. The findings were used in proposing adaptation measures at local level.

2. Study Area

The PR lies between 75°27′–79°54′ East longitudes and 10°9′–13°30′North latitudes Figure 1, and extends over 17 Village Development Committees (VDCs) of Kaski, Syangja and Parbat districts. It covers an area of 284 Km^2.

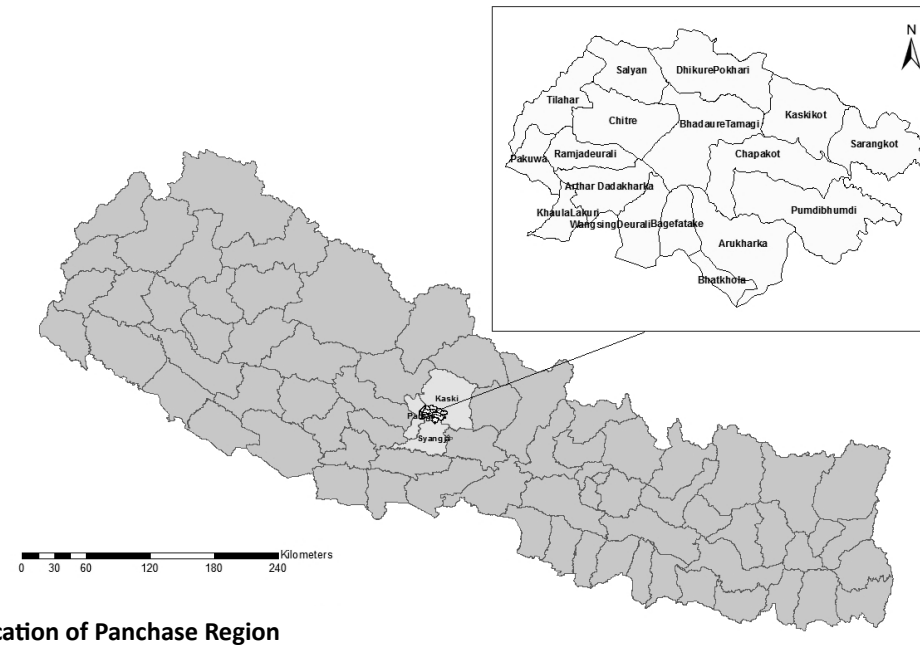

Figure 1: Location of Panchase Region

The elevation of the PR ranges from 742 m above sea level near Phewa Lake to 2517 m at the top of Panchase Peak. Around 79 per cent of the total area lies between altitudes of 1000 to 2000 m above sea level and just four per cent is above 2000 m and the remaining 17 per cent is lies at altitudes below 1000 m. The climate varies from subtropical to cold temperate. At lower elevations, summers are warm whereas at higher elevations these range from cold to very cold. In winter the Panchase peaks are covered in the snow. The data indicates that the mean maximum temperature in the PR is about 29°C and the mean minimum temperature is 5.3°C. The coldest month is January with an average monthly minimum temperature of 4.3°C. On average, PR receives 3882 mm of rainfall every year, well above the national average of 1857 mm (Practical Action, 2009). However, the amount of precipitation is greatly affected by the terrain.

The region is home to diverse ecosystems including forests and wetland, a wide vegetative variety, including rhododendrons and endemic orchid species, as well as religious and cultural diversity (Dixit et al., 2015). The PR comprises the headwaters of Phewa Lake and Aandhi Khola, two important water bodies used extensively for hydropower, irrigation, recreation, tourism and aquaculture. The Rati/Jare Khola drains the remaining area of the PR.

3. Data Used and Methodology

The rainfall data over PR for the period from 1972 to 2013 was obtained from the Department of Hydrology and Meteorology (DHM). Figure 2 shows the meteorological stations used in this study. These stations were chosen to represent the best possible coverage of the climatic regions of PR and availability of maximum data length and data accuracy.

Figure 2: Spatial distribution of meteorological station used for the study

Table 1: Meteorological stations used in study area along with their elevation

Station code	Station name
813 (1600 m)	Bhadaure deurali (Kaski)
814 (1740)	Lumle (Kaski)
830 (1160 m)	Pamdur (Kaski)
613 (1720 m)	Karkineta (Parbat)
829 (1000 m)	Sallyan (Parbat)
805 (460 m)	Putali Bazar (Syangja)
804 (827 m)	Pokhara Airport (Kaski)

Seasonal, annual and monthly rainfall data series of PR were computed using daily rainfall data of rain gauge stations located in and around PR region. Then average seasonal and annual precipitation amount was computed over the 42-year period to be able to examine precipitation trend. The trend detection methods were applied to annual, seasonal and monthly precipitation data. The yearly time scale was classified into four seasons: pre-monsoon, (March – May); monsoon (June–September), post-monsoon (October–November), and winter (December–January–February). The study applied Mann–Kendall trend test and Spearman's rank-order correlation tests (Sneyers, 1990; Turkes et al., 1995; and Tonkaz et al., 2007), coefficient of variation and liner trend to analyze the spatial and temporal rainfall variability. In the present study, confidence levels of 95% signify the positive or negative trends determined by the test statistic. At the 95% significance level, the null hypothesis of no trend is rejected if $|Z| > 1.96$. More details of the Mann-Kendall test and its statistical ability are documented in Yue et al. (2002).

Man-Kendall test

Man-Kendall test (Mann, 1945; Kendall, 1975) is used for trend detection in rainfall time series. It is the best methods for the trend analysis preferred by various researchers (Douglas et al, 2000; Yue et al., 2003; Jain and Kumar, 2012). Mann- Kendall test is used for analysis and ascertains statistical significance by hypothesis test of hydrological variables (Yue et al., 2002). Mann-Kendall test does not require that datasets follow normal distribution and show homogeneity in variance; transformations are not basically required if data already follows normal distribution, in skewed distribution greater power is achieved (Duhan and Pandey, 2013). It also discusses function of slope in the trend, coefficient of variation, and type of probability distribution (Yue et al., 2002). Further, trends are analysed both at the annual and at the seasonal scale.

The Mann-Kendall test is used to test the null hypothesis H_0 of no trend in a data series, against the alternate hypothesis H_1 of increasing or decreasing trend. In this test the data values are evaluated as an ordered time series. The test statistic of MK test can be computed as:

$$S = \sum_{i=2}^{n} \sum_{j=1}^{i-1} sign\,(x_i - x_j) \qquad \text{(i)}$$

where, S is sum of signs of the differences between any two observations for a series xn. Also, where sign (z) is 0 when z is zero, and 1 when z > and −1 when z < 1.

Coefficient of Variation

The coefficient of variation (CV) is a statistical measure of how the individual data points vary about the mean value. A greater value of CV is the indicator of larger spatial variability, and vice versa. For instance it indicates the amount of fluctuation in rainfall recorded over

a long period of time from the mean values. Statistically, the coefficient of variation of rainfall is defined as the standard deviation divided by the average areal rainfall, was used to characterize the monthly seasonal and annual spatial variability of rainfall.

Spearman's rank test

The existence of trends in the rainfall data was assessed by the rank-based non-parametric Spearman's rank or Spearman's rho statistical test (Dahmen and Hall, 1990; Sneyer, 1990). The presence or absence of trend was evaluated by using a confidence interval of 95%.

Further, the spatial variability was applied on monthly, seasonal and annual rainfall. The Spatial interpolation technique is employed to determine the spatial pattern of rainfall using Arc GIS 9.3. Additionally, the presence or absence of trend was evaluated by using Spearman's rank test. A confidence interval of 95% was also used to evaluate trend using Spearman's rank test. Both Mann-Kendall and Spearman's rank test was applied on seasonal and annual rainfall.

4. Result and Discussion

The outcome of the study revealed various facts about the spatial-temporal variation of rainfall in the PR. The variation included in different data series such as monthly, mean annual, seasonal variation of rainfall. The results of each series are discussed below:

4.1. Monthly rainfall

The figure 3 depict that PR receives highest amount of monthly rainfall in July followed by August and June while lowest amount of rainfall occurs in December followed by November. Monthly rainfall characteristics of the PR are presented in the Table 2 and in the Figure 3.

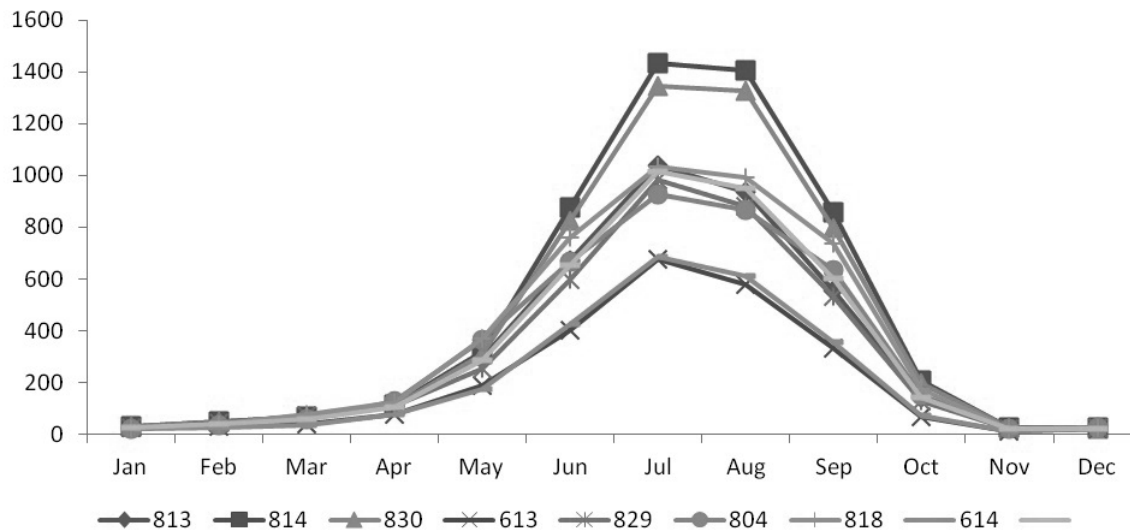

Figure 3: Annual profile of the monthly total rainfall (mm) for different stations in PR

Table 2: Mean monthly rainfall statistics of average of all station in PR

Month	Rainfall (mm)	Coefficient of Variation (%)
January	23.58	14.61
February	36.87	16.28
March	50.48	20.91
April	102.22	19.05
May	277.84	26.16
June	663.18	25.85
July	1029.95	26.92
August	947.11	30.18
September	605.93	32.18
October	145.41	36.58
November	18.80	31.88
December	17.00	18.71

The coefficient of variation (CV) of monthly variation varied from 14.61 to 36.58. It is highest in October (36.58 %), followed by September (32.18 %), November (31.88 %) and August (30.18 %) and the least during January (14.61 %) and February (16.28 %). It implies that the rainfall is highly variable in the month of October which lies in post monsoon season followed by September.

4.2. Seasonal rainfall characteristics

The PR experiences four distinct periods of rainfall (Figure 4) on the basis of the percentage of contribution to the annual rainfall: pre-monsoon (March to May), monsoon (June to September), post-monsoon (October to November), and winter (December to February). The PR receives copious rainfall (80 % of annual rainfall) during monsoon. This season has the maximum number of rainy days and is called the 'wet season'. The amount of rainfall ranges from 2075 mm to 3603 mm. The northern part of PR receives highest rainfall as depicted by isohyets (Figure 4b). During pre-monsoon, rainfall ranges from 292 mm to 613 mm. Isohyets of high rainfall values are located in the eastern parts of PR (Figure 4a). Contrary to this pattern, post-monsoon experience moderate rainfall ranging from 28 mm to 380 mm. The post-monsoon (Figure 4c) remains dry and contribute very low rainfall to the annual. Isohyets of post-monsoon indicate higher rainfall in north-western part of PR. The winter rainfall account (Figure 4d) for the lowest ranging from 5 mm to 173 mm. The isohyets denote highest rainfall in north-western part of PR.

Pre-monsoon (a)

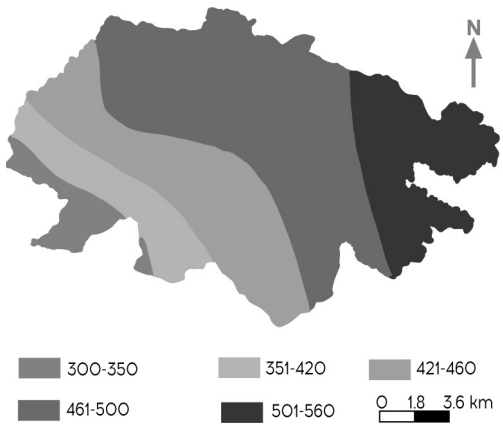

Monsoon (b)

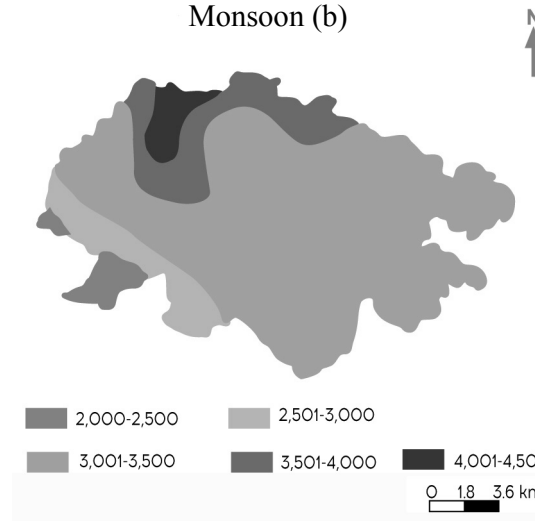

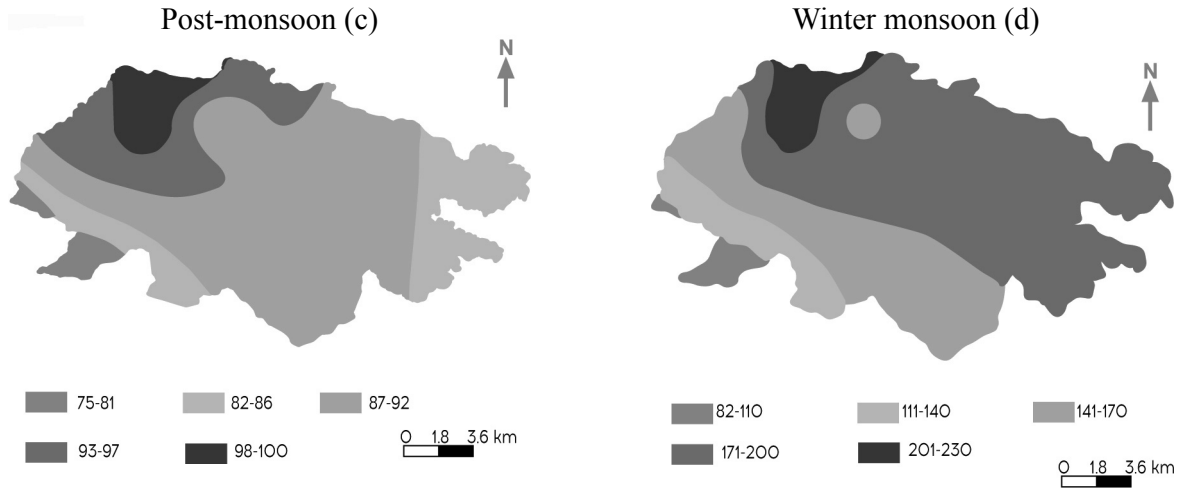

Figure 4: Spatial distribution of the mean seasonal rainfall over PR (1972–2013) (Dixit et.al, 2015) (Source: ISET-Nepal, 2015)

From the table 3, it is found that post-monsoon rainfall and winter rainfall shows high variability with CV of 54.47% and 58.07% respectively in comparison to pre-monsoon and monsoon rainfall with CV of 20.20% and 13.65% respectively. This implies that post-monsoon and winter rainfall show high rainfall variability.

Table 3: Seasonal rainfall statistics of PR

Seasons	Mean Rainfall (mm)	Coefficient of Variation (%)
Pre-monsoon	417.15	20.20
Monsoon	2772.80	13.65
Post-monsoon	132.18	54.47
Winter	68.78	58.07

4.3. Annual rainfall characteristics

The spatial distribution of annual rainfall is presented in figure 5. This map depicts the decreasing trend of rainfall from north western part to southern part of the PR. According to the performed analysis, high rainfall patterns are found in the north western region of PR with annual rainfall ranging from 4600 to 5300 mm. The south western part is the driest part of PR which receives rainfall between 2500 to 3100 mm annually. The southeast part of the PR gets moderate amount of rainfall from northeast part. The annual rainfall amounts to 3427.83 mm. The standard deviation of monsoon rainfall is 355.81 mm and co-efficient of variance is 10.38%.

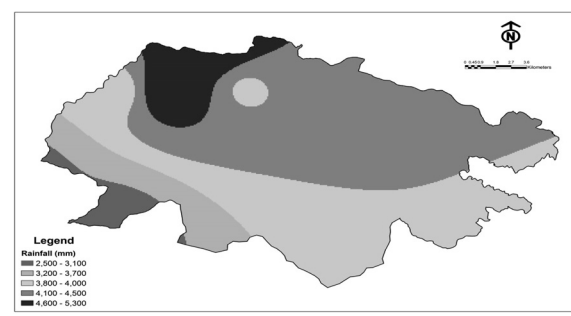

Figure 5: Spatial distribution of annual rainfall during the period 1972-2013

4.4. Temporal variation of seasonal trends

The analysis shows that the seasonal rainfall varies widely over different parts of PR. Decreasing trends for the pre-monsoon, monsoon, post-monsoon, and winter has been depicted by Mann-Kendall test. Additionally, results of Spearman's rank test as provided in table 4 does not reveal significant trend. The majority of the

rainfall time series of different stations depict negative values with non-significant decreasing trend. Monsoon rainfall shows increasing trend. But the trend is not significant.

Table 4: Mann-Kendall and Spearmen's trend statistics of seasonal rainfall over the PR region

Annual/ Stations	Mean Seasonal Rainfall (mm)	Mann-Kendall	Spearmen's Rank Test		Test Interpretation
		Test Z	Rho	P-value	
Pre-Monsoon	417	-0.27	-0.019	0.901	Not Statistically Significant
Monsoon	2773	0.04	-0.006	0.972	Not Statistically Significant
Post-Monsoon	132	-0.16	-0.187	0.229	Not Statistically Significant
Winter	69	-0.02	-0.139	0.379	Not Statistically Significant

The trend line manifested an insignificant decreasing trend in all seasons Figure 6. But the trend is not statistically significant. The rates of rainfall change in the pre-monsoon, monsoon, post-monsoon and winter are -0.264, -3.30, -1.054 and -0.215 mm/year respectively.

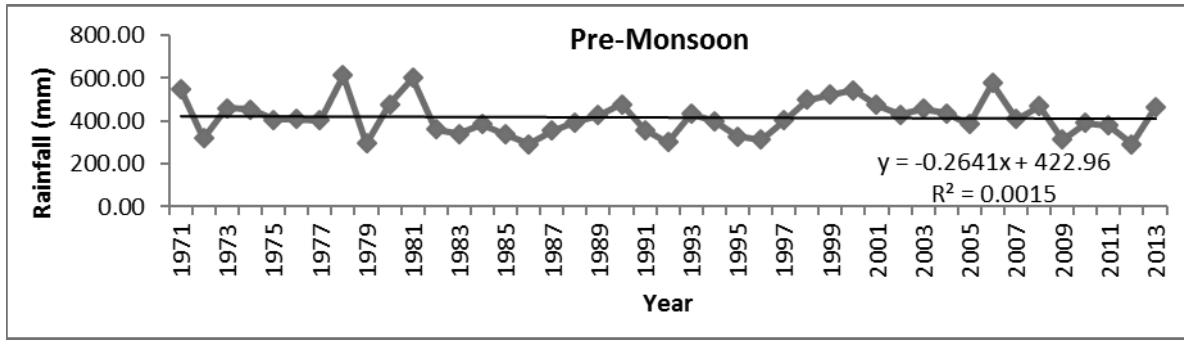

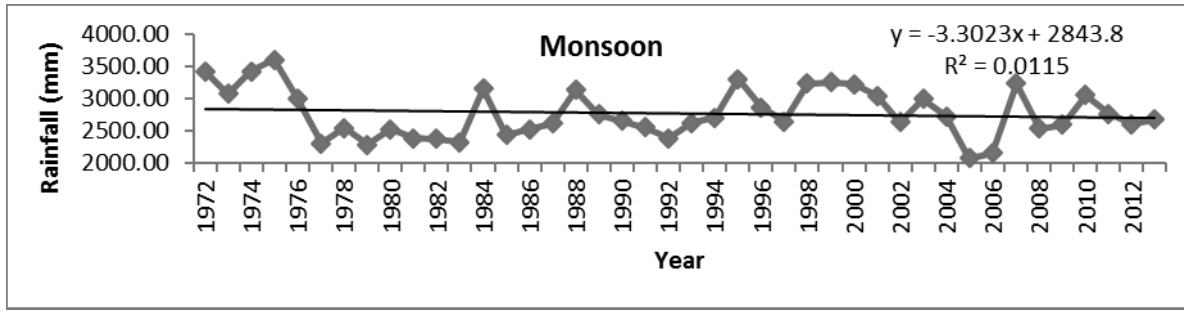

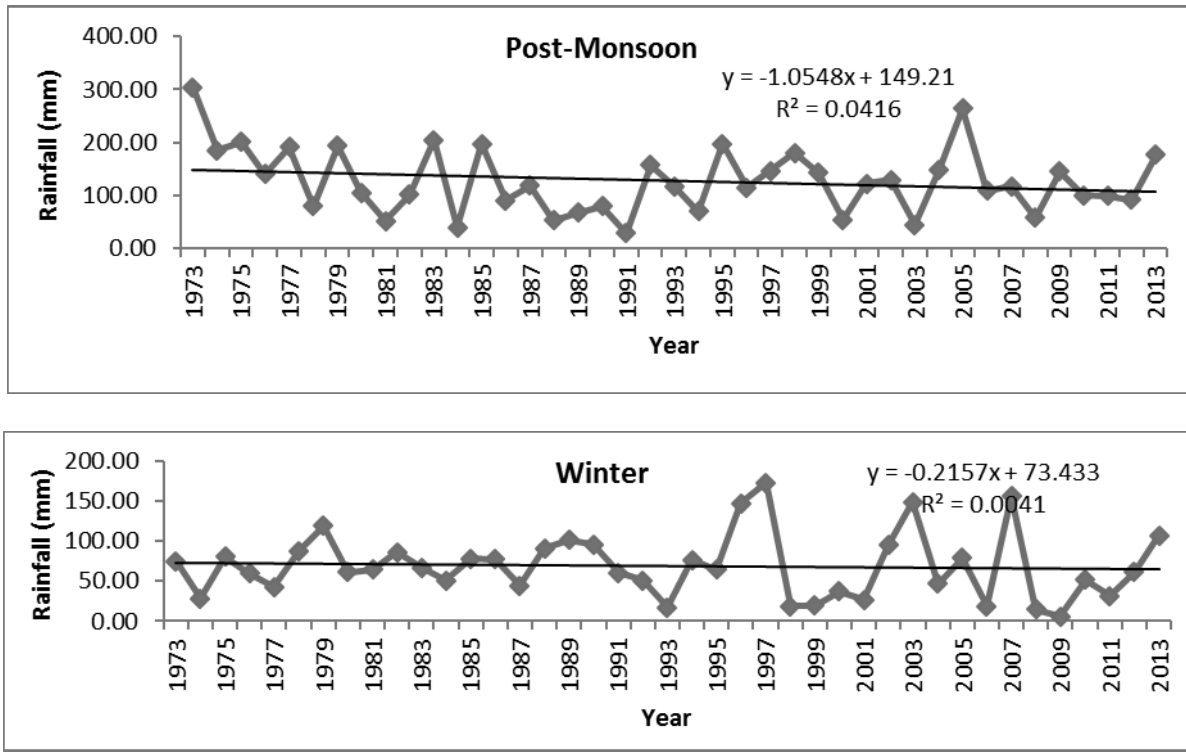

Figure 6: Time series trend line fit of seasonal rainfall over the PR (1972–2013)

4.5. Temporal variation of annual trends

The annual mean rainfall is subjected to the Mann-Kendall test individually together with the Spearmen's rank text at each station. Table 5 summarizes Mann-Kendall and Spearmen's trend statistics of annual rainfall over the PR region. Further, linear regression analysis was performed on annual mean rainfall data. The annual trends resulting from the three tests showed similar trends.

The station-wise analysis shows that the highest amount of monsoon rainfall occurs at station 814 (5413 mm) and lowest occurs at station 614 (2466 mm). Northern part of PR receives more 5413 mm of the annual rainfall during monsoon season which is the highest over Nepal.

Table 5: Mann-Kendall and Spearmen's trend statistics of annual rainfall over the PR

Annual/ Stations	Mean Seasonal Rainfall (mm)	Mann-Kendall	Spearmen's Rank Test		Test Interpretation
		Test Z	Rho	P-value	
Annual	3428	-0.02	-0.170	0.276	Not Statistically Significant
804	3894	-0.16	-0.055	0.730	Not Statistically Significant
813	4025	0.00	-0.240	0.219	Not Statistically Significant
814	5413	-0.25	0.254	0.101	Not Statistically Significant
818	4287	0.00	-0.185	0.240	Not Statistically Significant
613	2467	-0.27	0. 043	0.800	Not Statistically Significant
614	2466	-0.16	0.247	0.110	Not Statistically Significant
805	2889	-0.20	-0.078	0.630	Not Statistically Significant
829	3790	0.00	-0.193	0.391	Not Statistically Significant

Predominantly positive trends were found over the northern region, although the trends are not significant. The rainfall exhibits a decreasing trend in most of stations investigated; only three stations of (814, 818, and 829) showed insignificant increasing trend. Man-kendall Z value for those stations are -0.25, 0.00 and 0.00 respectively.

Spearmen's rho correlation coefficient has been calculated for all stations showing descending slope magnitude in five stations. Only the three stations (613, 614 and 814) showing increasing trend in Spearmen's rho correlation method. Their corresponding values are 0.043, 0.247, and 0.254 respectively. The results of the Spearmen's rho correlation test seem to be fairly similar to those obtained from the Mann-Kendall test.

The liner trend statistics reveal that, despite not showing an insignificant decreasing trend over the full period of record (1972–2013), the annual rainfall rate decrease in with rate of -4.89 mm/year (Figure 7). The trend analysis revealed that statistically insignificant (95% confidence level) negative trends of the mean annual rainfall appear in PR.

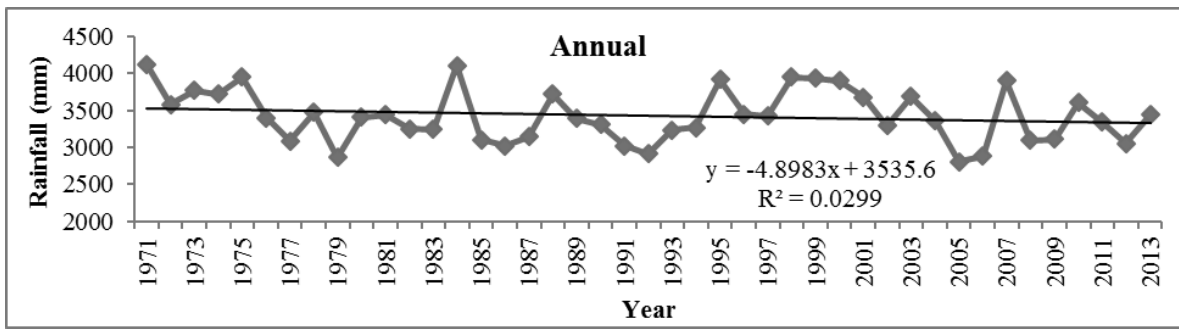

Figure 7: Time series trend line fit of annual rainfall over the PR (1972–2013)

5. Discussions and Conclusion

In Panchase region the local-scale features along with large-scale climate patterns plays detrimental role in producing variation in rainfall. The climate of a region is determined by two factors: and. The marked differences in elevation over short distances influence daily, seasonal and annual rainfall of PR. Rainfall varies significantly over short horizontal distances with sharp changes in the elevation. The spatial variations of year-wise rainfall show that the study area has fluctuations in rainfall both in space and time in all areas of the rain gauge stations. But, lack of data from some meteorological stations makes it impossible to confirm this hypothesis.

The study analysed rainfall time series, detected potential trends and assessed their significance over a wide area of about 284 km^2 of PR. The monthly rainfall shows high variability with monsoon season accounting for 80% of total annual rainfall. The seasonal and annual and monthly mean rainfall is subjected to the Mann-Kendall test together with the Spearmen's rank text. Further, linear regression analysis was performed on seasonal and annual mean rainfall data. The seasonal and annual trends resulting from the three tests showed similar trends. The changes are not seasonally and temporally homogenous over this time period. The result indicates an overall downward trend in annual and seasonal rainfalls by the both trends methods. The combined existence of positive and negative trends, along with the differences in the results referred to the particular observed time interval, does not allow drawing conclusions of a general tendency for the PR. However, the findings are helpful for planning and efficient use of agriculture water resources.

The decreased amount of monsoon and post-monsoon rainfall could have had negative impacts on agriculture and livelihood of the local people. The results of this study therefore have implications of the utmost importance in this sector. It is imperative to have further study to be carried out to establish other rainfall characteristics such as extreme rainfall, rain days, and other climate change parameters for this region to verify whether the significant trend has occurred and also to establish a correlation between temperature and extreme rainfall.

The unequal length of records renders the comparison of result with respect to different stations and seasons difficult. In Nepal, there is dearth of information on data quality. There are lots of missing data, which would affect the result related to the trend analysis substantially. Additionally, the long-term pattern of precipitation in Nepal is poorly constrained due to a lack of measurements of precipitation on spatial scales of a few tens of kilometres or less. The scarcity of information on spatial patterns of precipitation is in part due to the difficulty of measuring precipitation over appropriate spatial and temporal scales. But existing rain-gauge networks, especially in mountainous areas, are generally not dense enough to reveal variability in precipitation over spatial scales of tens of kilometres scales over which topography and precipitation can vary significantly. To this aim, further perspectives of the research, would require spanning spatial extension of the database to cover the whole region.

Acknowledgments

This research was supported by UNEP, UNDP and IUCN Government of Nepal. The authors gratefully acknowledge funding support

provided. The authors also thank Department of Hydrology and Meteorology for providing necessary data. The authors thank Mr. Ajaya Dixit, Executive Director of ISET-Nepal for his thoughtful support regarding this publication. The authors also wish to thank Kanchan Mani Dixit and Sneha Pandey for helping in editing which resulted in an improvement of the manuscript.

References

Alison, M. A. Gerard, H. R. Hallet, B. Montgomery, D. R. Finnegan, N and J. Putkonen, 2006: Spatial patterns of precipitation and topography in the Himalaya, Geological Society of America Special Paper, 398.

Barros, A. P. and T. J Lang, 2003: Monitoring the monsoon in the Himalayas: observations in central Nepal, June 2001, Monthly Weather Review, 131, 1408–1427.

Barros, A. P. Joshi, M. Putkonen, J and D.W. Burbank, 2000: A study of the 1999 monsoon rainfall in a mountainous region in central Nepal using TRMM products and rain gauge observations. Geophysical Research Letters, 27, 3683–3686.

Chalise, S. R. Kansakar, S. R. Rees, G. Croker, K and M. Zaidman M, 2003: Management of water resources and low flow estimation for the Himalayan basins of Nepal, Journal of Hydrology, 282, 25–35.

Dahmen, E. R and M. J. Hall, 1990: Screening of hydrological data: tests for stationarity and relative consistency, The Netherlands, 58, Publication #49.

Dixit, A., Karki, M. and A. Shukla, 2015: Vulnerability and Impacts Assessment for Adaptation Planning in Panchase Mountain Ecological Region, Nepal, Kathmandu, Nepal.

Douglas, E. M. Vogel, R. M and C. N. Knoll, 2000: Trends in flood and low flows in the United States: impact of spatial correlation, Journal of Hydrology, 240, 90–105.

Duhan, D and A. Pandey, 2013: Statistical Analysis of long term spatial and temporal trends of precipitation during 1901-2002 at Madhya Pradesh, India Atmospheric research, Elsevier, 122, 136-49.

Jain, S. K and V. Kumar, 2012: Trend analysis of rainfall and temperature data for India. *Current Science*, 102 (1): 37-49.

Kansakar, S. R. Hannah, D. M. Gerraed, J and G. Rees, 2004: Spatial pattern in the precipitation regime of Nepal, International Journal of Climatology, 24, 1645–1659.

Kendall, M. G., 1975: Rank Correlation Methods. Charles Griffin, London.

Lang, T. J and A. P. Barros, 2002: An investigation of the onsets of the 1999 and 2000 monsoons in central Nepal, Monthly Weather Review, 130, 1299–1316.

Mann, H. B., 1945: Nonparametric tests against trend. Econometrica 13 245–259.

Practical Action, 2009: Temporal and Spatial Variability of Climate Change over Nepal (1976-2005), Practical Action, Kathmandu.

Shrestha, A. B. Cameron, P.W. Paul, A.M. and E. D. Jack, 2000: Precipitation fluctuations in the Nepal Himalaya and its vicinity and relationship with some large scale Climatological parameters, International Journal of Climatology, 20, 317-327.

Sneyers, R, 1990: On the Statistical Analysis of Series of Observations. Technical Note no. 143, WMO-no. 415, World Meteorological Organization, Geneva, Switzerland.

Tonkaz, T. Çetin, M and T. Kâzım, 2007: The impact of water resources development projects on water vapour pressure trends in a semi-arid region, Turkey, Climatic Change, 82,195–209.

Turkes, M. Sumer, U. M. and G. Kilic, 1995: Variations and trends in annual mean air temperatures in Turkey with respect to climatic variability, International Journal of Climatology 15, 557– 569.

Xu, Z. X. Takeuchi, K and H. Ishidaira, 2003: Monotonic trend and step changes in Japanese precipitation, Journal of Hydrology, 279, 144–150.

Yue, S. Pilon, P and B. Phinney, 2003: Canadian stream flow trend detection: impacts of serial and cross-correlation, Hydrological Science Journal, 48(1), 51-63

Yue, S. Pilon, P and G. Cavadias, 2002: Power of the Mann-Kendall and Spearman's rho tests for detecting monotonic trends in hydrological series, J. Hydrol, 259, 254–271.

Water balance of Nepal and climatic classification based on moisture regimes

Rajendra Man Dongol
Freelancer, Kathmandu
Email: rajendra.dongol1@gmail.com

ABSTRACT

An attempt has been made to prepare the climatic map of Nepal based on moisture regime as defined by Thornthwaite. All together 97 meteorological stations throughout Nepal were selected for analyses. In order to calculate water balance, Modified Penman method has been used to estimate potential evapotranspiration. Due to the limitation of available meteorological parameter necessary for the computation, multiple regression formulae based on elevation, latitude and longitude is used. This paper also describes in detail the computation of potential evapotranspiration. Water balance of all the stations are calculated to obtain moisture index and other parameters viz., Actual Evapotranspiration, Water Deficit, Water Surplus and their corresponding maps are prepared and its parameters discussed. Finally climatic map based on the moisture regime is presented.

Keywords: *Climate Map, Water Balance, Water Deficit, Moisture.*

Introduction:

In 1948 Thornthwaite developed a climatic water budget procedure which permitted quantitative evaluation of hydrological parameters. These include soil moisture storage, actual evaporation, water deficit, water surplus, etc. This 1948 procedure has been modified over years (Thornthwaite & Mather, 1955; Rao & Subrahmanyam, 1961). While studying hydrologic parameters of Karnali river basin, Nepal, (Subrahmanyam et al , 1983) water balance was also used to study the climate of the basin. This method is widely used as it needs only precipitation and potential evapotranspiration as input variables.

The highest chain of mountains in the world, Himalaya, which extends over 2000 kilometres, running from Afghanistan, Kashmir in the west to Myanmar (Burma) in the east. Nepal is located along the southern slope of this Asiatic high Himalayas extending from longitudes 80º 14'E and 88º 12'E, latitude varies but lies within 26º 22'N and 30º 27'N. It is the extremes in altitude, from lowlands (Terai) in the south with less than 100 metres above sea level (masl) to the high Himalaya in the north, coupled with dry season and a rainy season, causes the extreme climatic contrasts in Nepal. This is also evident from Figure 1. (Chalise, 1994, reproduced with the author's permission), which represents the cross section for Central Nepal showing the dramatic altitudinal rise within a horizontal distance of 174 km. Similar north-south gradient exists throughout the length of about 800 km within Nepal and beyond. In the south, its elevation is

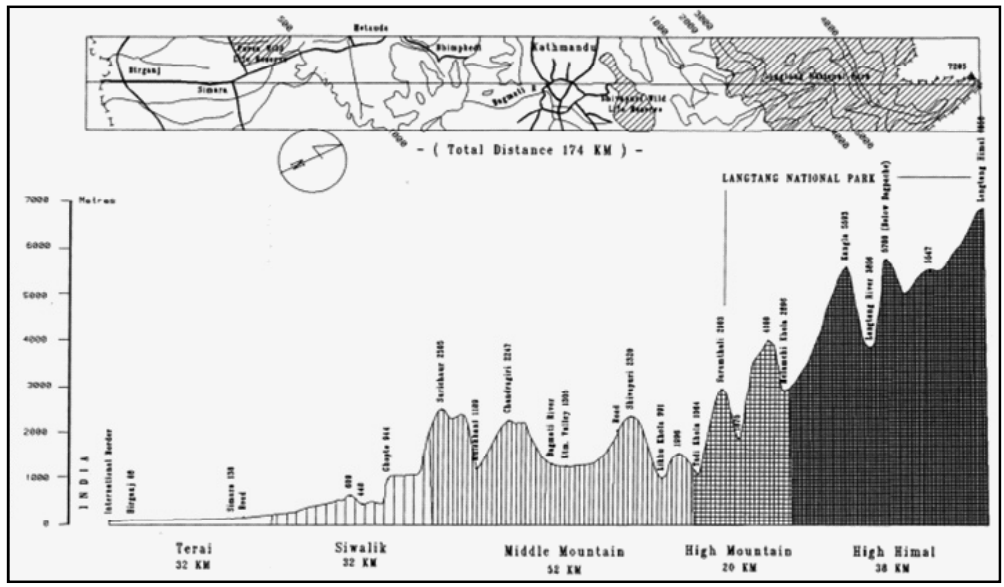

Figure 1: Cross-section of Central Nepal

less than 100 masl where, as in the north, it rises above 7000 masl (even up to 8848 masl, Mt. Everest) within less than 200 km. Due to the extremes in topography there exists wide range of climate. The high Himalayan region fits into polar climate due to altitude and tropical climate exists in the southern plains (Terai). Studies have shown that aerial distribution of precipitation is not linear mainly due to the varied topography (Subrahmanyam & Upadhyay, 1982; Shtrestha et al. 2000).

Climatic classification has been carried out by Nayava (1974) by applying Thornthwaites's 1931 scheme (Thornthwaite, 1931) and broadly divided into five climatic groups based on temperature. The study was limited by very few numbers of stations. Karki et al. (2015) classified climate of Nepal using Köppens classification scheme incorporating 74 climate stations data and 240 precipitation data from 1981 to 2010. According to them, the original Köppens-Geiger 1936 classification scheme, the Terai belt of Nepal resulted into temperate climate zone and therefore modified classification scheme was used following Peel et al. (2007) hence indicating the need for further study in this regard.

Data and Methodology

For the present study, monthly rainfall and other weather data required for computing potential evapotranspiration was collected from Department of Hydrology and Meteorology, Kathmandu. Department of Hydrology and Meteorology operates and maintains 267 meteorological stations, among which 97 stations including 4 high altitude stations, having Temperature and Humidity values, throughout the country establish over different years. In order to bring uniformity in the temporal data distribution, only stations established prior to 1981 was selected for this study. Rainfall, Humidity, Sunshine, Wind data and maximum & minimum temperature data are averaged from 1981 – 2010. In Figure 2, the spatial distribution of 97 meteorological stations used for this study is shown.

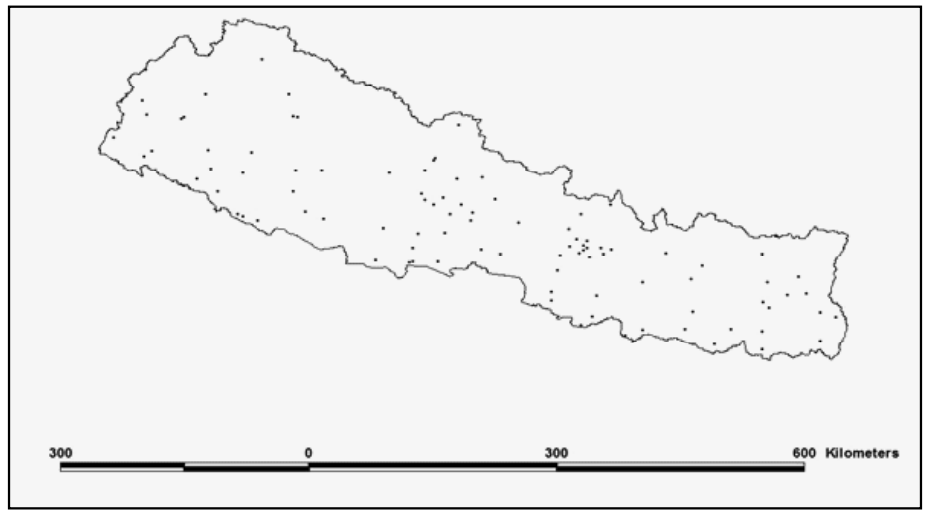

Figure 2: Spatial Distribution of Meteorological Stations considered for the Study

Potential evapotranspiration (PE) is the amount of moisture that would have been evaporated from water body, soil, and as well as transpirated from vegetation if it were available all the time. Large numbers of empirical methods are available for estimating evapotranspiration from different climatic variables. Prior water balance studies are based on PE estimated directly from temperature. Empirical relation to estimate potential evapotranspiration using elevation has been also developed (Lambert and Chitrakar,1989). For Nepalese condition, according to Nayava (2005), Penman method gives the best estimates of PE over Nepal.

FAO recommends the Penman-Monteith method as the sole method for determining reference crop evapotranspiration. The evapotranspiration rate from a reference surface, not short of water, is called the reference crop evapotranspiration or reference evapotranspiration and is denoted as ET_o. The reference surface is a hypothetical grass reference crop with specific characteristics (Allen et. al. 1998). The only factors affecting ET_o are climatic parameter and can be computed from weather data. The form of the Penman equation used to estimate PE for the current study is adopted from Hydrology and Agro-meteorology manual. The Penman equation is given by:

$$ET0 = C*\{Wg * Rn + (1 - Wg) * f(u) * (es - e)\} \quad \ldots\ldots\ldots\ldots\ldots (1)$$

where,

	ET0	=	evapotranspiration in mm/day
	Wg	=	a weighting factor
	Rn	=	net radiation in equivalent evapotranspiration mm/day
	f(u)	=	the wind function
	(es – e)	=	saturation deficits in millibar. es is the saturation vapour pressure and e is vapour pressure
	C	=	an adjustment factor to compensate for the effect of variations in day and night weather conditions

For each station, Potential evapotranspiration was estimated for each month using above formulae. The calculation of saturation deficit involves temperature and relative humidity. Based on the 97 stations mean monthly maximum and mean monthly minimum temperature data from 1981 to 2010, mean monthly maximum and minimum were estimated using multiple regression equation for all other stations without having temperature data. Similarly, relative humidity (RH) is taken as the midpoint between the two observations taken at 0845 NST and 1745 NST. Multiple regression method was again used to fill the missing stations. The saturation vapour pressure '$\mathbf{e_s}$' is a function of temperature which is given by Fig. 3 and vapuor pressure '**e**' is estimated using;

$$\mathbf{e = RH / 100 \times es} \quad \text{..... (2)}$$

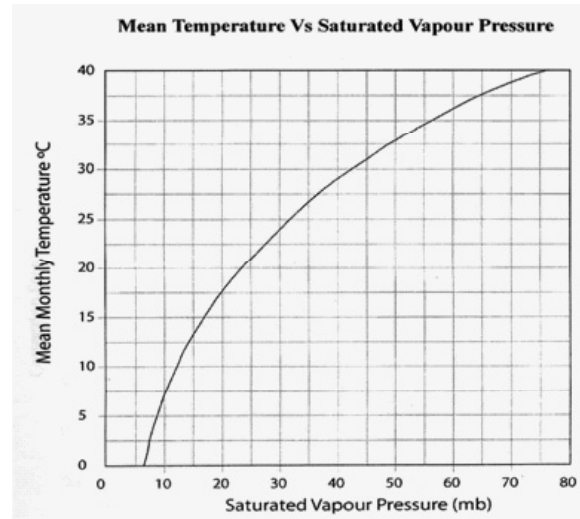

Figure 3

The net radiation '$\mathbf{R_n}$' is the difference between net short wave radiation '$\mathbf{R_{ns}}$' and net long wave radiation '$\mathbf{R_{nl}}$'.

$$\mathbf{ET0 = C*\{Wg * Rn + (1 - Wg) * f(u) * (es - e)\}} \quad \text{..... (1)}$$

where, $\mathbf{R_{ns}}$ = $0.75 \times (0.25 + 0.50 \times n/N) \times Ra$ ……..(4)

n is the sunshine duration in hours

N is the possible maximum sunshine hours and Ra the extra-terrestrial radiation in millimeters of water per day depending upon the latitude and time of the year (obtained from table given below).

$\mathbf{R_{nl}}$ = $f(t) \times f(e) \times (0.1 + 0.9 \times n/N)$ …….. (5)

f(t) is the Correction factor for temperature

f(e) is the Correction factor for vapour pressure obtained from thr graph given below.

Values of N for different Northern Latitude

Table 1

Lat	Jan	Feb	Mar	Apr	May	Jun	Jul	Aug	Sep	Oct	Nov	Dec
0	11.8	11.9	12.0	12.2	12.3	12.4	12.3	12.3	12.1	12.0	11.9	11.8
5	11.6	11.9	12.0	12.3	12.6	12.7	12.6	12.4	12.1	11.8	11.6	11.5
15	11.3	11.6	12.0	12.5	12.8	13.0	12.9	12.6	12.2	11.8	11.4	11.2
20	11.0	11.5	12.0	12.6	13.1	13.3	13.2	12.8	12.3	11.7	11.2	10.9
25	10.7	11.3	12.0	12.7	13.3	13.7	13.5	13.0	12.3	11.6	10.9	10.6
30	10.4	11.1	12.0	12.9	13.6	14.0	13.9	13.2	12.4	11.5	10.6	10.2

35	10.1	11.0	11.9	13.1	14.0	14.5	14.3	13.5	12.4	11.3	10.3	9.8
40	9.6	10.7	11.9	13.3	14.4	15.0	14.7	13.7	12.5	11.2	10.0	9.3
42	9.4	10.6	11.9	13.4	14.6	15.2	14.9	13.9	12.6	11.1	9.8	9.1
44	9.3	10.5	11.9	13.4	14.7	15.4	15.2	14.0	12.6	11.0	9.7	8.9
46	9.1	10.4	11.9	13.5	14.9	15.7	15.4	14.2	12.6	10.9	9.5	8.7
48	8.8	10.2	11.8	13.6	15.2	16.0	15.6	14.3	12.6	10.9	9.3	8.3
50	8.5	10.1	11.8	13.8	15.4	16.3	15.9	14.5	12.7	10.8	9.1	8.1

Values of Ra (mm of water per day) for different Northern Latitude

Table 1 (Cont.)

Lat	Jan	Feb	Mar	Apr	May	Jun	Jul	Aug	Sep	Oct	Nov	Dec
0	15.0	15.5	15.7	15.3	14.4	13.9	14.1	14.8	15.3	15.4	15.1	14.8
2	14.7	15.3	15.6	15.3	14.6	14.2	14.3	14.9	15.3	15.3	14.8	14.4
4	14.3	15.0	15.5	15.5	14.9	14.4	14.6	15.1	15.3	15.1	14.5	14.1
6	13.9	14.8	15.4	15.4	15.1	14.7	14.9	15.2	15.3	15.0	14.2	13.7
8	13.6	14.5	15.3	15.6	15.3	15.0	15.1	15.4	15.3	14.8	13.9	13.3
10	13.2	14.2	15.3	15.7	15.5	15.3	15.3	15.5	15.3	14.7	13.6	12.9
12	12.8	13.9	15.1	15.7	15.7	15.5	15.5	15.6	15.2	14.4	13.3	12.5
14	12.4	13.6	14.9	15.7	15.8	15.7	15.7	15.7	15.1	14.1	12.8	12.0
16	12.0	13.3	14.7	15.6	16.0	15.9	15.9	15.7	15.0	13.9	12.4	11.6
18	11.6	13.0	14.6	15.6	16.1	16.1	16.1	15.8	14.9	13.6	12.0	11.1
20	11.2	12.7	14.4	15.6	16.3	16.4	16.3	15.9	14.8	13.3	11.6	10.7
22	10.7	12.3	14.2	15.5	16.3	16.4	16.4	15.8	14.6	13.0	11.1	10.2
24	10.2	11.9	13.9	15.4	16.4	16.6	16.5	15.8	14.5	12.6	10.7	9.7
26	9.8	11.5	13.7	15.3	16.4	16.7	16.6	15.7	14.3	12.3	10.3	9.3
28	9.3	11.1	13.4	15.3	16.5	16.8	16.7	15.7	14.1	12.0	9.9	8.8
30	8.8	10.7	13.1	15.2	16.5	17.0	16.8	15.7	13.9	11.6	9.5	8.3
32	8.3	10.2	12.8	15.0	16.5	17.0	16.8	15.6	13.6	11.2	9.0	7.8
34	7.9	9.8	12.4	14.8	16.5	17.1	16.8	15.5	13.4	10.8	8.5	7.2
36	7.4	9.4	12.1	14.7	16.4	17.2	16.7	15.4	13.1	10.6	8.0	6.6
38	6.9	9.0	11.8	14.5	16.4	17.2	16.7	15.3	12.8	10.0	7.5	6.1
40	6.4	8.6	11.4	14.3	16.4	17.3	16.7	15.2	12.5	9.6	7.0	5.7
42	5.9	8.1	11.0	14.0	16.2	17.3	16.7	15.0	12.2	9.1	6.5	5.2
44	5.3	7.6	10.6	13.7	16.1	17.2	16.6	14.7	11.9	8.7	6.0	4.7
46	4.9	7.1	10.2	13.3	16.0	17.2	16.6	14.5	11.5	8.3	5.5	4.3
48	4.3	6.6	9.8	13.0	15.9	17.2	16.5	14.3	11.2	7.8	5.4	3.7

Net short wave radiation depends largely upon the ratio of sunshine duration '**n**' in hours of the station to the maximum possible sunshine hours '**N**' which depends on the latitude and time of the year and extra terrestrial radiation '$\mathbf{R_a}$'. For stations not having sunshine duration data, the ratio (**n/N**) is estimated as described in Hydrology and Agro-meteorology manual, Assistance in the establishment of design criteria and manuals for irrigation projects in Nepal (Sir M MacDonald & Partners Ltd, 1989).

Net long wave radiation depends mainly upon the mean temperature, vapour pressure and the n/N ratio. Using the mean temperature and vapour pressure, the value for **f(t)** and **f(e)** is obtained from Fig. 4 & 5. Then net long wave radiation, $\mathbf{R_{nl}}$ is calculated from eqn (5).

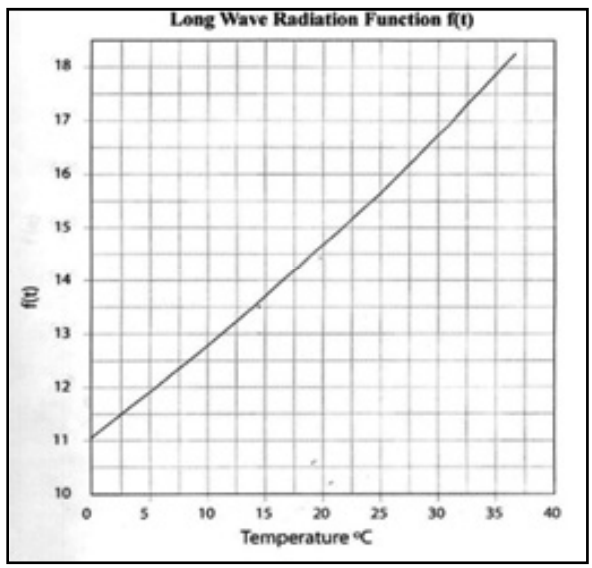

Figure 4

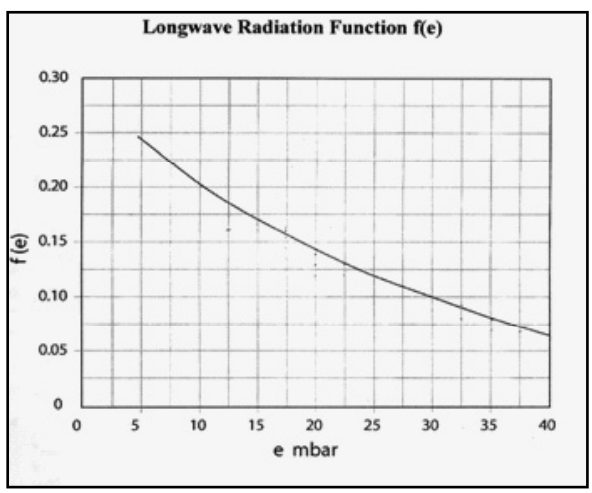

Figure 5

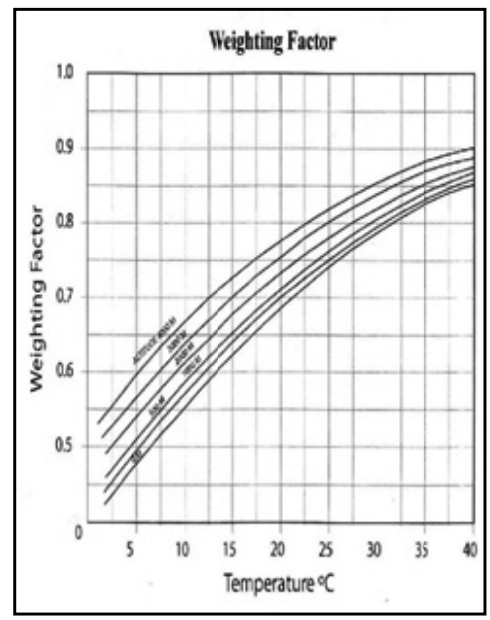

Figure 6

There are very few stations reporting wind speed over Nepal and that too are recorded at different heights. Where wind speed records are not measured at 2 metres above the ground, a correction factor using the graph (Mac Donald, 1989) is obtained to estimate wind speed at 2 metres (Fig. 7). The value for wind function '**f(u)**' is obtained by transferring daily wind speed to 24 hour wind run in kilometers. For stations not reporting wind, regression equations (Nayava, 2005) were used to estimate wind run and finally '**f(u)**' is obtained from a f(u) – wind run graph (Fig. 8) ((Mac Donald, 1989).

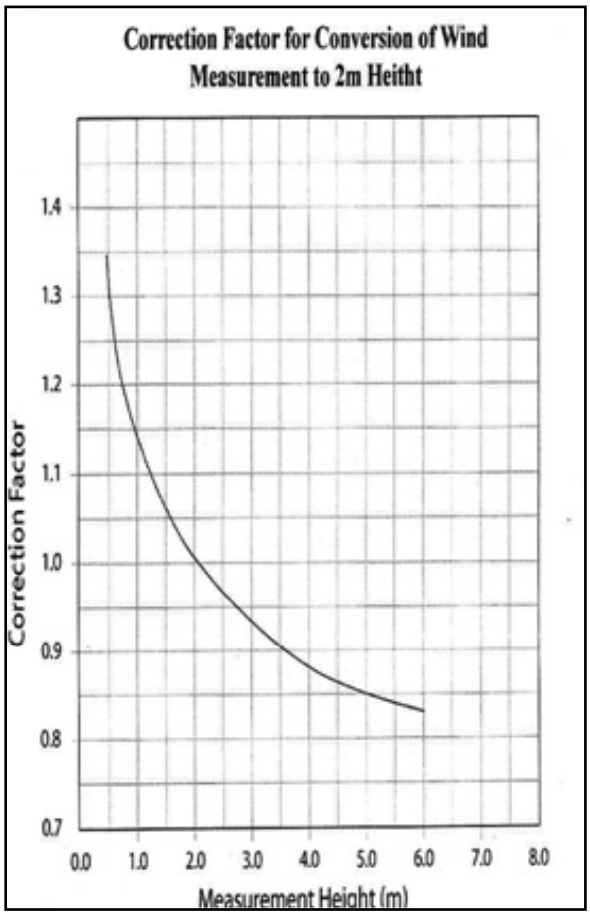

Figure 7

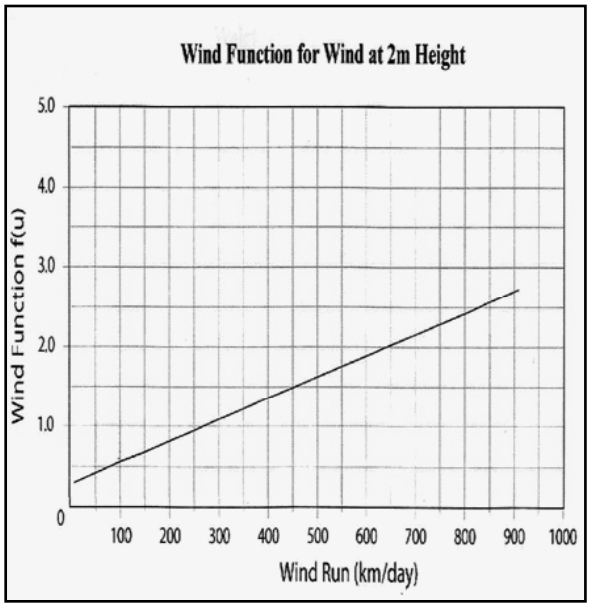

Figure 8

The water loss generated by available energy is greater in summer than in winter. By comparing the amount of water available from precipitation with water loss, it is possible to assess the moisture conditions to determine seasonal surplus or deficiencies. As much as potential evapotranspiration represents a transfer of both heat and moisture to the atmosphere and is primarily a function of energy received from the Sun. It is an index of thermal efficiency as well as water loss and so combines both the moisture and heat factors in climate. The moisture holding capacity of a soil depends upon the depth of the soil layer considered and its structure. It can vary from just few millimeters (mm) on a shallow sand to well over 400 mm on deep well aerated silt, loam. For the current study, the moisture holding capacity is taken from Upadhyay (1984). Where it is not available, we have considered 200 mm for stations over lowlands, 150 mm for middle mountain and 100 for higher elevations.

Using the book-keeping procedure (Thornthwaite and Mather, 1955), the water balance elements for all the stations have been computed. The input parameters for this model are monthly values of precipitation (**P**), monthly values of potential evapotranspiration (**PE**) and moisture holding capacity of the soil. Monthly total average values of the rainfall are based on the measured values. Monthly potential evapotranspiration values were estimated from other climatic parameters.

Results and Analysis

It has already been mentioned that rapid changes in the altitude and aspect along the latitudes have made existence of wide range of climatic conditions in Nepal. Therefore, within

a span of less than 200 km, Nepal captures almost all types of climates, subtropical to alpine/arctic. Therefore to capture all these aspect meteorological stations should also be distributed accordingly.

Table 2 illustrates the distribution of stations with elevation. There are fairly good amount of stations distributed up to 2000 masl, after which it decreases sharply.

Table 2: Distribution of Meteorological Stations with Altitude

Elevation (masl)	No of stations
< 500	32
< 1000	14
< 1500	22
< 2000	10
< 2500	9
< 3000	6
>= 3000	4

With the help of Arc View 3.1, rainfall distribution over Nepal (Fig. 9) shows that it varies from 138 mm at Lomathang (83º 97'E, 29º 18'N) to 5515 mm at Lumle (83º 47'E, 28º 18'N) with average of 1795 mm. There are numerous areas of rainfall greater than 3000 mm but generally it is minimum towards north-west area with minimum precipitation over Mustang area. Mustang area which lies north of Mt Dhaulagiri, is thus a rain shadow area and spatially very closes to Lumle.

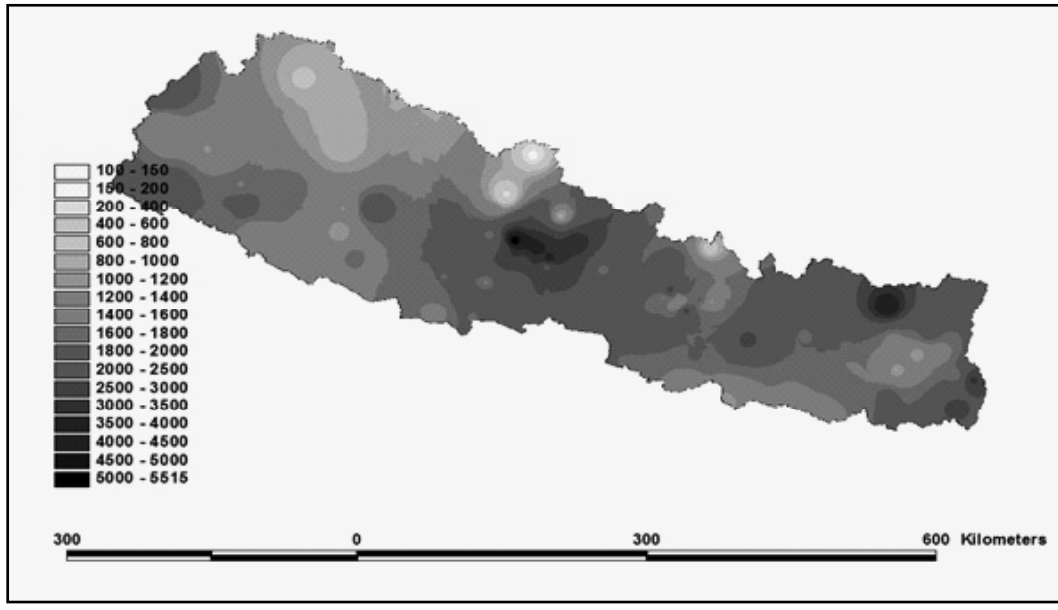

Figure 9: Spatial Distribution of Annual Rainfall (mm) over Nepal

The distribution of annual potential evapotranspiration is represented in Figure 10. It may be seen that the annual water need is more in the southern plains of the country where it is more than 1100 mm. As one proceeds north, it decreases and is less than 800 mm around 83º 95'E and 28º 53'N (Annapurna area).

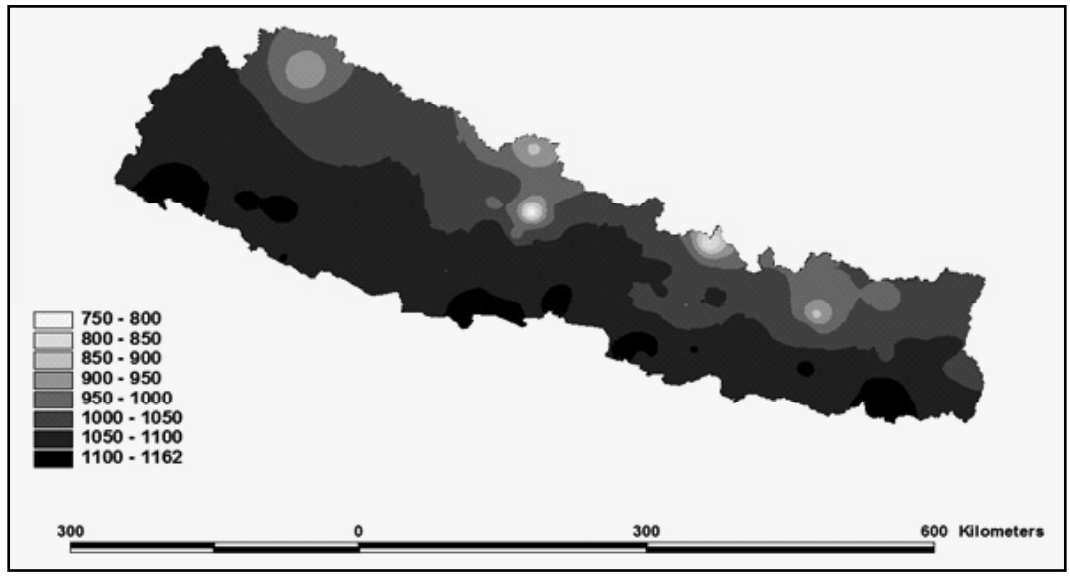

Figure 10: Spatial Distribution of Annual Potential Evapotranspiration (mm) over Nepal

Water balance of Nepal

The output parameters of the water balance model are monthly available soil moisture (**St**) for plants utilization, monthly values of actual evaporation (**AE**), monthly values of water deficit (**WD**) and monthly values of water surplus (**WS**). As an example, the water balance for the whole country is presented in Table 2 and their elements discussed.

Table 3: Water Balance Table of Nepal

	Jan	Feb	Mar	Apr	May	Jun	Jul	Aug	Sep	Oct	Nov	Dec	Total
$P_{(mm)}$	22	28	34	55	132	272	479	419	264	66	10	15	1795
$PE_{(mm)}$	51	62	97	119	124	110	98	102	100	85	60	50	1059
P-E	-29	-34	-64	-64	8	162	381	317	164	-19	-51	-36	
$St_{(mm)}$	61	49	32	21	29	150	150	150	150	132	95	74	
Cst	-13	-12	-17	-11	8	121	0	0	0	-18	-38	-20	
$AE_{(mm)}$	35	41	50	66	124	110	98	102	100	84	48	35	892
$WD_{(mm)}$	16	22	47	53	0	0	0	0	0	1	13	16	167

	Jan	Feb	Mar	Apr	May	Jun	Jul	Aug	Sep	Oct	Nov	Dec	Total
$WS_{(mm)}$	0	0	0	0	0	41	381	317	164	0	0	0	903
$RO_{(mm)}$	13	7	3	2	1	21	201	259	212	106	53	26	903

It is clear from Table 3, that precipitation (**P**) is greater than the potential evapotranspiration (**PE**) from June to September. Precipitation above water need (PE) is stored in a soil and is brought to field capacity in the month of June itself. After the soil moisture has reached field capacity, any precipitation more than evapotranspiration is considered to be surplus and ultimately losses as runoff. Climatically, Nepal has an annual water surplus of 903 mm accumulated from June to September. October is the month when climatic water need exceeds precipitation and it failed to supply water need by 19 mm but however 18 mm is supplied by water stored in soil so that actual evapotranspiration is 84 mm which is nearly equal to potential evapotranspiration with deficit of only 1 mm. From this month onwards till the month of May, deficit occurs totaling to 167 mm.

Distribution of Water balance parameters

Actual evapotranspiration, the water that is actually lost from the vast vegetation covered area, equals potential evapotranspiration when 'P' exceeds 'PE' (Table 2) and when 'P – PE' is negative, actual evapotranspiration equals the sum of precipitation for the month plus soil moisture availability. The map (Figure 11) of the actual evapotranspiration shows that maximum values of AE are along the belt of high rainfall area and where the precipitation is less, actual evapotranspiration value is also less. This is clearly reflected over Mustang area.

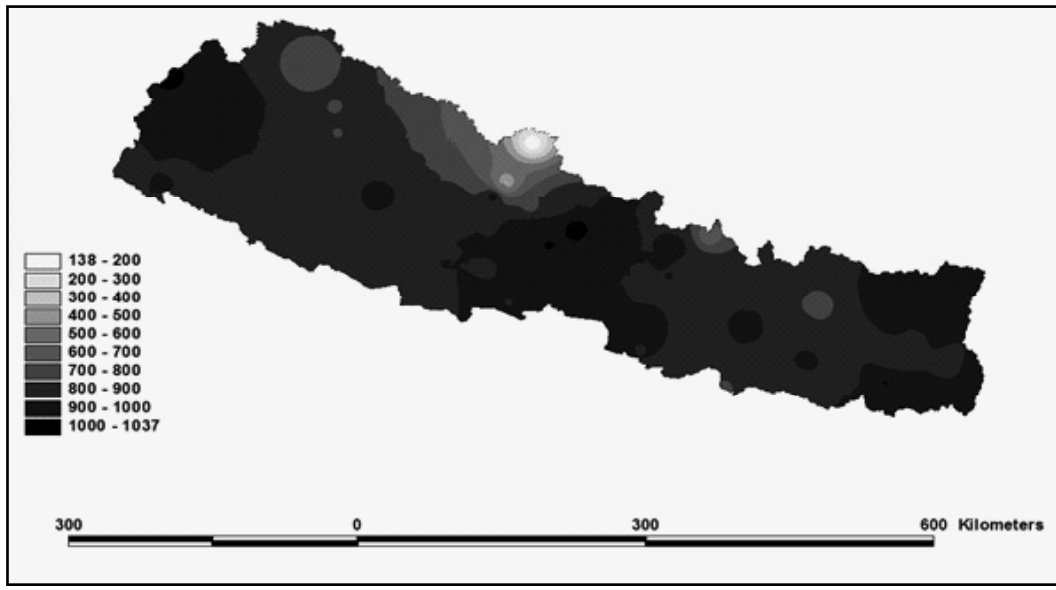

Figure 11: Spatial Distribution of Annual Actual Evapotranspiration (mm) over Nepal

Water deficiency represents the amount by which precipitation is not able to meet the demands of evapotranspiration. Its knowledge is essential in understanding feasibility of irrigation and for a definite measure of drought. Annually in Nepal, there is 167 mm water deficiency accumulated over various months. Water deficiency map (Figure 12) reveals the fact that even fairly humid regions have large water deficiency specially over the southern plains. This is due to the strong seasonal concentration of precipitation during the monsoon season (June – September) and very low rainfall during rest of the year. Large deficiency over Mustang area is obviously due to very little precipitation.

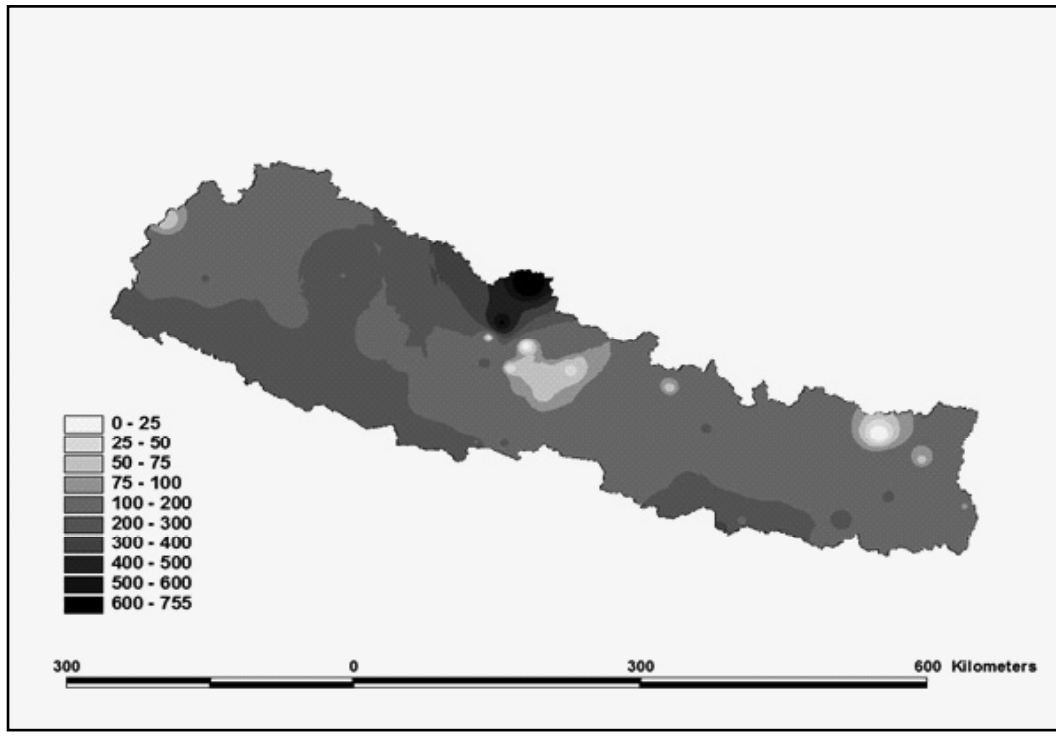

Figure 12: Spatial Distribution of Annual Water Deficit (mm) over Nepal

Distribution of annual water surplus (WS), obtained from the book-keeping procedure indicates that except over north-western Nepal, there is fairly good amount of water surplus over the whole country. Concentration of water surplus is high over the pockets of high precipitation areas. Water surplus occurs from June to September, the monsoon season. It is clear from Table 3 that a large fraction of the rainwater in the early period of the rainy season i.e. Monsoon season goes to soil and therefore less water is available for runoff.

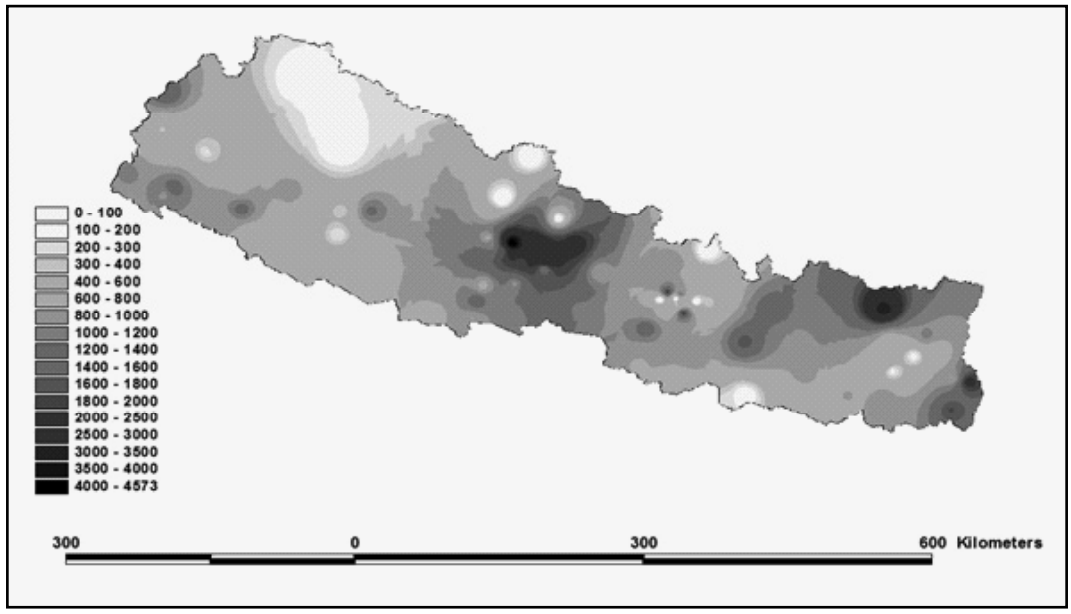

Figure 13: Spatial Distribution of Annual Water Surplus (mm) over Nepal

Climatic type

The ultimate aim of the study is to classify the climatic types of Nepal based on the moisture regions - 1955 Thornthwaite Climatic Classification is shown in Figure 14. It can be seen that in Nepal, there exist semi-arid to per-humid type of climate. Large area of the country is occupied by humid climate. Per-humid type of climate is found over the high precipitation areas. Mustang areas fit into semi-arid type of climate and extending from there towards west, sub-humid type of climate are found.

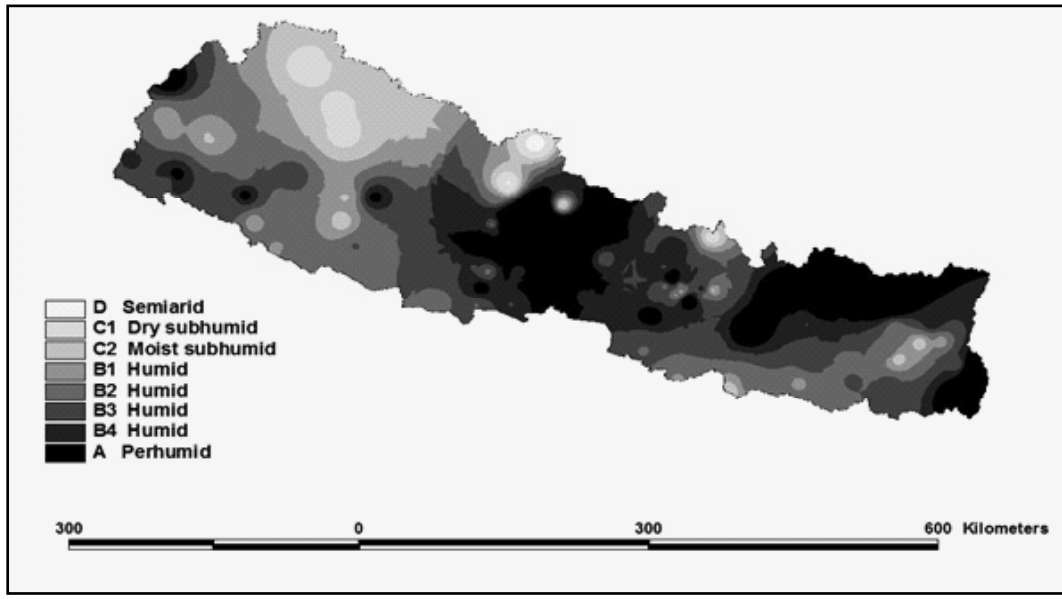

Figure 14: Spatial Distribution of Moisture (mm) over Nepal according to Thornthwaite' Classification

Conclusion

In general, Nepal has fairly good amount of water surplus accumulated mostly during the monsoon season which can be effectively used for irrigation during other seasons when water deficiency occurs.

The present study shows that Thornthwaite's water balance model captures well the different climate types or moisture regimes. Different climate type in Nepal is due to altitude. Therefore, in order to reflect its true climate type, it is important to have meteorological stations over higher elevation.

If a comparison is made between the amount of water available from precipitation and the water need, it is easy to assess the moisture condition to determine the seasonal distribution of moisture deficits or surpluses and whether a climate is dry or wet.

Acknowledgement

The author would like to thank the Department of Hydrology and Meteorology, Nepal for providing the meteorological data for the present study. The author is also grateful to Prof. Rupak Man Rajbhandari, Tribhuvan University, Nepal for his overall guidance during the preparation of this manuscript.

References

Allen, R.G., L. S. Pereira, D. Raes and M. Smith (1998) **Crop evapotranspiration - Guidelines for computing crop water requirements- FAO Irrigation and Drainage paper 56.** Food and Agriculture Organization of the United Nations.

Chalise, S. R. (1994) **Mountain environments and climate change in the Hindu Kush-Himalayas.** In: Beniston, M. (ed.), Mountain Environments in Changing Climates, 383-404.

Hagen, T. (1998) **Nepal** Himal Books, 251p

Inoue, J. (1976) **Climate of Khumbu Himal.** Seppyo, Vol. 38, Special Issue, 66-73p

Karki, R; R. Talchabhdel; J. Aalto and S.K. Baidya (2015) **New climatic classification of Nepal.** Theor Appl Climatol (published online), DOI 10.1007/s00704-015-1549-0

Lambert, L. and B. D. Chitrakar (1989) **Variation of potential evapotranspiration with elevation in Nepal.** Mountain Research and Development, Vol.9, No. 2, 145-152p

Nayava, J. L. (1974) **Climate of Nepal.** The Himalayan Review, Vol. 11, 15-20p.

Nayava, J.L. (1981) **Areal rainfall in the Kathmandu valley.** Mausam, Vol. 32, No. 4, 343-348p

Nayava, J. L. (2005) **The estimation of evapotranspiration by climate models for Western Nepal.** Journal of Hydrology and Meteorology, 2(1): 16-23.

Peel, M.C.; B. L. Finlayson; T. A. McMahon (2007) **Updated world map of the Köppen-Geiger climate classification.** Hydrol Earth Syst Sci 5: 1633–1644

R. Suresh (2005) **Watershed Hydrology**

P.W., Jack, E.D. and Paul, A.M. (2000) **Precipitation fluctuations in the Nepal Himalaya and its vicinity and relationship with some large cale climatological parameters.** Int. J. Climatol., 20, 317-327

Shrestha, M. L. (2000) **Interannual variation of summer monsoon rainfall over Nepal and its relation to Southern Oscillation index.** Meteorology and Atmospheric Physics, 75, 21-28.

Sir M MacDonald & Partners Ltd (1989) **Assistance in the establishment of design criteria and manuals for irrigation projects in Nepal.** Hydrology and Agro-meteorology manual, Department of Irrigation, Nepal.

SubbaRao and V. P. Subrahmanyam (1961) **Estimation of yields from river basins by a modification of the water balance procedure of Thornthwaite.** Indian Journal of Meteorology and Geophysics, Vol. 12, No. 2, 339-344p

Subrahmanyam, V.P.; Upadhyay, B.P. (1982) **A Study of rainfall patterns in Nepal.** In: Proceedings of the Hydrological Investigations during the last 25 years in India, India, Waltair, Andhra University, 43-50p.

Subrahmanyam, V.P. (1983) **The concept and usage of water balance in eco-climatic planning.** In: Subrahmanyam, V.P. (ed.), Applied Climatology, 13-31p

Subrahmanyam, V.P.; B. P.Upadhyay and R. M. Rajbhandari(1983)**Hydrometeorology and water balance of Karnali river basin in Nepal.** In: Proceedings of the Seminar on "Hydrology", India, Andhra Pradesh, Osmania University, 73-80p

Thornthwaite, C.W. (1931) **The climates of North America according to new classification.** Geogr Rev XXXI:633–655

Thornthwaite, W.C. (1948) **An approach toward a rational classification of climate.** Geographical Review, Vol. 38, 55-94p

Thornthwaite, W. C. and J. R. Mather (1955) **The water balance.** Publication in Climatology, Laboratory of Climatology, Drexel Institute of Technology, Vol. 8, No. 1

Upadhyay, B. P. (1984) **Water balance of Nepal with reference to water resources and agricultural development.** (Ph. D. Thesis) Department of Meteorology and Oceanography, Andhra University, India, 320p.

Climate Change Impact on Water Availability: A Case Study of West Seti, Gopaghat of Karnali Basin Using SWAT Model

Binu Maharjan[1], Tirtha Raj Adhikari[1], Laxmi Devi Maharjan[2]

[1] *Central Department of Hydrology and Meteorology*

[2] *President Chure-Terai-Madhesh Conservation Development Board*

ABSTRACT

Climate change has significant impact on important natural phenomena viz precipitation, temperature and consequently on the water supply in streams. This study was carried out for understanding and predicting the impacts of climate change on water availability and future flows in streams of West Seti River Basin using physically based hydrological model, Soil and Water Assessment Tool (SWAT). The fluctuations in Precipitation, Net Water yield (NWY) and Evapotranspiration (ET) due to climate change were also studied. For sensitivity analysis, calibration, validation and uncertainty analysis SWAT-CUP was used. Recent climate change scenario data; Representative Concentration pathways (RCP) was used in the study. Projected WRF model data was used for medium emission scenario; RCP4.5 (1996-2050). Climate change impact analysis on water balance components with future climate data shows that annual Precipitation is increasing overall in future whereas Ground water, ET and Stream flow is decreasing for RCP4.5 which is due to significant increase in surface runoff at basin level. The model efficiency 0.77 and Nash-Sutcliffe Efficiency 0.72 shows a satisfactory result with volume deviation of 4.3% between observed and simulated flow.

Keywords: *Climate Change, Water Availability, West Seti River Basin, SWAT, RCP*

1. INTRODUCTION

Climate change has become a raging global issue that has influenced almost every field. It can be considered as one of the factors, that has caused degradation of water resources in Nepal. Under the changing climate, availability and quality of water will be major issues that society will face in near future (Kundezewicz, 2007). These water challenges will be further increased by climate change, causing water scarcity globally. Climate change will contribute to increased variability of river runoff due to changes in timing and intensity of precipitation as well as melting of glaciers (Agrawala et. al, 2003). Nepal's temperature is rising faster than the global average, and rainfall is becoming unpredictable (Dhakal et. al, 2010). Globally, temperature is increasing and the amount and distribution of rainfall is being altered (Cubasch, 2001). Erratic rainfall events (i.e. higher intensity of

rains but less number of rainy days and unusual rain) with no decrease in total amount of annual precipitation have been experienced (Malla, 2008). Himalayan country like Nepal is very sensitive to Climate change and is vulnerable as they have limited means to adapt it (Gurung P. et. al, 2013). Therefore, the projection of climate is necessary in other to estimate the fluctuation in precipitation, evapotranspiration, Net Water Yield and ultimately estimate the flow of water in streams for strategic planning and management of water resources, agricultural management in upcoming days. Climate change effects on every sector, among them, water resources and hydropower ranks the highest impacted by climate change followed by agriculture (Agrawala et. al, 2003).

The overall agriculture production system in Nepal is still traditional, unmanaged and too slow to adopt new technology due to which changes in water availability during the monsoon, pre-monsoon and the post-monsoon season have a direct impact on Nepali agriculture (WECS, 2011) . The impact of climate change shows that summer crop yields will decrease and winter crop yields will increase in West Seti River basin (Gurung P. et. al, 2013).

Hydrological models help in understanding the relationship between climate and water resource by providing a conceptual framework (Xu, 1999). The reliability of hydrological models relies on the calibration process from which a best set of parameter value can be obtained for increasing the accuracy of model (A.J Jakeman, G.M Hornberger, 1993) that governs the validation of the hydrological model. This paper aims to investigate the impact of climate change on Precipitation pattern, ET, NWY, stream flow and predict future water availability in West Seti River basin with help of SWAT model, SWAT-CUP and climate change data downscaled from Weather Research Forecasting (WRF) for Representative Concentration Pathways (RCP). Representative Concentration Pathways (RCPs) (Wyane, 2013) are the latest now in use emission scenarios (Richard M. et. al, 2007). There are four: RCP8.5, RCP6, RCP4.5, and RCP2.6. "Each RCP defines a specific emissions trajectory and subsequent radiative forcing. A radiative forcing is a measure of the influence a factor has in altering the balance of incoming and outgoing energy in the Earth-atmosphere system, measured in watts per square meter" (P.B Urich. et. al, 2013). The Weather Research and Forecasting (WRF) Model is a mesoscale numerical weather prediction model designed for both atmospheric research and operational forecasting needs. (WRF, 2016)

2. STUDY AREA

West Seti River Basin lies in geographic location $80^{o}26'0E$ to $81^{o}37'0E$ and $30^{o}7'0N$ to $29^{o}5.4'0N$ and drains an area of about approximately 4300 sq. km at Gopaghat gauging station. The average altitude of West Seti is 3803m but altitudinal variation of the basin ranges from 625m – 6980m. Kali Gad, Sani Gad, Ghat Khola, Mugu Khola are few tributaries of West Seti River. West Seti falls in first group of rivers that is originated from snow covered high Himalayas and fed by snow, ice and glaciers which cover 9% of total basin area. This basin includes Bajhang, and few parts Bajura, Doti, Baitadi, and Dadeldhura which are among rural places of Nepal. The climate in the catchment ranges from alpine in the high altitude upper catchment, to warm temperate, subtropical monsoon in lower catchment.

The land use patterns of West Seti River Basin

are Agriculture, forest, barren land, snow/ glacier, agriculture land, pasture and water sources. The major soil types for the basin include Gelic Leptosols, Eutric Cambisols, Chromic Cambisols, Eutric Regosols, Glaciers, Humic Cambisols and, Gleyic Cambisols. For HRU definition multiple slope classes were chosen which were divided as class: 0 to 20 %, class2: 20 to 40 % and class3: 40 to 60% and 60% and above.

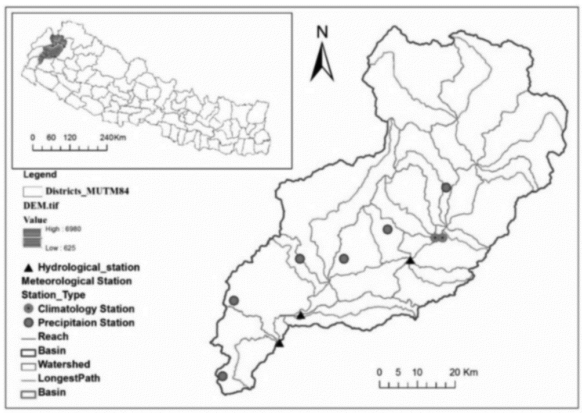

Figure 1: Location map showing Hydrological and Meteorological Station

3. METHODOLOGY

"The Soil and Water Assessment Tool (SWAT) (Arnold, 1998) , (Neitsch, 2005)is a physically based, continuous time (Lenhart T. et. al, 2002) and computationally efficient hydrological model, which uses readily available inputs". In SWAT, a watershed is discretized into multiple sub watersheds, which are then further discretized into hydrologic response units (HRUs) which is a unique combination of homogeneous land use, management, topographical, and soil characteristics exceeding a certain user-defined threshold. SWAT simulates the hydrological cycle based on the water balance equation.

$$SW_t = SW_0 + \sum_{i=1}^{t}(\sum_{i=1}^{t}(R_{day} - Q_{surf} - E_a - W_{seep} - Q_{gw}) \quad \text{..... (3.1)}$$

Where, SW_t is the final soil water content (mm), SW_0 is the initial soil water content on day i (mm), t is the time (days), R_{day} is the amount of precipitation on day i (mm), Q_{surf} is the amount of surface runoff on day i (mm), E_a is the amount of evapotranspiration on day i (mm), W_{seep} is the amount of water entering the vadose from the soil profile on day i (mm), and Q_{gw} is the amount of return flow on day i (mm).

Digital Elevation Model (DEM) taken from Shuttle Radar Topographic Mission (SRTM) 90m Digital Elevation Database v4.1 was used for automatic watershed delineation in database. Soil data of Soil Terrain digital zone (SOTER) and Land use data from International Centre for Integrated Mountain Development's (ICIMOD) geoportal were used for determination of HRUs within basin. The available Climate data (Precipitation, Temperature, Solar radiation, Wind Speed, Relative Humidity and Discharge) provided by Department of Hydrology and Meteorology (DHM) was used for calibration and validation. The calibration and uncertainty program of SWAT- CUP; SUFI2 was used in this study. **The goodness of fit of each set is determined by the value of the employed objective functions;** coefficient of determination (R^2), Nash-Suttcliffe simulation efficiency (NSE). The future climatic data; daily precipitation, maximum and minimum temperature of RCP 4.5 (from 1996 to 2050) was extracted from GRADs and then bias was corrected using Mean Correction Method. Since, "GCM outputs are related to model-related uncertainties and involve a great deal of biases" (Ahmed, 2011). However, the climate change data were used from 2020 to 2050 period of time for model input. In this study following equations were used to correct the bias in

climate change data. Equation (i) and Equation (ii) were used to de- bias daily temperature and Precipitaion data repectively.

$T_{deb} = T_{scen} - (\overline{T_{cont}} - \overline{T_{obs}})$.....i

$P_{deb} = P_{scen} \times (\frac{\overline{P_{obs}}}{\overline{P_{cont}}})$.....ii

Where. $T_{deb}T_{deb}$ and $P_{deb}P_{deb}$ are bias corrected daily temperature and precipitation respectively and $\mathbf{T_{SCEN}}$ and $\mathbf{P_{SCEN}}$ are daily temperature and precipitation obtained from downscale data (WRF). $\overline{T_{obs}}\,\overline{T_{obs}}$ and $\overline{P_{obs}}$ $\overline{P_{obs}}$ are long term monthly mean of observed temperature and precipitation respectively, while $\overline{T_{CONT}}\,\overline{T_{CONT}}$ and $\overline{P_{CONT}}\,\overline{P_{CONT}}$ are long term monthly mean of temperature and precipitation simulated using WRF for observed period.

4. RESULTS AND DISCUSSION

The temperature data from one station (Chainpur west) and precipitation data from seven stations were used in this study as shown in Figure 1. Based on the data provided by department of Hydrology and Meteorology, the total annual precipitation of West Seti River Basin is about 1980mm. The basin experiences the highest rainfall of about 530mm in month of August and lowest rainfall of only 10mm in November. The Average surface temperature of West Seti River Basin is 14.61 °C. The highest average maximum temperature is observed to be 26.16 °C in month of May while average minimum temperature is experienced in month of December which is almost 0°C. The linear temperature trend (1985-2013) suggested the increase in observed temperature with rate 0.048°C/yr. whereas observed precipitation was in decreasing trend with rate -1.43mm/yr. as shown in Figure 2. The annual average temperature trend of Chainpur_0202 west was also verified statistically using Mann Kendell's test which showed that the temperature trend in station has increasing trend of significance level 0.001 whereas precipitation didn't show any significant trend under 95% confidence level.

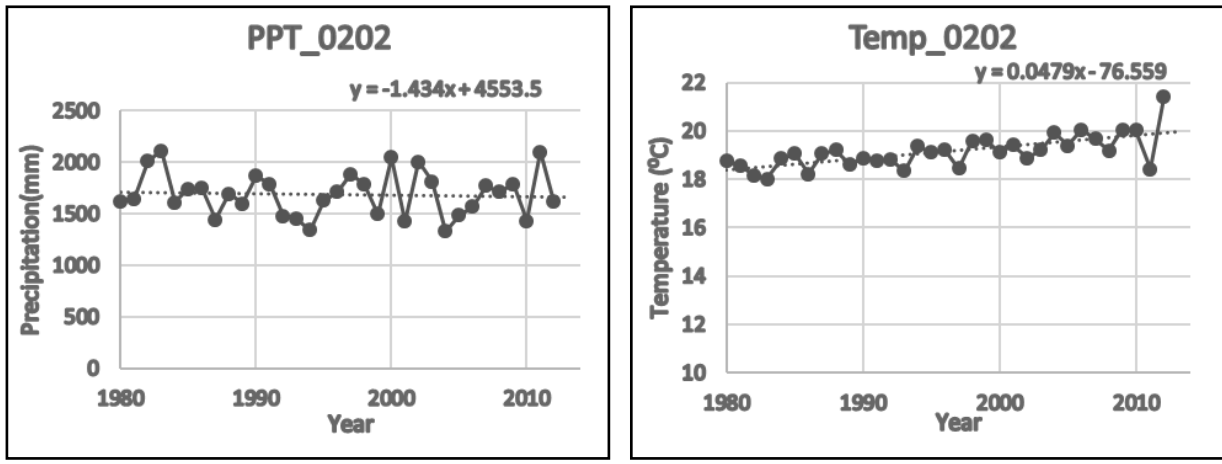

Figure 2: Annual Average Precipitation and Annual average temperature trend of Basin

Table 1: Mann Kendell's test results

Time series	First year	Last Year	n	Test S	Test Z	Significance
PPT_0202	*1981*	*2012*	*32*		-0.39	
TEMP_0202	*1981*	*2012*	*32*		4.26	***

The sensitivity analysis of 17 parameters using SUFI2 showed four parameters; CH_N2, CH_K2, ALPHA_BNK and SOL_K has the value of P-stat less than 0.05, therefore they are considered to be the most sensitive parameters, Whereas SURLAG, ESCO, EPCO, SOL_AWC, CN2 are the less sensitive parameters. The t-stat provides a measure of sensitivity (larger in absolute values are more sensitive) p-values determined the significance of the sensitivity. The value closer to 0 is more significant (Abbaspour, 2011).

Table 2: Sensitivity Analysis of parameters

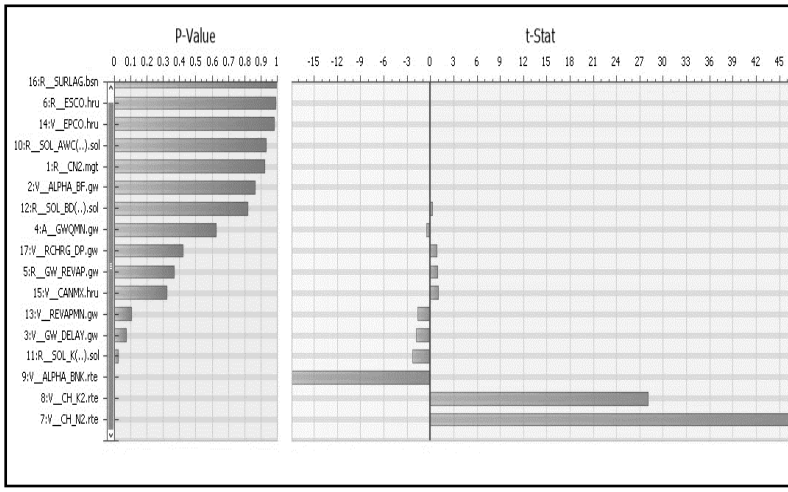

Parameter Name	t-Stat	P-Value
16:R__SURLAG.bsn	-0.001972518	0.998426560
6:R__ESCO.hru	-0.012406561	0.990103770
14:V__EPCO.hru	-0.023170565	0.981518925
10:R__SOL_AWC(..).sol	-0.087577357	0.930230454
1:R__CN2.mgt	-0.094695997	0.924575616
2:V__ALPHA_BF.gw	-0.168885624	0.865921387
12:R__SOL_BD(..).sol	0.228653292	0.819186008
4:A__GWQMN.gw	-0.487346009	0.626121918
17:V__RCHRG_DP.gw	0.806146841	0.420353360
5:R__GW_REVAP.gw	0.905746256	0.365292346
15:V__CANMX.hru	0.996211937	0.319392589
13:V__REVAPMN.gw	-1.631747131	0.103053385
3:V__GW_DELAY.gw	-1.792957977	0.073287309
11:R__SOL_K(..).sol	-2.270124428	0.023416039
9:V__ALPHA_BNK.rte	-17.867922090	0.000000000
8:V__CH_K2.rte	28.103020097	0.000000000
7:V__CH_N2.rte	46.273841063	0.000000000

The most sensitive parameters resulted from sensitivity analysis were adjust manually by hit and trail method on Daily basis. In the process of calibration, the base flow of simulated flow seemed very low. So, the base flow parameters like GWQMIN, GW_REVAP, REVAP, RCHRG_DP were adjusted. The calibration was done for 17 years of data from 1987 to 2003. The simulated flow was adjusted with reference to observed flow at outlet results the values of statistics, R^2 =0.77 and NSE= 0.72 for calibration which indicates good predictive capability of model. Validation period yielded satisfactory value of R^2 =0.61 and NSE=0.55. However, the simulated model discharge didn't match the peak flow of observed discharge at the station.

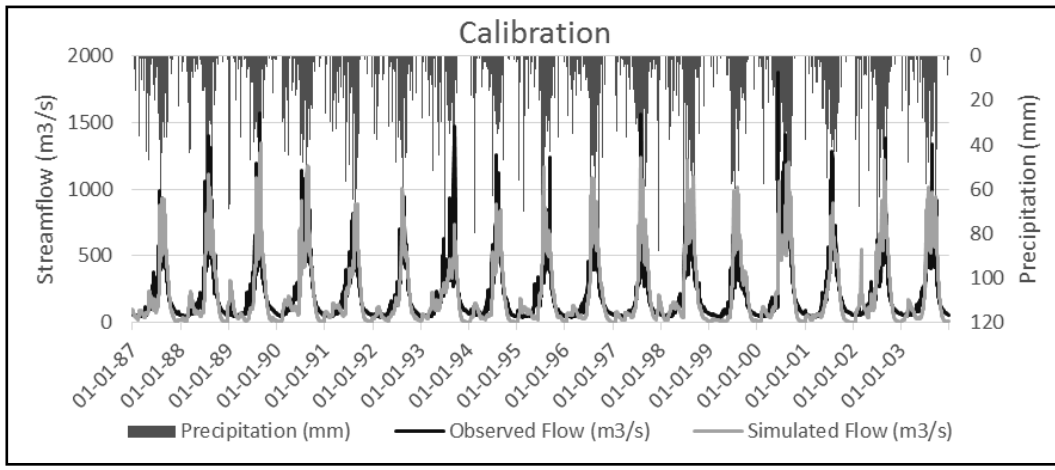

Figure 3: Observed and simulated hydrograph for calibration period with simulated rainfall

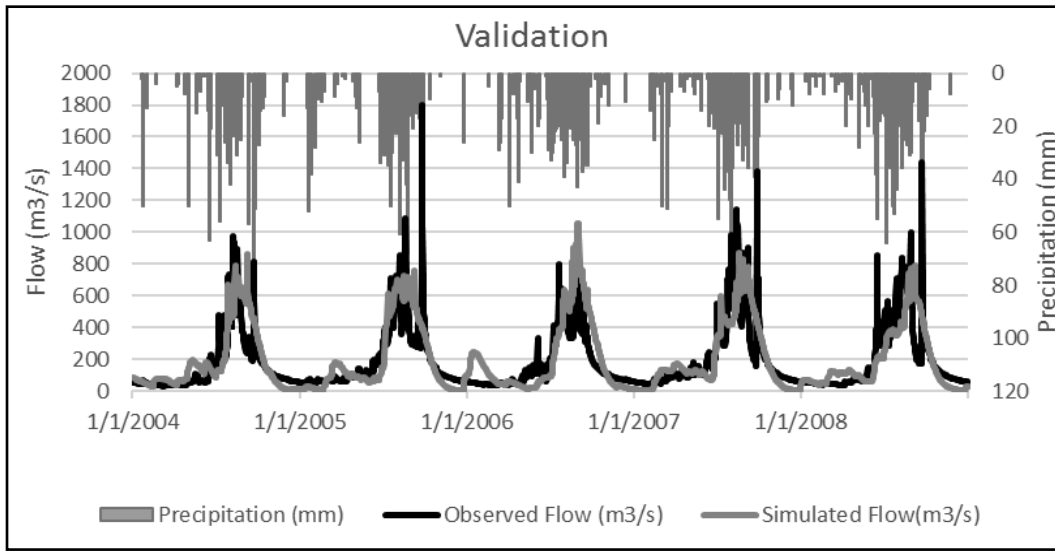

Figure 4: Observed and simulated hydrograph for Validation period with simulated rainfall

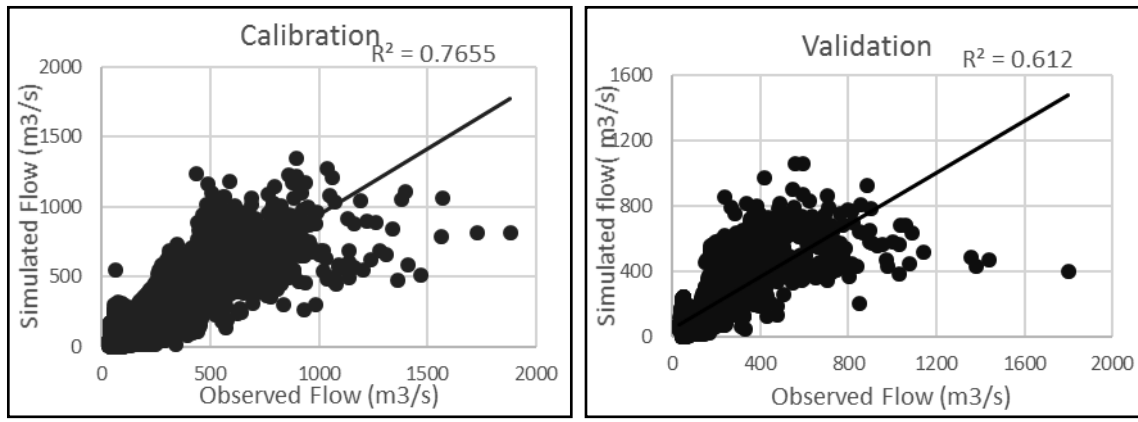

Figure 5: Value of R^2 during calibration period (1987- 2003) and Validation period (2004-2008)

Table 3: Volume deviation between observed and simulated flow

Time Period	Average annual Discharge Volume		Volume Deviation
	Observed(m3/s)	Simulated (m3/s)	
Calibration (1987-2003)	200.19	191.57	4.3 %
Validation (2004-2008)	186.20	192.54	-3.4 %

Table 4: Adjustment of parameters for flow calibration

Parameter Name	Range for parameters		Best Range for parameters		Best Fitted Value
	Lower	Upper	Lower	Upper	
CN2	35	98	36.210	49.570	47.098
ALPHA_BF	0	1	0.900	1.000	0.938
GW_DELAY	0	500	107.950	247.000	179.561
GWQMN	0	5000	1.000	5.400	4.234
GW_REVAP	0.02	0.2	0.020	0.040	0.036
ESCO	0	1	0.062	0.088	0.068
CH_N2	-0.01	0.3	0.068	0.126	0.090
CH_K2	-0.01	500	409.290	463.030	439.653
ALPHA_BNK	0	1	0.004	0.280	0.154
SOL_AWC	0	1	0.400	0.800	0.494
SOL_K	0	2000	20.900	32.110	24.767
SOL_BD	0.9	22.5	0.900	1.000	0.940
REVAPMN	0	500	408.580	472.690	452.495
EPCO	0	1	0.160	0.260	0.164
CANMX	0	100	1.390	11.950	6.089
SURLAG	0.05	24	14.620	19.040	17.648
RCHRG_DP	0	1	0.880	1.000	0.980

Bias Correction of projected Climate Data

For the study, the baseline and future climate data were downscaled by WRF which were later extracted using GRADS for climate change scenarios RCP4.5 from 1996 to 2050. The modelled baseline period is from 1996 to 2013 and simulated period is from 2020 to 2050. The observed baseline data for most of station was available from 1981-2012. There is always some degree of biases for both temperature and precipitation data from such GCMs and RCMs. The reasons for such biases include systematic model errors cause by imperfect conceptualization, discretization and spatial averaging within the grids (Teutschbein C. & Seibert J., 2012). It was found that the modelled baseline data have different trend than observed baseline data i.e. there is no effect of monsoon on June, July, August and September. Since the model simulate the future data based on baseline data, future data will have same trend as modelled baseline data which is referred as modelled bias. So, these modelled biases are necessary to be corrected. Hence, the projected climate change data was bias corrected using

mean correction method for using in model. In the Chainpur (West) station the observed data has highest rainfall in month of august followed by July which is due to pronounced effect of Monsoon. But for future projected data almost all month have similar average precipitation with little variation. The future simulated precipitations were not much diverted and after its bias correction it follows the trend of observed baseline in RCP4.5 as shown in Figure 6(ii).

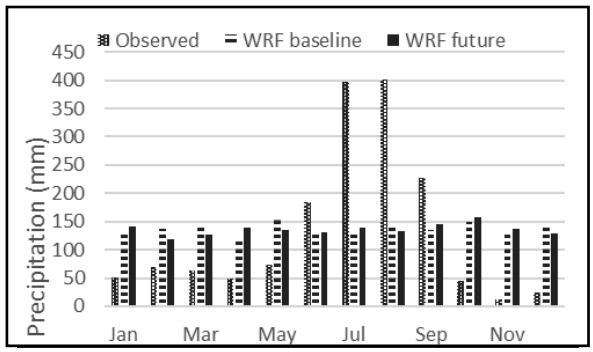

i) Before Bias Correction

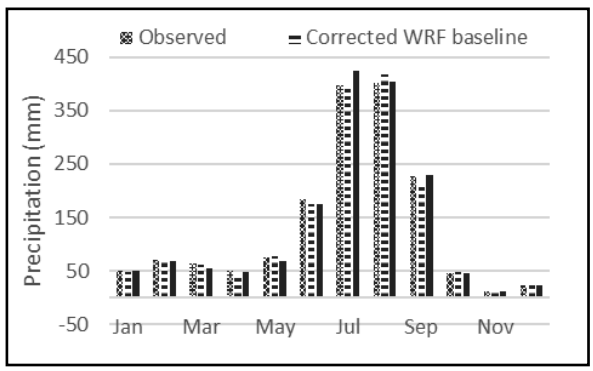

ii) After Bias Correction

Figure 6: Monthly average precipitation of Chainpur (West) for observed, baseline and projected period for RCP4.5

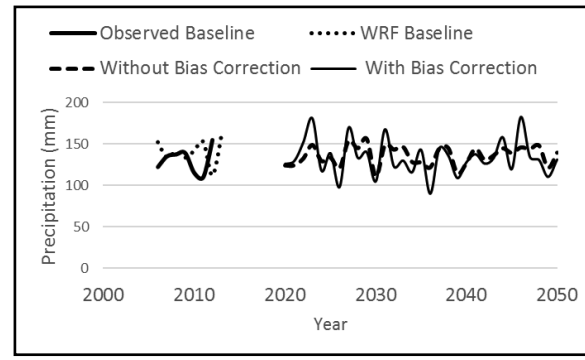

Figure 7: Bias correction of projected precipitation for Chainpur (West) of RCP4.5

The monthly average maximum temperature for WRF baseline and WRF future is very low in every month compared to observed station data. The future climate data is then bias corrected and which showed result as in graph (Figure 8). Now the bias corrected WRF baseline and WRF future data shows similar trend to observed data. The projected annual maximum temperature shows lesser values than that observed at the station. After the modelled bias was reduced, its trend was shown quite like observed baseline trends as in Figure 9.

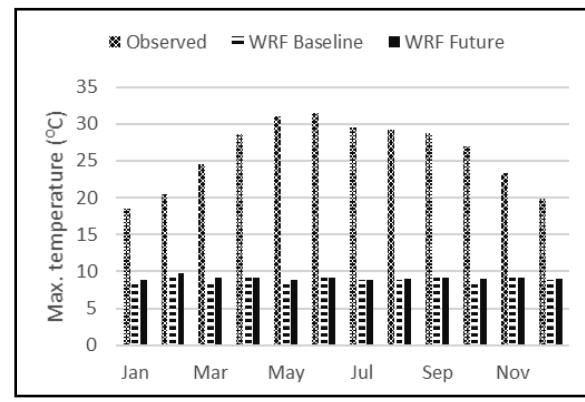

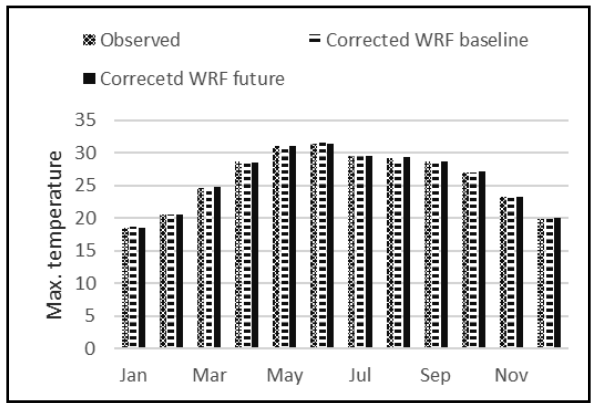

Figure 8: Monthly average Max. temperature of Chainpur(west) for observed, baseline and projected period RCP4.5

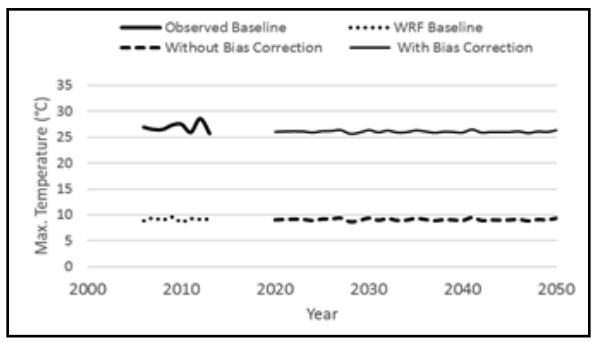

Figure 9: Bias correction of projected Maximum Temperature of Chainpur (West) for RCP4.5

The monthly average minimum temperature is negative in almost every month for the scenario whereas the monthly average observed station data didn't show any negative values. Therefore, the downscaled data were bias corrected using mean correction method which yielded the graph in Figure 10. The projected annual minimum temperature for baseline period is very low than observed baseline for RCP4.5. Hence bias correction was done for future projection data, which gave model usable data as shown in Figure 11.

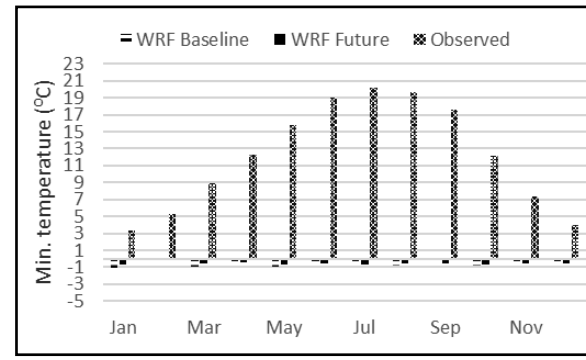

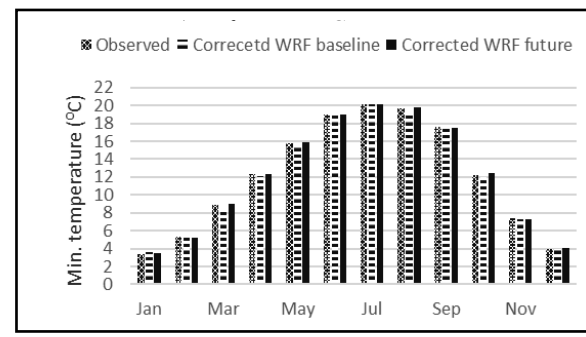

ii) After Bias Correction

Figure 10: Monthly average Minimum temperature of Chainpur (West) for observed, baseline and projected period RCP4.5

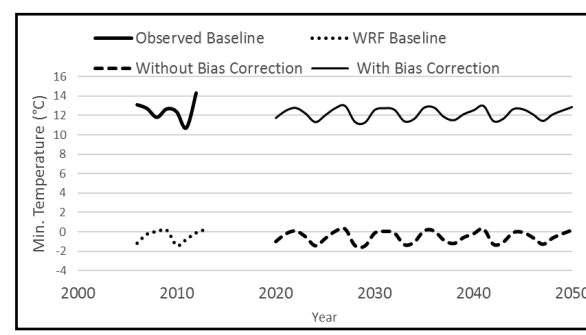

Figure 11: Bias correction of projected Minimum Temperature of Chainpur (West) for RCP4.5

Water Balance of Basin and impact of climate Change for RCP4.5

The water balance condition of the basin is presented considering the most essential water balance component such as precipitation, surface runoff and evapotranspiration, Ground

water, from the model output. Table 5 shows the average monthly water balance values for major water balance component. The component with the positive sign is input (rainfall) to the system whereas component with negative sign is output from the system and storage change. Considering the average of monthly for 24 years rainfall, ET and NWY, 48% is estimated to be lost from the system as evapotranspiration and around 51% of the rainfall goes to the drainage of the basin as Surface runoff, Groundwater, storage and transmission loss.

Table 5: Monthly water balance within the basin

Month	Precipitation (mm)	Evapotranspiration (mm)	Water Yield (mm)	Balance closure
Jan	46.48	20.85	17.39	8.23
Feb	64.23	32.86	23.32	8.05
Mar	59.96	46.46	23.34	-9.84
Apr	48.76	45.36	16.42	-13.02
May	92.09	61.96	30.30	-0.17
Jun	225.24	99.81	92.67	32.75
Jul	470.62	145.89	251.11	73.62
Aug	447.92	149.91	271.06	26.95
Sep	241.14	137.99	141.85	-38.70
Oct	33.03	69.12	20.80	-56.89
Nov	9.34	26.81	6.09	-23.57
Dec	21.80	14.80	9.67	-2.67
Total	1760.60	851.82	904.02	4.75
Percentage		48.38%	51.35%	0.27%

The water balance of the basin represented by Precipitation, ET, Surface runoff, streamflow, Storage for observed station data and downscaled RCP4.5 data is shown in Table 6. It shows that the Precipitation will increase (0.23%) and Groundwater Flow will decrease (-8.49%) due to land use change in the study area. Similarly, the surface runoff will increase (51.6%) for RCP4.5 may be due to deforestation which causes decrease in ET (2.73%) as well. With possible increase in demand for water use in the basin, model output also demonstrates increase in water yield (33.4%) as depicted in the table 6.

Table 6: Changes in Water balance of basin for RCP4.5

Parameters	WTR_BLC_OBS	WTR_BLC_4.5	Increase or decrease %
Precipitation (mm)	1760.60	1764.64	0.23
Evapotranspiration (mm)	851.82	828.59	-2.73
Surface Runoff (mm)	180.86	274.24	51.63
Groundwater Flow (mm)	29.37	26.88	-8.49
Water yield (mm)	698.54	931.71	33.38

Annual distribution of Precipitation, Evapotranspiration and Net Water Yield and impact of climate change

The distribution of three components Precipitation, ET, and NWY is shown in Figure 12(a, b & c). The middle part of the basin gets more rain than the high mountain region where as the lowest part of basin gets comparatively less amount of rain. The annual average evapotranspiration is also higher in middle part of basin where most of land use is covered by agriculture and forests. The net water yield is related to precipitation and shows the distribution according to rainfall distribution in the sub-basins.

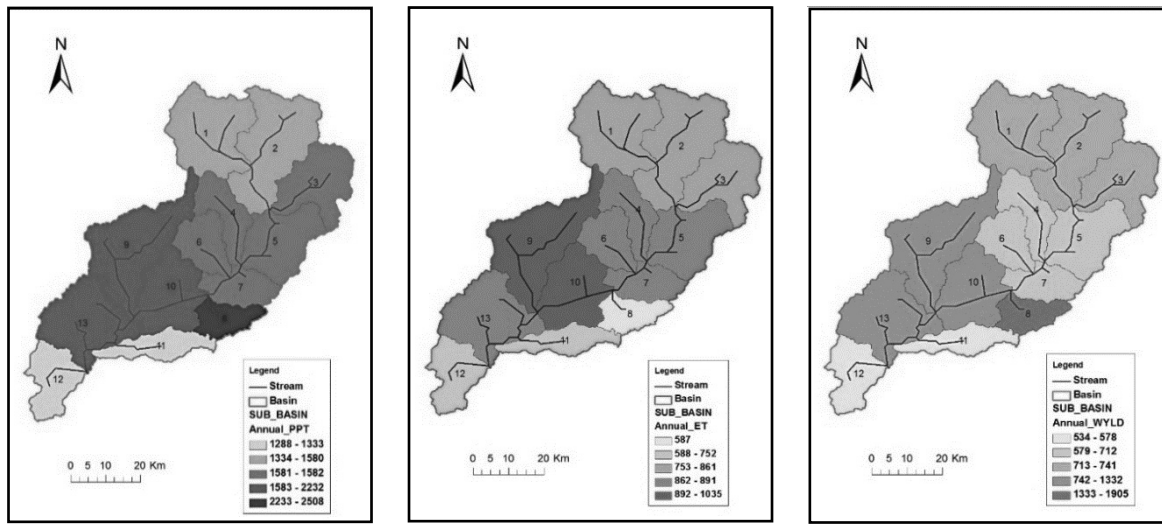

a) *b)* *c)*

Figure 12: Annual distribution of Precipitation, Evapotranspiration and Net Water Yield

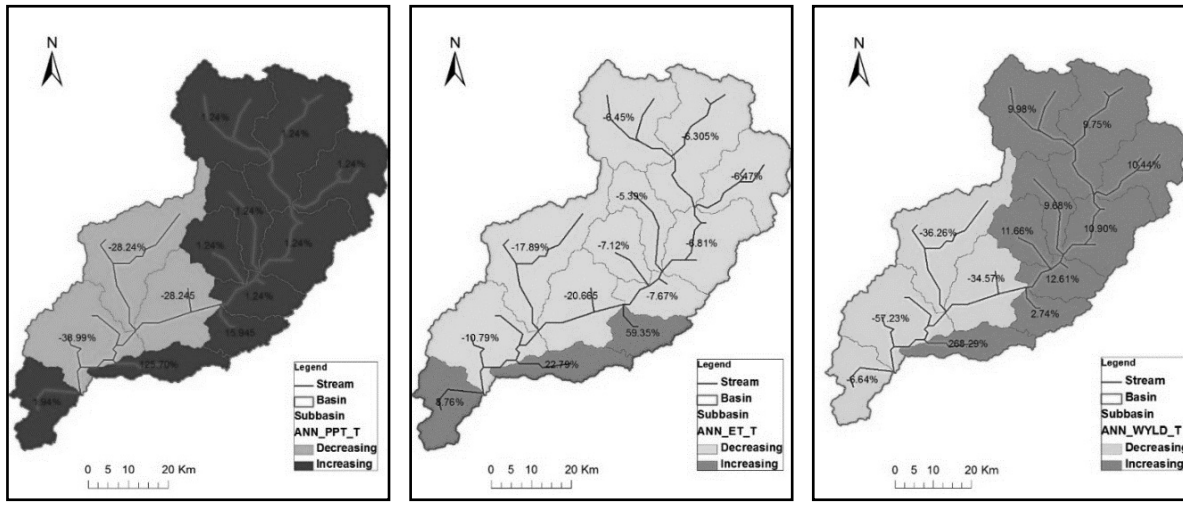

Figure 13: Impact of Climate Change Annual Change in Precipitation, Evapotranspiration and Net Water Yield for RCP4.5

The annual changes in precipitation, evapotranspiration and net water yield were analysed from Baseline to projected data (Figure 13). The annual results for basin from RCP 4.5 indicate that the average annual change in rainfall ranges from -36% to 125%. There will be increase in rainfall in upper Himalayas and decrease in middle part of basin. ET change is ranging from -20% to 60% and -57% to 268% change in NYW. Decrease in ET in middle part of basin where agriculture and forest is major land use type may be due to deforestation for development or human settlement.

The future flow simulated by SWAT model showed some year with increasing peak discharge for both emission scenarios. The annual observed and projected discharge of RCP4.5 shows a decreasing trend of -0.76 m^3/s/ year (Figure 14) and -0.80m^3/s/year respectively. The statistical verification of trend analysis for simulated streamflow using Mann Kendell's test didn't show any significance under 95% confidence level.

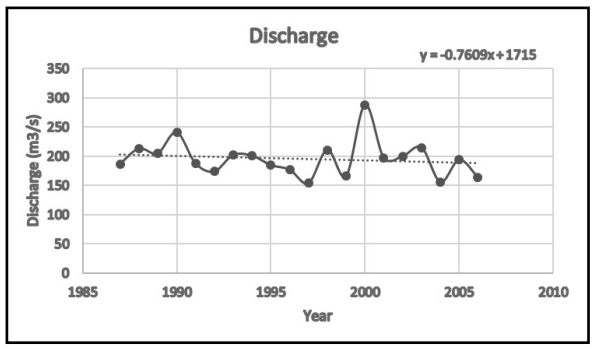

Figure 14: Annual Observed Streamflow in West Seti Basin (1987-2006)

5. Conclusion

The observed precipitation is decreasing but projected precipitation is increasing whereas both observed and projected temperature is increasing. The ET in the basin is decreasing compared to observed ET due to change in land use of basin. The observed and projected discharge in West Seti basin shows decreasing trend. There is significant increase in projected water yield in basin with respect to observed NWY probably because of excessive water use causing water deficit in water balance in most of the months.

Acknowledgement

I am thankful to Department of Hydrology and Meteorology, Government of Nepal for providing Hydrological and Meteorological data. In addition, my thanks go to International Centre for Integrated Mountain Development (ICIMOD) for land use data and Bjerknes Center for Climate Research (BCCR), University of Bergern, Norway for WRF projected data.

References

A.J Jakeman, G.M Hornberger. (1993). How much complexity is warranted in a rainfallrunoff? Water Resource Research vol.29(8). 2637-2649.

Abbaspour, K. C. (2011). *SWAT-CUP4, SWATCalibration and Uncertainty Programs- a user manual.* Swiss Federal Institute of Aquatic Science and Technology, Eawag.

Agrawala S., V. Raksakulthai, M. Aalst, P. Larsen, J. Smith, J. Reynolds. (2003). *Development and Climate Change in Nepal: Focus on Water Resources and Hydropower. Paris: Organization for Economic Co-operation and Development.*

Ahmed, K. F. (2011). Bias Correction and Downscaling of Climate Model Outputs Required for Impact Assessments of Climate Change in the U.S. Northeast.

Arnold, J. G. (1998). *Large area hydrologic modeling and assessment: Part I.* Model development. J. American Water Resource. Association. 34(1).

Claudia Teutschbein, Jan Seibert. (2012). Bias correction of regional climate model simulations for hydrologicalclimate-change impact studies: Review and evaluation of different methods. Journal of Hydrology. 12-29.

Cubasch, U. M. (2001). *Projections of future climate change. Climate change 2001: The Scientific Basis. Contribution of Working Group I to the Third Assessment Report of the Intergovernmental Panel on Climate Change.* (Eds.), Houghton, J.T., Ding, Y., Gri.

Dhakal, K., Silwal, S., & Khanal, G. . (2010). *Assessment of Climate Change Impacts on Water Resources.* . Kathmandu: Ministry of Environment/ Government of Nepal.

Gurung P., Bharati L., Karki S. (2013). Application of SWAT model to assess Climate Change on Water Balances and Crop Yields in West Seti River Basin. *SWAT Conference.* France.

Kundezewicz, Z. M. (2007). *Freshwater resources and their managent. Climate Change 2007: Impacts, Adaptation and Vulnerability. Contribution of Working Group I.* IPCC.

Lenhart, T., Eckhardt, K., Fohrer,N., Frede, H.G. (2002). Comparison of two different approaches of sensitivity analysis. Physics and Chemistry of the Earth . Elsevier Science Ltd.

Malla, G. (2008). *Climate Change and its Impact on nepalese Agriculture, The IPCC's fifth assessment report; What's in it for South Asia? Executive Summary.* IPCC.

Neitsch, S. A. (2005). . *Soil and Water Assessment Tool-TheoreticaDocumentation-Version 2005.* Texas: Grassland: Soil and Water Research Laboratory, Agricultural Research Service and Blackland Research Center,Texas Agriculture Experiment Station.

P.B Urich, P. Kouwenhoven, Y. Li. (2013). *The IPCC Fifth Assessment Report in Context: Implications for End Users in the Transition from AR5.* New Zealand: CLIMsystems Ltd.

Richard, M., Mustafa, B., Sander, B., Eduardo, C., Tim, C., Jae, E., ... & Roger, J. (2007). *Towards new Scenarios for Analysis of Emissions, Climate Change, Imapcts and Response Strategies, Technical Summary.* Geneva: IPCC.

WECS. (2011). *Water resources of Nepal in the context of Climate Change. Kathmandu: Waer and Energy Commission Secretariat.* Government of Nepal.

WRF. (2016). *The Weather Research & Forecasting Model*. Retrieved 7 3, 2016, from http://www.wrf-model.org/index.php

Wyane, G. (2013). *A guide to the IPCC's new RCP emissions pathways*. Retrieved 7 6, 2016, from The Guardian: http://www.theguardian. com/environment/climate-consensus-97-percent/2013/aug/30/climate-change-rcp-handy-summary

Xu, C.-y. (1999). From GCMs to river flow:A review of Downscaling Methods and Hydrological Modelling Approaches. *Progress in Physical Geography 23,2*, 229–249.

Recent Evolution of Glacial Lakes in Sagarmatha National Park, Nepal

Sudeep Thakuri[*1,2] and Franco Salerno[2]

[1] *Department of Earth Sciences "Ardito Desio", University of Milan, Milan, Italy and*

[2] *National Research Council, Water Research Institute, 20861 Brugherio, Italy*

[*] *Corresponding author: Sudeep Thakuri, E-mail: sthakuri@hotmail.com*

ABSTRACT

High altitude ecosystems are especially considered vulnerable to changing environments. Glacial lake evolution and their surface area variation are highly visible and easily measurable signal of the impact of climate change in such ecosystems. In this paper, evolution of glacial lakes is examined using the satellite imagery and topographic maps between 1963 and 2013 in the Sagarmatha (Mt. Everest) National Park (SNP), Nepal. Three types of glacial lakes (supra, pro, and unconnected) are present in the SNP that have their distinctive characteristics to explain the glaciological and climatic conditions. During the study period (1960s–2013), both number and surface area of supraglacial lakes has continuously increased (number +109.7%; area +13.3%) with an accelerated rate in the last decade. Proglacial lakes are more or less constant in both numbers and size, except Imja Lake that have exceptionally increased, while the surface area of unconnected lakes has increased from 1960s–1990s (+4.3%) and decreased from early 1990s afterward (-10.9%). Supraglacial lakes behaviour confirms the acceleration of the negative mass balance of glaciers due to the reduced ice velocities caused by decreased precipitation. The unconnected lakes are evaluated as a useful indicator of precipitation trend. The decrease in the precipitation is not only impacting to lakes, but also significantly impacting to the glaciers in the Himalaya. The paper underlines a clear need to extend this analysis at broader areas to gain regional perspective.

Keywords: *Glacial lakes, Temporal Change, Satellite data, Sagarmatha, Indicator.*

1. INTRODUCTION

Studies of abundance, size distribution, and changes of glacial lakes play a significant role in assessing the glacier and snow melt, biogeochemical cycles, and ongoing climate change (Shijin and Zhang, 2014). Three types of glacial lakes can be distinguished, according to Ageta et al. (2000), in Mt. Everest region. They are *(a) Supraglacial lakes,* which develop on the surface of the glacier, *(b) Proglacial lakes,* which are moraine-dammed lakes and are in contact with glacier front, and *(c) Unconnected glacial lakes,* which are not directly connected with glaciers, but may have a glacier located in their basin (Figure 1). Gardelle et al. (2011), considering supraglacial and proglacial lakes, noted that the southern side of Mt. Everest is the region that is most characterized by glacial lakes

in the Himalaya. Glacial lakes are considered as a suitable indicator for evaluating the impact of climate change at high elevation (Richardson and Reynolds, 2000; Benn et al., 2001).

After the first pioneering work by Löffler (1969) in the 1960s, other studies focused on these lake environments only after the late 1980s. The research activities were initially addressed on the hydro-geochemical characterization of the lakes over a wide spatial extent (Tartari et al., 1998; Bortolami, 1998; Smiraglia, 1998). In seven expeditions conducted between 1989 and 1997, 48 lakes were visited (Tartari et al., 1998), leading to the identification of many temporary water bodies. Tartari et al. (2008) provided a complete review of the limnological studies carried out in Mt. Everest region.

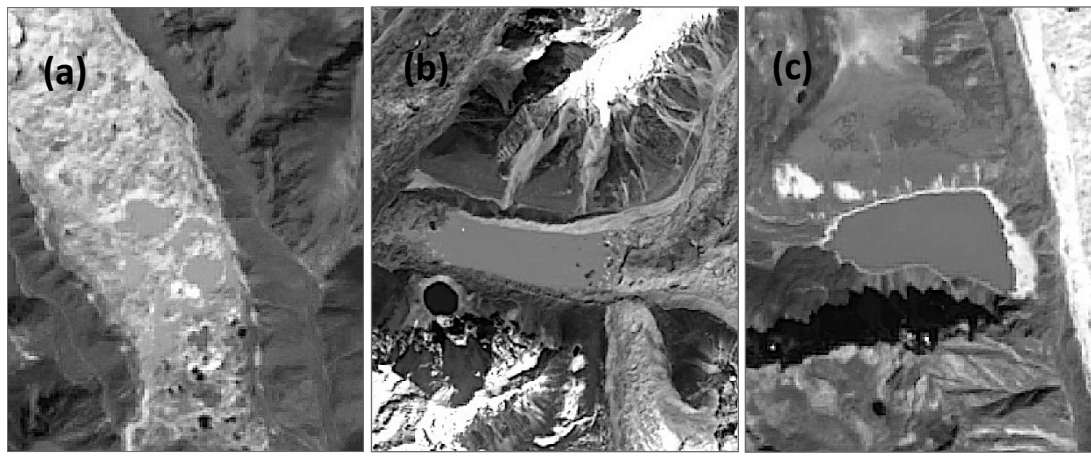

Figure1: Three types of glacial lakes: (a) Supraglacial, (b) Proglacial, and (c) Unconnected lakes, in the Sagarmatha National Park (SNP), as seen from Landsat 8 OLI image of 10 October 2013.

A first cartographic study was carried out to compile a lake cadastre using the Mount Everest map (scale 1:50,000), published by National Geographic Society, Washington D.C. (1988), which represented the lakes morphology of the Northeastern sector of the SNP in December 1984 (Tartari et al., 1998). This initial cadastre was after 10 years integrated for the same territory with the Official Nepali map (scale 1:50,000; Survey Department of His Majesty's Government of Nepal, 1997) dated December 1992 (Tartari et al., 2008). Including this study of Tartari et al. (2008), some other studies revealed that areas of proglacial lakes increased on the south slopes of Mt. Everest (central Himalaya) since the early 1960s (Tartari et al., 2008; Bolch et al., 2008; Bajracharya and Mool, 2009; Gardelle et al., 2011). Gardelle et al. (2011) found that strong increasing of lake surface area in this region (33% in 1990 to 2009). Salerno et al. (2012) demonstrated that the slope of the glacier where lakes are located influence the supraglacial lake formation. Further, the slope of upstream glacier favours the formation of the supraglacial lakes as a boundary condition. The formation of proglacial lakes is related to the growing and coalescing of the supraglacial lakes.

Studies have indicated that the current moraine-dammed or ice-dammed lakes are the consequences of coalesce and the growth of supraglacial lakes (Sakai et al., 2000; Fujita et al., 2009; Watanabe et al., 2009; Thompson

et al., 2012). These growths of lakes pose a potential threat of the Glacial Lake Outburst Floods, GLOFs (Reynolds, 2000; Richardson and Reynolds, 2000; Benn et al., 2012) with the potential consequent loss of human life and property in the downstream valley. One of such proglacial lakes in Mt. Everest region, Imja Tsho (lake; hereafter referred as 'Imja Lake'), that evolved and in the continuing growth since the early 1960s, has been of great research interest due to its potential GLOF risk (Thakuri et al., 2016). Considering these issues, in this study, the evolutions of three types of glacial lakes are examined for the last 50 years based on the satellite data and available topographic maps.

2. STUDY SITE

This study was conducted in the Sagarmatha (Mt. Everest) National Park (SNP) in the southern slope of Mt Everest (Figure 2). The SNP includes an area of 1,148 km² covering lower alpine forest areas to upper grassland and nival zone that extends from 2,845 (at Jorsale) to 8,848 m asl, the Sagarmatha (Mt. Everest)-top of the world. The buffer zone covers an area of 275 sq. km lying just outside the southern part of the park.

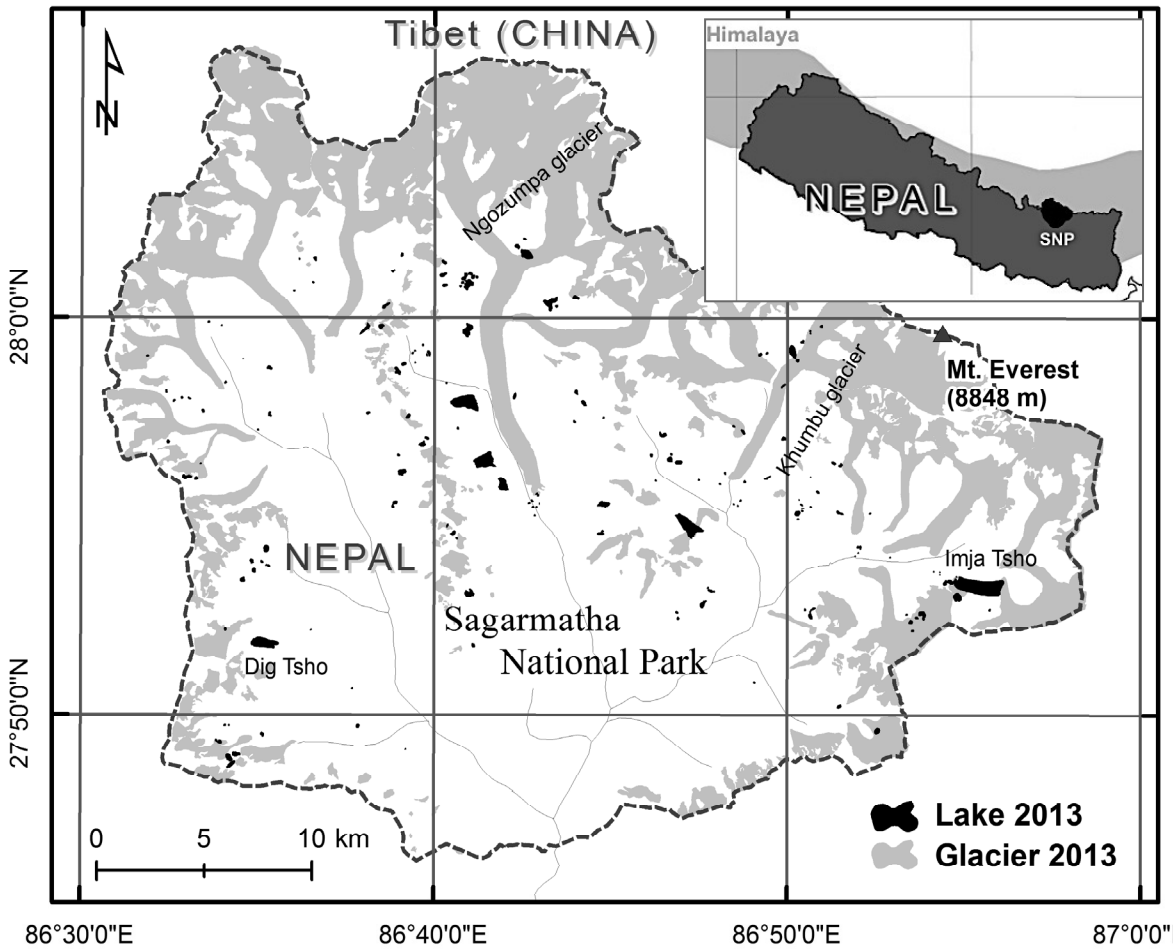

Figure 2: Map of the Sagarmatha National Park (SNP) indicating the lakes and glaciers in 2013.

3. DATA AND METHODS

The satellite imagery from different sensors from the 1960s to 2013 (Table 1) and a topographic map of Indian Survey 1963 (scale 1:50000) were used in this study. Using these data, it was possible to analyze the temporal evolution of supraglacial, proglacial, and unconnected lakes between 1960s and 2013. The satellite imagery of 1962 was a panchromatic image and thus, was not very promising data for all the glacial lakes inventory, but instead, was used to validate the lakes inventory from the topographic map of 1963. For this reason, the year 1963 was considered as the reference year. The ASTER GDEM ver. 2, a product of the Ministry of Economy, Trade, and Industry of Japan and the NASA, was used for extracting morphometric information on lakes parameters.

Table 1: Satellite data used in this study.

Acquisition date	Mission/Sensor	Resolution (m)	Scene ID
15 Dec, 1962	Corona KH-4	~8	DS009050054DA175_175
17 Nov, 1992	Landsat 5 TM	30	LT51400411992322ISP00
30 Oct, 2000	Landsat 7 ETM+	15*	LE71400412000304SGS00
24 Oct, 2008	ALOS AVNIR 2	10	ALAV2A14647304
10 Oct, 2013	Landsat 8 OLI	15*	LC81400412013283LGN00

** Pan-sharpened images*

The mapping of glacial lakes was conducted with both manual and semi-automatic methods. In the semi-automatic method, to extract the lake outlines from the Landsat imagery, blue (0.45–0.52 μm) and near-infrared (NIR; 0.77–0.90 μm) wavelength bands were used to calculate a normalized difference water index (NDWI): NDWI = [NIR – blue]/[NIR + blue]. The method, originally proposed by McFeeters (1996) and successfully adapted to our region by Bolch et al. (2008), Thakuri et al. (2016), was applied using a manual post-correction. The manual post-correction involved adjustment of the lake outlines by visual inspection of the objects in the satellite imagery. This step was useful for correcting the outlines affected by shadows and ice areas.

Furthermore, the outlines of lake basins were extracted using Spatial Analyst Hydrology tools in ArcGIS (Wu et al., 2008). The morphometric characteristics (e.g., elevation) and surface areas were computed for the mapped lakes. In each analysis, a particular emphasize was provided for introducing the uncertainties of the measurements.

4. RESULTS AND DISCUSSION

Overall, the surface area of glacial lakes in the SNP has increased by 1.742 km^2 (28.9%) from a total area of 6.047 km^2 in 1963 to 7.789 km^2 in 2011 (Table 2). Moreover, the numbers of lake have increased from 337 to 626 (by 86%). The new lakes have appeared at higher elevations (~42 m higher than the lakes in the 1960s) following the glaciers retreat.

Table 2: Lake statisticsin the 1963–2011 period.

Lake type	Surface area (km^2)						
	1963	*1992*	*2000*	*2008*	*2011*	*2013*	*Uncertainty*
Supraglacial	1.373	1.344	1.338	1.522	1.555	-	±45%
Proglacial	0.305	1.882	1.448	1.766	2.043	2.132	±7%
Unconnected	4.394	4.153	4.542	4.278	4.131	4.012	±14%
Total	6.047	7.378	7.328	7.566	7.789	-	±18%

4.1 Supraglacial Lake

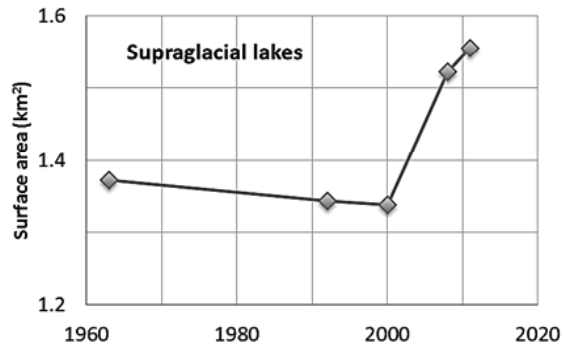

Figure3: Temporal surface area change of supraglacial lakes in the Sagarmatha National Park (SNP from 1963 to 2011.

The debris-covered ablation part of glaciers in the Mt. Everest region holds many supraglacial lakes. Such lakes are very small in size, but numerous. Both numbers and surface areas of supraglacial lakes have increased (109.7% and 13.3%, respectively) in the SNP during the 1960s to 2011 (Table 1; Figure 3). Due to their very small sizes, the associated uncertainties are large (±45%). Such supraglacial lakes are ephemeral and very unstable in space and time as they can suddenly drain through sub-glacial drainage system (Benn et al., 2001). However, total surface area of the lakes was more or less stationary until 2000, but increased rapidly after.

Figure4: An example of glacier mass loss: Supra-glacier lake in Lobuje Glacier. (a) July 2012 and (b) September 2014, indicating substantial mass loss of debris-covered ice (Photo: Sudeep Thakuri).

The increasing of the lakes in the last decades can be associated to the glacier flow velocities decrease caused by reduced precipitation and increased ablation of glacier ice (Thakuri et al., 2016). The reduced precipitation induces and increased ablation of the glacier ice which lowers ice velocities and trigger evolution of such lakes. Furthermore, as a feedback, evolutions of the

supraglacial lakes on the surface make glacier susceptible to enhanced mass loss (Figure 4). Glaciers are extensively losing mass in last few years, particularly those glacier which have lakes on their surface. The evolutions of lakes on surface of glaciers are increasing the loss of glaciers ice mass, primarily by ice calving.

4.2 Proglacial Lake

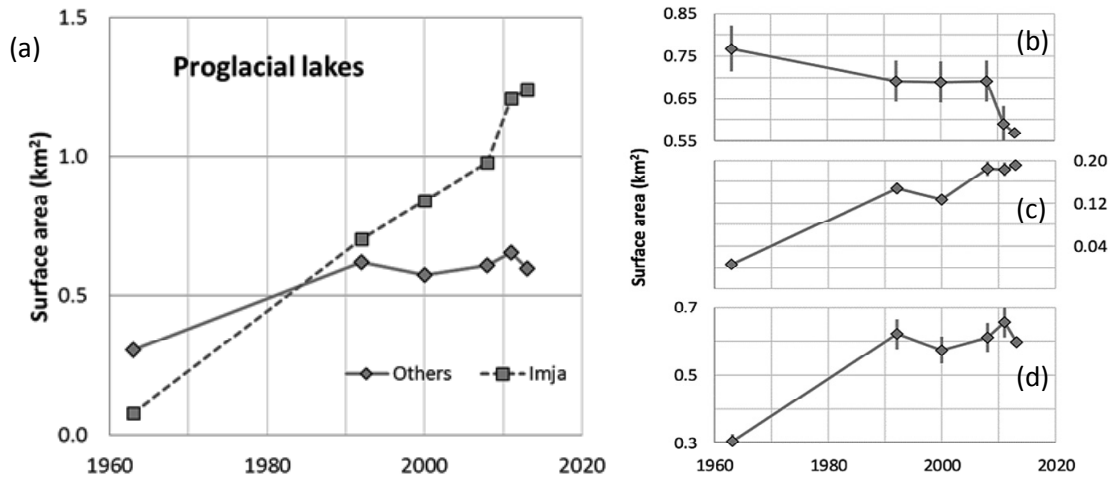

Figure5: Temporal trends of proglacial lakes in the SNP from 1963 to 2013. (a) A comparison between Imja Lake and other proglacial lakes for their surface area change. Surface area change for (b) the lakes that were proglacial before 2000s and no more proglacial now, (c) recent new proglacial lakes those were not present in past, and (d) the lakes that remained always proglacial lake.

The surface area of the proglacial lakes has remained quite stationary more so after 1992, except Imja Lake (Figure 5a). For a group of lakes that were proglacial in the past (before 1990s) and became unconnected lakes recently, it is observed that their surface area have decreased continuously (Figure 5b). The lakes that appeared as proglacial lakes recently have increased in their surface area (Figure 5c). Small number of lakes were becoming unconnected (leaving the glacier) and a similar number of small lakes became the proglacial lake, without changing total surface area. Just four proglacial lakes (except Imja Lake) continued to be proglacial lakes, independently to the glacial they belong, in the last 50 years. They increased in the first period (1963–1992) and then, remain constant (Figure 5d).

Imja Lake was the only Proglacial Lake that has increased continuously from 0.029 ± 0.010 km2 in 1963 to 1.352 ± 0.054 km2 in 2013. No significant changes in the surface areas for other proglacial lakes were found. As a case study on Imja Lake, Thakuri et al. (2016) demonstrated that the continuous increase of the lake is associated with decrease of flow velocities of Imja Glacier and increased elevation of zero degree isotherms of maximum temperature. Flow velocities of Imja Glacier have significantly decreased from 1992 to 2013 (Thakuri et al., 2016), particularly in the upper debris-covered ablation part of the glaciers.

4.3 Unconnected Lake

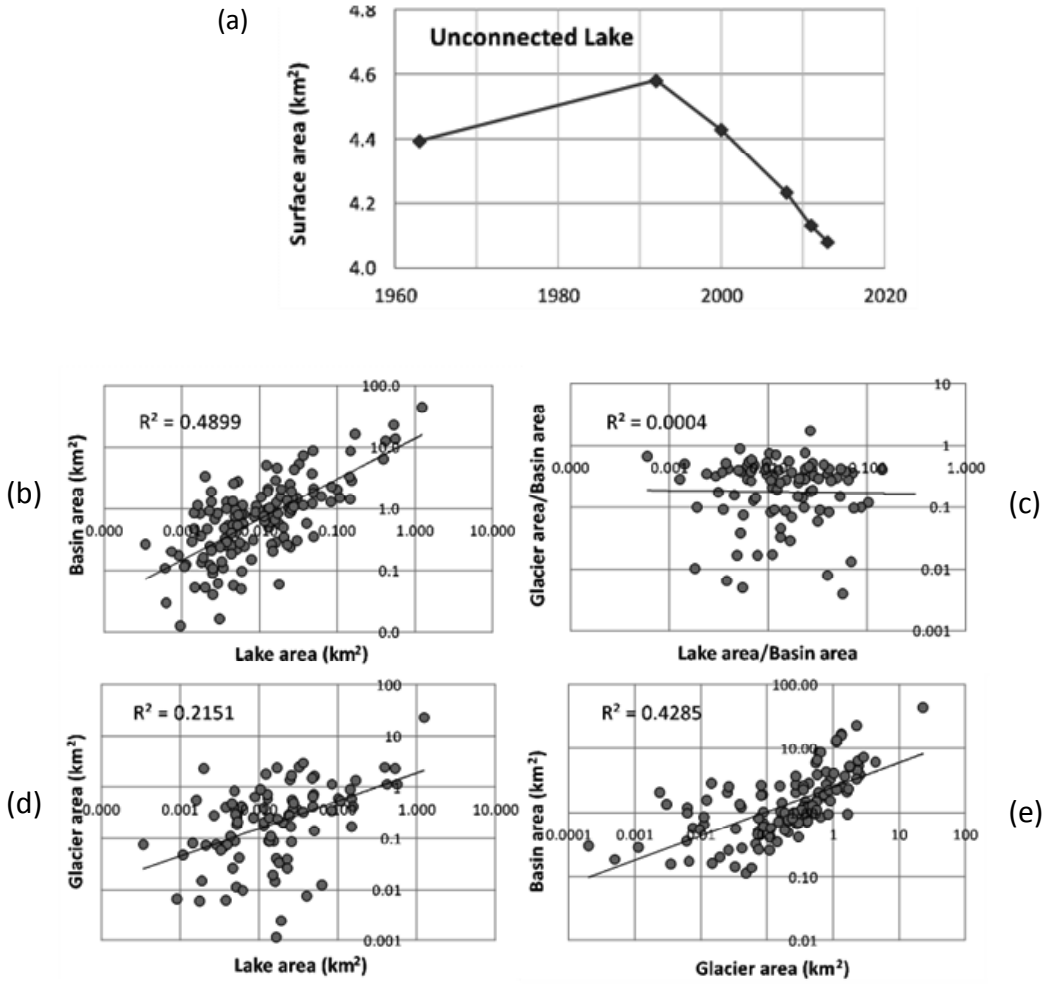

Figure6: Unconnected lakes. (a) Temporal trend of average surface area in 1963–2013 period; (b–e) Relationships between lake surface area, their basin surface area, and glacier area in the basin, indicating that Unconnected lake act as an indicator of precipitation trend at high-altitude.

The surface area of unconnected lakes has increased from 1960s to 1990s (4.3%) and decreased (10.9%) of the surface area from 1990s to 2013 (Table 2; Figure 6a) with an overall decreasing by 7.2% (from 4.395 to 4.080 km2). This observation is in line with slightly increased precipitation until the beginning of 1990s and a significantly reduced precipitation then after (Thakuri, 2015).

The surface areas of the unconnected lakes are strongly dependent on their basin area ($r = 0.70$; $p < 0.001$; Figure 6b). There are no correlations with the glacier surface area (Figure 6c). In Figure 6d, the glacier surface areas are plotted against the lake area. It indicates that the lake surfaces are slightly correlated with the glacier area ($r = 0.46$), but it is due to autocorrelation, because the glacier surface is a function of

the basin (r = 0.65; Figure 6e). Figure 6d suggests that there are no correlation between the ratios, Lake/Basin area and Glacier area/ Basin area (r = 0.02). Thus, considering that the evaporation/precipitation ratio at these altitudes is approximately 0.34, it can be interpreted that the evolution of such lakes acts as an indicator of precipitation trend of these high-altitude regions.

5. CONCLUSIONS

In this paper, the recent evolutions of three types of glacial lakes (*supra, pro,* and *unconnected*) are examined using the satellite imagery and topographic maps in the SNP. Based on the findings of the analysis, it is possible to underline that the three types of lakes are capable of representing the unique condition of glaciers and climate variations in the region. Supraglacial lakes behaviour confirms the acceleration of the negative mass balance of glaciers due to the reduced ice velocities caused by decreased precipitation. Unconnected lakes have been observed most likely a good indicator of the precipitation change in the region.

ACKNOWLEDGES

This work was a part of Ph.D. work of S. Thakuri, supported by the IPCC Scholarship Programme (Switzerland) and the IRSA-CNR/ Ev-K2-CNR (Italy).

REFERENCES

Ageta, Y., Iwata, S., Yabuki, H., Naito, N., Sakai, A., Narama, C., and Karma, T., 2000. *Expansion of glacier lakes in recent decades in the Bhutan Himalayas*. IAHS Publication, 264, 165–175.

Bajracharya, S.R. and Mool, P., 2009. *Glaciers, glacial lakes and glacial lake outburst floods in the Mount Everest region, Nepal*. Annals of Glaciology, 50, 81–86.

Benn, D., Wiseman, S., and Hands, K., 2001. *Growth and drainage of supraglacial lakes on debris-mantled Ngozumpa Glacier, Khumbu Himal, Nepal*. Journal of Glaciology, 47 (159), 626–638.

Benn, D.I., Benn, T., Hands, K., Gulley, J., Luckman, A. Nicholson, L.I., Quincey, D. Thompson, S., Toumi, R., and Wiseman, S., 2012. *Response of debris-covered glaciers in the Mount Everest region to recent warming, and implications for outburst flood hazards*. Earth-Science Reviews, 114, 156–174.

Bolch, T., Buchroithner, M.F., Peters, J., Baessler, M., and Bajracharya, S., 2008. *Identification of glacier motion and potentially dangerous glacial lakes in the Mt Everest region/Nepal using spaceborne imagery*. Natural Hazards Earth System Science. 8, 1329–1340, doi: 10.5194/nhess-8-1329-2008.

Bortolami, G., 1998. *Geology of Khumbu Region, Mt. Everest, Nepal. In: Lami, A. and G. Giussani (Eds), Limnology of high altitude lakes in the Mt. Everest Region (Nepal)*. Mem. Ist. ital. Idrobiol., 57, 41-49.

Fujita, K., Sakai, A., Nuimura, T., Yamaguchi, S. and Sharma, R.R., 2009. *Recent changes in Imja Glacial Lake and its damming moraine in the Nepal Himalaya revealed by in situ surveys and multi-temporal ASTER imagery*. Environ. Res. Lett., 4, 045205, doi: 10.1088/1748-9326/4/4/045205.

Gardelle, J., Arnaud, Y., and Berthier, E., 2011. *Contrasted evolution of glacial lakes along the Hindu Kush Himalayan mountain range between 1990 and 2009*. Global and Planetary Change, 75, 47-55.

McFeeters, S.K., 1996. *The use of the Normalized Difference Water Index (NDWI) in the delineation of open water features*. Int. J. Remote Sensing, 17(7), 1425-1432.

Löffler, H., 1969. *High altitude lakes in Mt. Everest region*. Verh. int. Ver. Limnol., 17, 373-385.

Reynolds, J.M., 2000. *On the formation of supraglacial lakes on debris-covered glaciers*. IAHS Publication, 264 (Symposium at Seattle 2000 – Debris-Covered Glaciers), 153–161.

Richardson, S.D. and Reynolds, J.M., 2000. *An overview of glacial hazards in the Himalayas*. Quatern. Int., 65/66(1), 31–47.

Sakai, A., Takeuchi, N., Fijita, K., and Nakawo, M., 2000. *Role of supraglacier ponds in ablation process of a debris-covered glacier in the Nepal Himalaya*. IAHS Publication. 264, 119-130.

Salerno, F., Thakuri, S., D'Agata, C., Smiraglia, C., Manfredi, E.C., Viviano, and Tartari, G., 2012. *Glacial lake distribution in the Mount Everest region: uncertainty of measurement and conditions of formation.* Global and Planetary Change. 92–93, 30–39, doi: 10.1016/ j.gloplacha.2012.04.001.

Shijin, W. and Zhang, T., 2014. *Spatial change detection of glacial lakes in the Koshi River basin, the Central Himalayas*. Environ. Earth Sci., doi: 10.1007/ s12665-014-3338-y.

Smiraglia, C., 1998. *Glaciers and glaciology of Himalaya*. In: Baudo, R., G. Tartari, and M. Munawar (Eds.), Top of the World Environmental Research: Mount Everest – Himalayan Ecosystem. Ecovision World Monograph Series, Backhuys Publ., Leiden, 65-100.

Tartari, G., Salerno, F., Buraschi, E., Bruccoleri, G., and Smiraglia, C., 2008. *Lake surface area variations in the north-eastern sector of Sagarmatha National Park (Nepal) at the end of the 20th century by comparison of historical maps.* Journal of Limnology, 67, 139–154.

Tartari, G., Previtali, L., and Tartari, G.A., 1998. *Genesis of the lake cadastre of Khumbu Himal Region (Sagarmatha National Park, East Nepal).* In: Lami, A. and G. Giussani (Eds.), Limnology of high altitude lakes in the Mt. Everest Region (Nepal). Mem. Ist. ital. Idrobiol., 57: 139-149.

Thakuri, S., 2015. *Coupling glacio-hydrological response to climate variability in Mt. Everest Region (Central Himalaya).* Ph.D. Thesis. University of Milan, Italy. p.181.

Thakuri S., Salerno, F., Bolch, T., Guyennon, N., and Tartari, G., 2016. *Factors controlling the accelerated expansion of Imja Lake, Mount Everest region, Nepal.* Annals of Glaciology. 57(71), 245-256.

Thompson, S.S., Benn, D.I., Dennis, K., and Lukman, A., 2012. *A rapidly growing moraine-dammned glacial lake on Ngozumpa Glacier, Nepal.* Geomorphology, 145-146, 1-11.

Watanabe, T., Lamsal, D., and Ives, J.D., 2009. *Evaluating the growth characteristics of a glacial lake and its degree of danger of outburst flooding: Imja-Lhotse Shar glacier, Khumbu Himal, Nepal.* Norsk Geogr. Tidssk, 63, 255–267.

Wu, S., Li, J., and Huang, G.H., 2008. *A study on DEM-derived primary topographic attributes for hydrologic applications: Sensitivity to elevation data resolution.* Applied Geography, 28(3), 210-223.

Modeling the impacts of climate change on hydrology of Sunkoshi river basin, Nepal

Mohan Rana Magar[1], Tirtha Raj Adhikari[2], Dhiraj Gyawali[3]

[1] *Goldden Gate International College, Tribhuwan University, Kathamandu, Nepal (memohan88@gmail.com)*

[2] *Central Department of Hydrology and Meteorology, Tribhuwan University, Kirtipur, Nepal*

[3] *Water Modeling Solutions Pvt. Ltd. Lalitpur, Nepal*

Abstract

Sunkoshi river basin is extended into Nepal and China, lying at geographic location between 27.62˚E, 85.55˚N in northern region and 27.33˚E, 86.0˚N in southern region. An altitude of basin is ranging between 389m – 7928m, covered by snow, forest, agriculture and barren land with catchment area of 10129 km2. This study is focused on likely impact of climate change on the hydrology of Sunkoshi river basin using regional climate model (RCM); PRECIS-ECHAM5 under A1B emission scenario and RegCM4-ECHAM4 under A2 emission scenario coupled with hydrologic model called Soil and Water Analysis Tool (SWAT) for the projection periods 2041-2050 and 2051-2060. Bias correction of projected precipitation and temperature from RCM was carried out using power transformation method. The results revealed that the climate change has less impact on mean annual flow at outlet (Khurkot gauging station), slightly decreased by 2% under A1B scenario while it would decreased by 15% under A2 scenario for projected period 2041-2060. The average seasonal flow was found to be increasing in monsoon season while it was significantly decreasing for rest of the seasons. The future water balance component was observed increasing in comparison to historical period. It was evident that the change of future climatic variables has crucial impacts on changes of flow regimes in sub-basins which has significant implications on water availability and development of infrastructure.

Key words: *Climate change, SWAT, GIS, modeling, Sunkoshi, RCM*

1. Introduction

Nepal is rich in water resources include more than 6000 rivers originated from snow covered higher Himalayas, middle hills of Mahabharat and Chure hills which contributes about 225 billion cubic meters of water annually (WECS, 2011). The hydropower potential of Nepal is 83,000 MW of which 45,610 MW has been identified economically feasible. Nepal has monsoonal climate in which 80 % of annual precipitation occurs during a very short period from June to September and feeds number of small and large rivers in mountains (WECS, 2011). Water availability is variable in time and space, governed by many natural, environmental, geographical and meteorological parameters (Chaulagain, 2003). Nepal is agrarian country

where more than 80% of population depends on subsistence agriculture for livelihoods (World Bank, 2009), which contributes about 40% to GDP and provides employment to two-thirds of the population. Nepalese agriculture is mainly rain fed and partly irrigated, are all being affected badly due to droughts, flooding, erratic rainfall and other extreme weather events (MoPE, 2004).

According to precipitation trend analysis, the annual average precipitation over Nepal is decreasing at the rate of 9.8 mm/decade (WECS, 2011; MoPE, 2004), however based on data from 1947 to 1993, the precipitation trend in the Koshi Basin shows an increasing trend (Sharma et al., 2000). Many of the studies suggest that the intensity of precipitation is likely to increase in coming decades (Immerzeel et al. 2012; Kumar et al., 2011). Research based on the available data found that, the average warming in annual temperature between 1977 and 2000 was 0.06˚C/yr. (Shrestha et al, 1999); temperature on the Tibetan Plateau increased at a rate of 0.16°C per decade between 1955 and 1996 (Liu and Chen, 2000). It has been projected that the annual temperature in Nepal will be increased by 1.4°c in 2030, 2.8°c in 2060 and 4.7°c in 2090 (MoE, 2010; ISET-N, 2009). The warming is found to be more noticeable in the higher altitudinal regions of the Nepal such as Middle Mountain and Himalayan. In Bagmati river basin, the average annual mean maximum temperature was predicted to increase by 2.1°C under A2 scenario and by 1.5° C under B2 scenario in 2080s (Babel et al., 2014) and in Koshi basin it will increase by 0.86°C under A2 and by 0.79°C under B1 scenarios in 2030s compared to baseline 1976 – 2005 (Bharati et al., 2014). The rate of evaporation will be high due to increased temperature, ultimately affects the intensity and duration of drought. The study carried out for the projection of precipitation under A1B scenario for the future period 2020s, 2055s and 2090s in Koshi basin is expected to increase (Agrawal et al., 2014). Under these projected scenarios, the water balance of the region will change, which could affect water availability downstream (Akhtar et al., 2008; Nepal et al., 2014)

Climate change is generally expected to lead to an intensification of the global water cycle as a result of change in hydrologic variables such as precipitation and temperature (Huntington, 2006). The study suggested that the overall annual runoff in Himalayan watersheds will increase with change in climate as a result of an increase in precipitation as well as an increase in net glacier melt (Immerzeel et al., 2013 and Lutz et al., 2014). The intra annual variability of stream flow is significantly increased by impact of climate change (Agrawala et al., 2003). For example, the flow of Bagmati River, Nepal would increase from 268m^3/s to 371.6m^3/s with temperature raised by 4° and precipitation increased by 10% (Chaulagain, 2006). Due to increased river flow, the number of flood disaster has increased compared to other forms of disaster in South Asia (Dutta and Herath, 2005). The agriculture system particularly in Nepal mostly based on monsoonal precipitation, any further change in water availability especially during non-monsoon seasons would affect agriculture production, which will have direct impact on the livelihood of people (WECS, 2011).The snow in high Himalayas is melting rapidly due to increased temperature, expected to create or expand the GLOFs as well as increase river water flows initially.

Although GCMs are used to predict climate variables, they are not designed for climate change impact studies and do not provide a direct estimation of the hydrological response to climate change (Mohammed, 2009). They are generally operated in very coarse resolution. Apparently, it is necessary to convert GCM outputs into a reliable daily rainfall series at the watershed scale levels to which the hydrological impact is going to be investigated. It is also important to investigate potential impacts of climate change in smaller scale catchments where the conditions can be modelled more precisely (Nepal, 2016). In addition to that, various types of regional climatic models have been developed for future climate change study at regional scale. Providing Regional Climate for Impact Studies (PRECIS) PRECIS of ECHAM5 under A1B scenario and Regional Climate Model version 4 (RegCM4) of ECHAM4 under A2 emission scenario are used in this study. Despite the increasing use of RCM simulations in hydrological climate-change impact studies, their application is challenging due to the risk of considerable biases (Lenderink et al.,, 2007; Teutschbein and Seibert, 2012; Leander and Buishand, 2007; Teng et al., 2014). To deal with these biases, several bias correction methods have been developed recently, ranging from simple scaling to rather sophisticated approaches (Teutschbein and Seibert, 2012)

In a mountainous country like Nepal, the data required by the models are found insufficient. In such cases, a physically based, semi-distributed parameter model with a robust hydrologic model, Soil and Water Analysis Tool (SWAT) compatible for both ArcGIS is used in this study to illustrate overall hydraulic simulation of entire basin. The major objective of this study is to assess potential impact of climate change on the hydrologic regimes of Sunkoshi river basin using SWAT2009.

2. Study area

Sunkoshi River is one of the major river of Nepal contributing massive amount of water flow (about 44%) to Koshi river basin. Sunkoshi river basin covers three distinct latitudinal physiographic zones: Mountain, Siwalik also known as Hills and Terai of Nepal. Sunkoshi river basin lying at geographic location between 27.62˚E, 85.55˚N in northern region and 27.33˚E, 86.0˚N in southern region, after joining with the Tamakoshi river at Khurkot (gauging station) of Sindhuli district in the eastern region of the Nepal. The total catchment area of Sunkoshi basin is 10129 km^2 at Kurkot gauging station delineated by using SWAT, out of which some portion (3418 km^2) of the basin covers Tibet region, with relatively dry and very low annual precipitation as shown in figure 1.

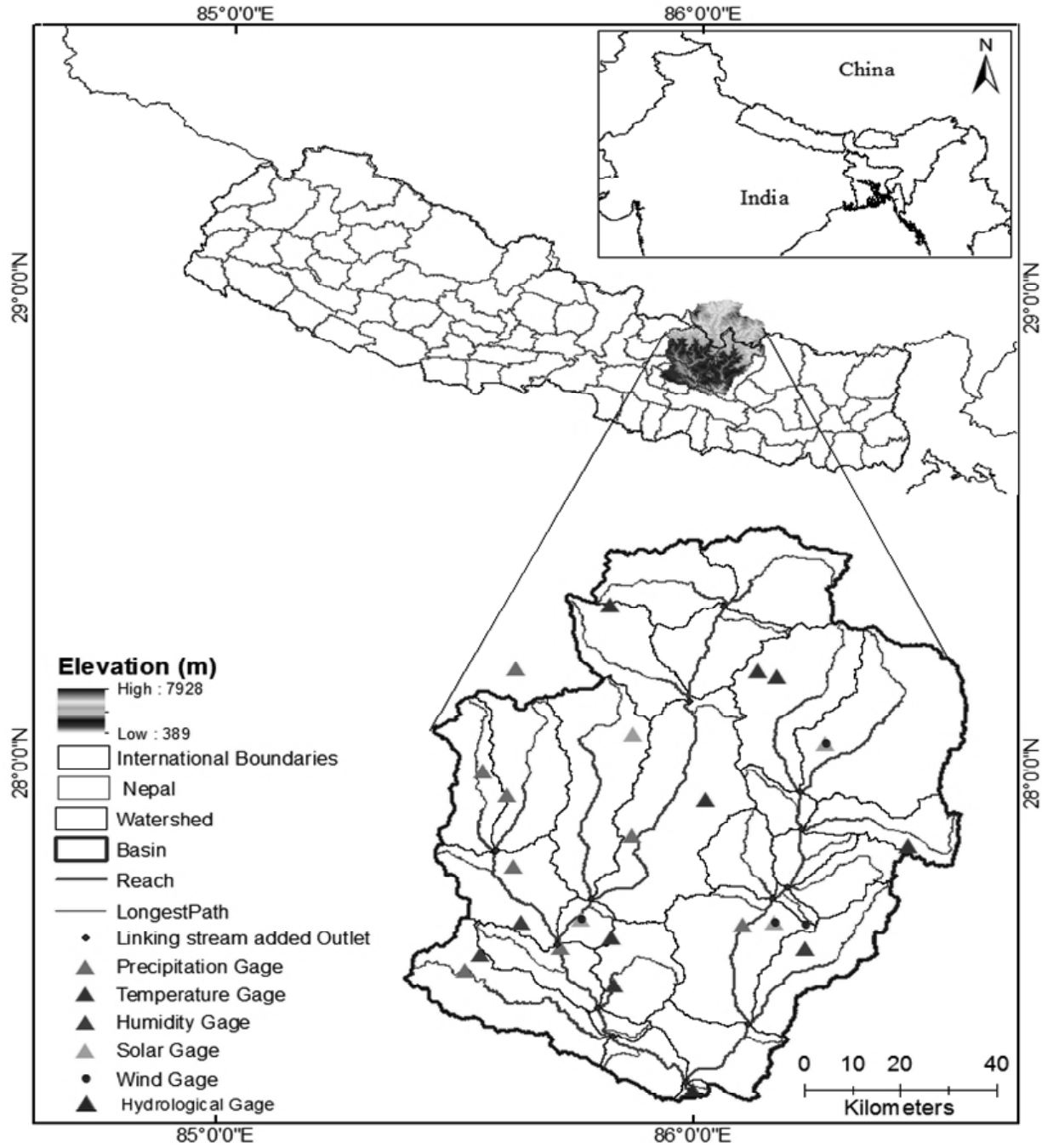

Figure 1: Sunkoshi river basin with sub-basin, elevation, climate and flow stations

Sunkoshi river basin is located in north eastern region of Nepal covered dominantly by forest (39.97%), barren land (38.84%) and snow (12.32%) as in figure 2. The region above 5000 m is covered by permanent snow and glacier included many glacial lakes. Altitudinal variation of the basin ranges from 389m in southern part to 7928m in northern region. Tamakoshi, Indrawati and Sunkoshi rivers are major rivers within this basin. The amount of water availability in this river basin plays vital role multi-purpose projects like Tamakoshi hydropower, reservoir, irrigation and some other household purposes. During monsoon season, the downstream region of basin gets affected by catastrophe like landslide and flooding while in summer season, the people in lower region is threatened by events like flash floods, GLOFs, drought etc.

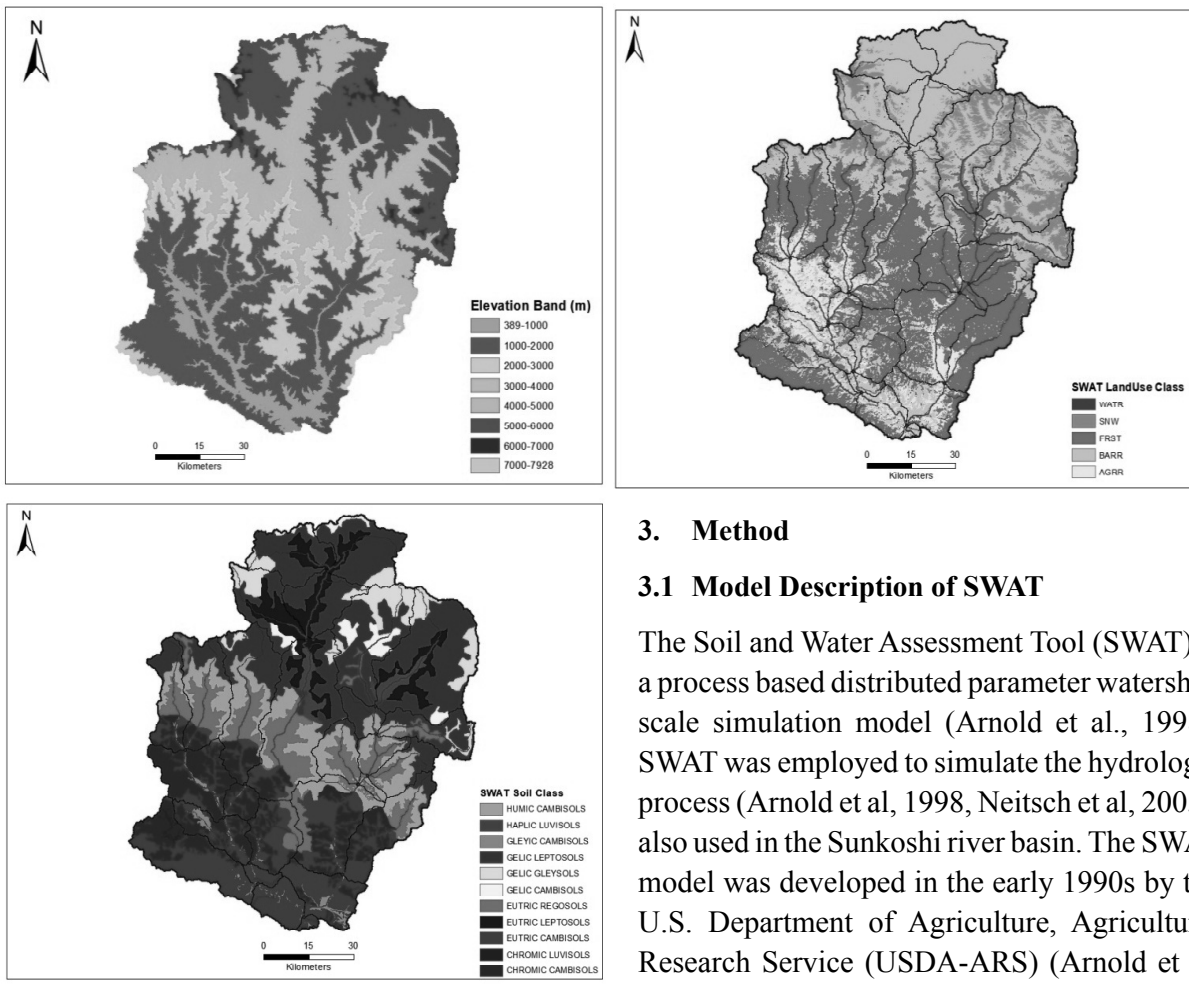

Figure 2: Digital Elevation Model (DEM), Land use and soil maps of Sunkoshi river basin

3. Method

3.1 Model Description of SWAT

The Soil and Water Assessment Tool (SWAT) is a process based distributed parameter watershed scale simulation model (Arnold et al., 1998). SWAT was employed to simulate the hydrologic process (Arnold et al, 1998, Neitsch et al, 2005), also used in the Sunkoshi river basin. The SWAT model was developed in the early 1990s by the U.S. Department of Agriculture, Agricultural Research Service (USDA-ARS) (Arnold et al, 1998). SWAT is a river basin or watershed scale model developed to predict the impact of land management practices on water, sediment and agricultural chemical yields in large, complex

watersheds with varying soils, land use and management conditions over long periods of time (Winchell et al, 2013).

SWAT is a semi-distributed, continuous watershed modelling system which simulates different hydrologic responses using process based equations. The model computes the water balance from a range of hydrologic process such as evaporation, snow accumulation, snowmelt, infiltration and generation of surface and subsurface flow components (Shrestha et al, 2011). Spatial variability within a watershed is represented by dividing the area into multiple sub-watersheds, which are further subdivided the area into unique soil, land use characteristics called hydrologic response units (HRUs). The water balance of each HRU in SWAT is represented by four storage volumes: snow, soil profile (0-2m), shallow aquifer (typically 2-20m) and deep aquifer (>20m) (Gosain et al, 2010). Flow generation, sediment yield and non-point source loadings from each HRU in a sub-watershed are summed and the resulting loads are routed through channels, ponds and/or reservoirs to the watershed outlet.

SWAT uses a temperature index approach to estimate snow accumulation and melt. Snowmelt is calculated as a linear function of the difference between average snowpack maximum temperature and threshold temperature for snowmelt. Snowmelt is included with rainfall in the calculation of infiltration and runoff. SWAT does not include an explicit module to handle snow melt processes in the frozen soil, however it includes a provision for adjusting infiltration and estimating runoff when the soil is frozen (Neitsch et al, 2005). Despite this limitation, SWAT was considered to be most appropriate integrated model currently available for application in the cold regions environment (Shrestha et al, 2011). SWAT computes actual soil water evaporation using an exponential function of soil depth and water content. The model generates surface runoff using a modified Soil Conservation Service (SCS) curve number method based on the local land sue, type of soil and antecedent moisture conditions. Lateral sub-surface flow in the soil profile is calculated simultaneously with percolation. Groundwater flow contribution to total stream flow is simulated by routing the shallow aquifer storage components to the stream. Runoff is routed through the channel network using the variable storage routing method or Muskingum method (Neitsch et al, 2005).

3.2 Regional Climate Model (RCM)

RCM is a climate model of higher spatial resolution than a Global Climate Model (GCM). GCM are not able to account climate change influenced by significantly by local topographical features such as mountains as they use relatively coarse spatial resolution. In this study, PRECIS of ECHAM5 under A1B (2030-2060) and RegCM4 of ECHAM4 under A2 (2040-2069) emission scenarios were used.

PRECIS model stands for Providing Regional Climate for Impact Studies is one of the best dynamical downscaling tools developed at Met Office and Hadley Center with 25 km resolution. It is based on atmospheric component of the HadCM3 (Hadley Centre Couple Model, UK) and ECHAM5 (Max Planck Institute for Meteorology, Germany) Global Climate Model (Gordon et al., 2000, Jones et al., 2004). In PRECIS model, dynamical flow, the atmospheric sulphur cycle, clouds and precipitation, radiative processes, land surface and deep soil are all

described at the limits of the model's domain to provide the meteorological forcing for the RCM (Graiprab et al., 2010).

The RegCM system is a community model and in particular, it is designed for use by a varied community composed of scientists in industrialized countries as well as developing nations (Pal et al. 2007). RegCM4 includes new land surface, planetary boundary layer and air sea flux schemes, a mixed convection and tropical band option, modifications to the pre-existing radiative and boundary layer schemes and a full upgrade of the model code (Elguindi et al., 2011).

PRECIS in conjunction with SWAT has been used in Koshi river basin, Nepal for disaster risk reduction and climate change adaptation (NDRI, 2013). The future change in climatic pattern over Hindu Kush Himalayan region (Kulkarni, 2013) and its impact on hydrology of upper Ganges river basin (Bharati et al., 2011) were studied by using high resolution climate model, PRECIS. Separately, climate change scenario was studied in Nepal based on regional climate change model, RegCM3 (DHM, 2007).

3.3 Data

Sunkoshi River basin covers distinct type of geographical location having major land use pattern; snow cover and barren land in higher altitudinal region while forest, agriculture and water body in lower altitudinal region. SWAT watershed model was constructed using time series and spatial data overlaying the basin. Observed weather and discharge data are the data required by SWAT model. The weather data includes rainfall, maximum and minimum temperature, relative humidity and observed stream flow data were collected from Department of Hydrology and Meteorology (DHM) for the period of 1980 – 2009, while solar radiation (sunshine duration) and wind data were downloaded from https://climatedataguide.ucar.edu_for the respective period. SWAT model divides whole sub-basin to be split into a maximum of ten elevation bands, and snow cover and snowmelt are simulated separately for the each elevation band (Fontaine et al., 2002). To adjust observed temperature for each elevation band, following equation was used;

$$T_B = T + (Z_B - Z).dT/dZ \quad \text{.....(i)}$$

SWAT requires DEM, land use and soil data as spatial data. For Digital Elevation Model (DEM), ASTER GDEM V2.0 of 30 X 30 m resolution was used. LANDSAT image (2009) taken from ICIMOD was classified using ERDAS IMAGINE 9.2 for land use pattern layer. As Sunkoshi basin is located partly in China, the global and national soil terrain digital database (SOTER) of China and Nepal were merged together for soil layer.

3.4 SWAT Model Setup and Calibration

Sunkoshi river basin was delineated using ArcSWAT into 27 sub-basins with 471 hydrological response units (HRUs). The data such as precipitation, maximum and minimum temperature, relative humidity, solar radiation and wind velocity and spatial data; land cover and soil data were used for model setup.

In SWAT, both manual and automated calibrations could be used for model calibration. Manual calibration is by far the most widely used approach for complex models, including those of the distributed type (Refsgaard and Knudsen, 1996; Refsgaard, 1997; Senarath et al., 2000). Govender and Everson (2005) used

an automatic Parameter Estimation (PEST) programme. Both manual and automated methods have been developed for calibration of SWAT simulations (Arnold, 2012). It was reported that manual calibration results are more accurate for predictions than PEST approach (Doherty, 2004). However it is tedious, time consuming and success of it depends on the experience of the modeler and knowledge of the eater being modeled (Eckhardt & Arnold, 2001). When the number of parameters used in the manual calibration is large, especially for complex hydrologic models, manual calibration can become labor-intensive (Balascio et al., 1998) and automated calibration methods are preferred. Manual calibration method was used in this study as it is more accurate and most widely used method.

Due to missing data of observed discharge for first few years, calibration period was started from 2000-2004 and validation period 2005-2009 adjusting few years as warm period so that the initial condition does not affect model calibration. The Nash-Sutcliffe coefficient of efficiency (NSCE) and coefficient of determination (R^2) was employed for independent evaluation of model performance as in table 1.

Table 1: Model Performance Evaluation Statistics

Name	Description	Formulae
R2	Coefficient of Determination	$\left[\frac{\sum_{t=1}^{T}(Q_{m,t}-\overline{Q}_m)(Q_{s,t}-\overline{Q}_s)}{\sum_{t=1}^{T}\left[(Q_{m,t}-\overline{Q}_m)^2\right]^{0.5}\sum_{t=1}^{T}\left[(Q_{s,t}-\overline{Q}_s)^2\right]^{0.5}}\right]^2$
NSCE	Nash Sutcliffe Coefficient of Efficiency	$1-\frac{\sum_{t=1}^{T}(Q_{m,t}-Q_{s,t})^2}{\sum_{t=1}^{T}(Q_{m,t}-\overline{Q}_m)^2}$

3.5 Bias correction

The RCM simulations of precipitation and temperature often show significant biases (Christensen et al., 2008; Teutshbein and Seibert, 2010; Varis et al., 2004), it must be handled with caution. The reasons for such biases include systematic model errors caused by imperfect conceptualization, discretization and spatial averaging within grid cells (Teutshbein and Seibert, 2012). These model biases caused the result more complicated when they are used in hydrological models for the impact study. Therefore, it is of major importance that RCM output is validated with historical observations before calibrating the hydrological model with the RCM data (Terink et al., 2010).

In this study, power transformation method was used to correct for both future precipitation and temperature based on A1B and A2 scenario. Leander and Buishand, (2007) used a power transformation method which corrects the coefficient of variation (CV) as well as the mean. The details of power transformation could also be found in Shabalova et al., 2003, Terink et al., 2010 and Teutshbein and Seibert, 2012). In this nonlinear correction, each daily precipitation amount P is transformed to a corrected P^* using:

$$P^* = aP^b \quad \text{.....(ii)}$$

The parameters a and b were determined for every five day period of the year with data from

all year available in a window including 30 days before and after the considered five day period. The determination of value of *b* parameter was done iteratively. It was calculated in way that the CV of the corrected daily precipitation matched the CV of the observed daily precipitation. In this study, macro developed by NDRI, (2013) was used for power transformation method to correct biases of projected precipitation.

Since the temperature is known to be approximately normally distributed, power law cannot be used to correct temperature as used for correcting precipitation (Terink et al., 2010). Leander and Buishand, (2007) mentioned that, the correction of temperature only involves shifting and scaling to adjust the mean and variance. Therefore, a different technique for correcting temperature for each grid was used as follows:

$$T^* = T_{obs} + \sigma T_{obs} / \sigma T_{era} (T_{era} - T_{obs}) + (T_{obs} - T_{era}) \ldots\ldots (iii)$$

Where T_{obs} is the observed daily temperature, T_{era} is the uncorrected daily temperature, σ is the standard deviation and overbar denotes the average over the considered period. This method may result negative values and considered as inappropriate in correcting precipitation.

4. Results and Discussion

4.1 Hydrological Modeling

SWAT model has been used in every geographic location of river basins all round the world for simulation of hydrological response, impact studies with combination of RCM. Several trial and error experiments were made for model calibration to obtain best fit results (table 2) for the analysis of future impacts due to climate change. Initially, the model was run for 30 years (1980-2009) long period of time. For model calibration, period; 2000-2004 was assigned while period; 2005-2009 was selected for model validation. The validation of model was carried out with the same existed parameters obtained from calibration period to analyse how well the calibrated parameters fit for rest of independent period. Firstly, the sensitive parameters on the system impacts surface response such as CN2, SOL_AWC and ESCO were adjusted followed by GW_REVAP, GWQMN, ALPHA_BF, GW_DELAY, SOL_Z, those which impacts sub-surface response. Later on, the parameters CH-K2, SURLAG, ALPHA_BF were adjusted for the accurate shape of the hydrograph.

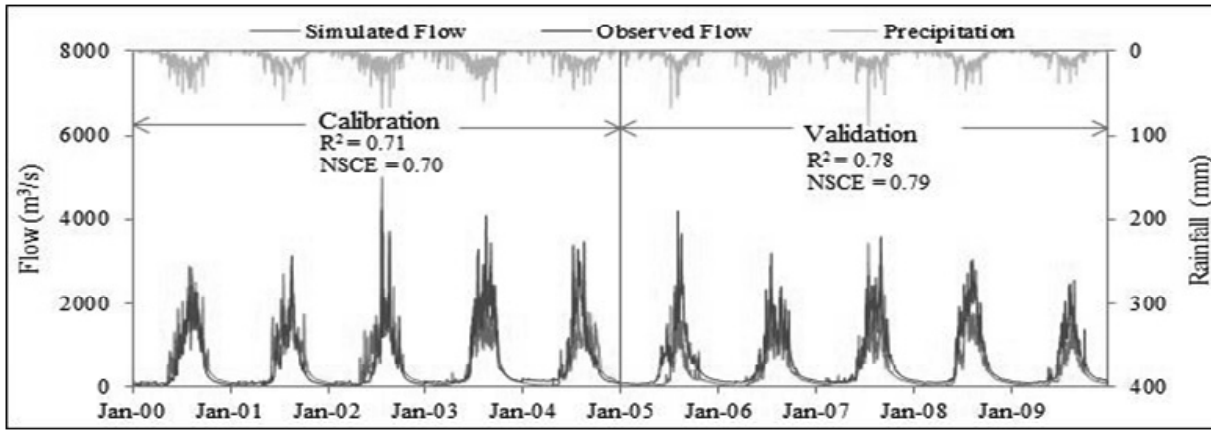

Figure 3: Observed vs. simulated hydrograph for the calibration period (2000-2004) and validation period (2005-2009) with rainfall

The performance of SWAT model was tested using statistics such as R^2 and NSCE which were calculated as 0.71 and 0.70 for calibration period and 0.78 and 0.79 for validation period respectively (Figure 3). The calculated value of statistics for calibration and validation were found within the valid requirements, $R^2 > 0.6$ and NSCE > 0.5 as suggested by Santhi et al., (2001). Based upon model evaluation statistics, the calibrated parameter's values (Table 2) were used for simulation of future hydrologic response.

Table 2: Range for SWAT parameters and best adjusted parameters of calibration and validation period

Parameters	Description	Parameter Range	Best Parameter
CN2	SCS runoff curve number	-35% to 35%	-35%
ESCO	Soil evaporation compensation factor	0 - 1	0.6
CANMX	Maximum canopy storage (mmH2O)	0.1 - 10	0.5,0.5,0.5,2,3
SOL_Z	Soil depth	-25% to 25%	16.67%
SOL_AWC	Available water capacity	-50% to 50%	-35%
SURLAG	Surface runoff lag time (days)	0.01-10	8
GWQMN	Threshold water depth in the shallow aquifer for flow(mm)	0-500	200
GW_DELAY	Ground water delay(days)	0-50	25
SOL_K	Saturated hydraulic conductivity (mm/hr)	-25% to 25%	-25%
GW_REVAP	Ground water revap coefficient	0.02-0.2	0.1
CH_K2	Effective hydraulic conductivity in main channel (mm/hr)	0-150	60
ALPHA_BF	Base flow alpha factor	0-1	0.07

4.2 Historic and Future flow comparison

In this study, 30 years period of climate data was allocated for model setup. For historical and future flow series, only 20 years period was considered for comparison of flow (based on availability of data). The historical flow was limited to1990 – 2009 while future flow (PRECIS under A1B and RegCM4 under A2) was considered to 2041 – 2060. The flow date of 20 years period was divided into two parts with 10 years interval for understanding of changes in future flow as shown in figure 4. In this study, it was assumed that the percentage change of flow was calculated based on comparison between historical and future flow.

4.2.1 Changes in annual flow

The study shows that an average annual future flow would decreased by 2% based on PRECIS, A1B scenarios while it would decreased by 15% based on RegCM4, A2 scenarios in comparison to historical flow as shown in table 3 . The study carried out in Koshi river basin using similar method by Devkota and Gyawali, (2015) found that the future flow was slightly less than baseline period (1987-2006). While Nepal, (2016) mentioned that an increase in average annual future flow in Koshi river basin by 13% followed by decreasing trend after mid-century. Sharma et al, 2000 studied the test of sensitivity of hydrology to change in climatic

conditions in Koshi river basin projected that; runoff would decreased by 2-8% with current precipitation levels and a rise in temperature by 4°. The study shows similar decreasing trend for the major rivers of Nepal; Narayani, Karnali, Kaligandaki (WECS, 2011).

Table 3: Percentage change of average seasonal flow at outlet (Khurkot) in response to climate change scenarios (A1B & A2)

Year	Scenario	Pre-monsoon (%)	Monsoon (%)	Post-monsoon (%)	Winter (%)
2041-2050	A1B	-28	1	-17	-81
2051-2060	A1B	-23	12	-19	-79
2041-2050	A2	26	-8	19	-43
2051-2060	A2	9	-25	-15	-76

The result shows that, climate change have slight impact on average annual flow at outlet under A1B whereas it has significant impact on average annual flow under A2 emission scenarios, as coupled with SWAT model under the present conditions of land use, soil types, and climatic data. In fact, projected average annual flow would decreased slightly (2%) under A1B and decreased by 15% under A2 scenario which is significantly relevant with the study conducted by Bharati et al., (2014) concluded that average projected annual flow of Koshi river basin would decreased by less than 5% under climate change scenarios A2 and B2 coupled with SWAT. The result in this basin was also relevant to Dudh Koshi river basin, in which the average annual flow would decrease by 4% for projected period 2045 – 2054 under IPCC AR5 scenario (Soncini et al., 2016). Overall projected flow seems to be less in comparison to historical flow in Sunkoshi river basin as a result of climate change which ultimately affect irrigation, hydropower and flood control system

4.2.2 Changes in monthly flow

In Nepalese river basin like Sunkoshi, heavy rainfall occurs in the months of June to August. There is surplus amount of water in river basin in these months causing disaster like flooding, sedimentation in reservoir, dam; whereas there is water deficient in rest of the months causing less agricultural production as Nepalese agriculture is solely depends on monsoonal precipitation. The peak flow was observed in the month of July and August which was decreased significantly for projected time period based on RCMs (PRECIS and RegCM4) used as shown in figure 4. The monthly water availability provides the way of operation of hydrological infrastructure like dam, hydropower, reservoir (Devkota and Gyawali, 2015).

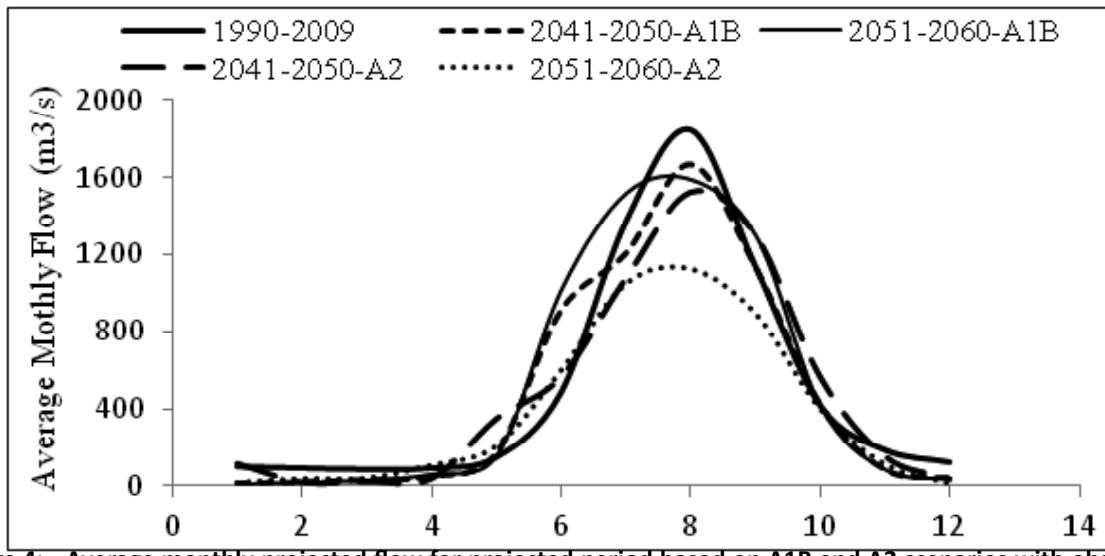

Figure 4: Average monthly projected flow for projected period based on A1B and A2 scenarios with observed period

Table 4 shows percentage change of seasonal flow at basin's outlet (Khurkot gauge station). The average monthly flow would decreased by 25% (average) and 18% (average) for pre-monsoon and post monsoon season, while it would increase by 7% (average) in monsoon season under A1B scenario. In pre-monsoon season, an average monthly flow would increase by 18% (average) and slightly increases in post monsoon season, while it would decreased by 16% (average) under A2 scenario for the projected period. Dixit et al., (2009) and NCVST, (2009) for the analysis of impacts of projected climate change concluded that wet seasons in Koshi basin are likely to become wetter and the dry seasons are likely to become drier, with increasing likelihood of both drought and flood. Also, it was noted that there was significant decrease in seasonal flow in winter in Sunkoshi river basin. Soncini et al., (2016) predicted that the average future flows in Dudh Koshi River would increase in monsoon season and at the end of century, the future flow would decrease by 26%.

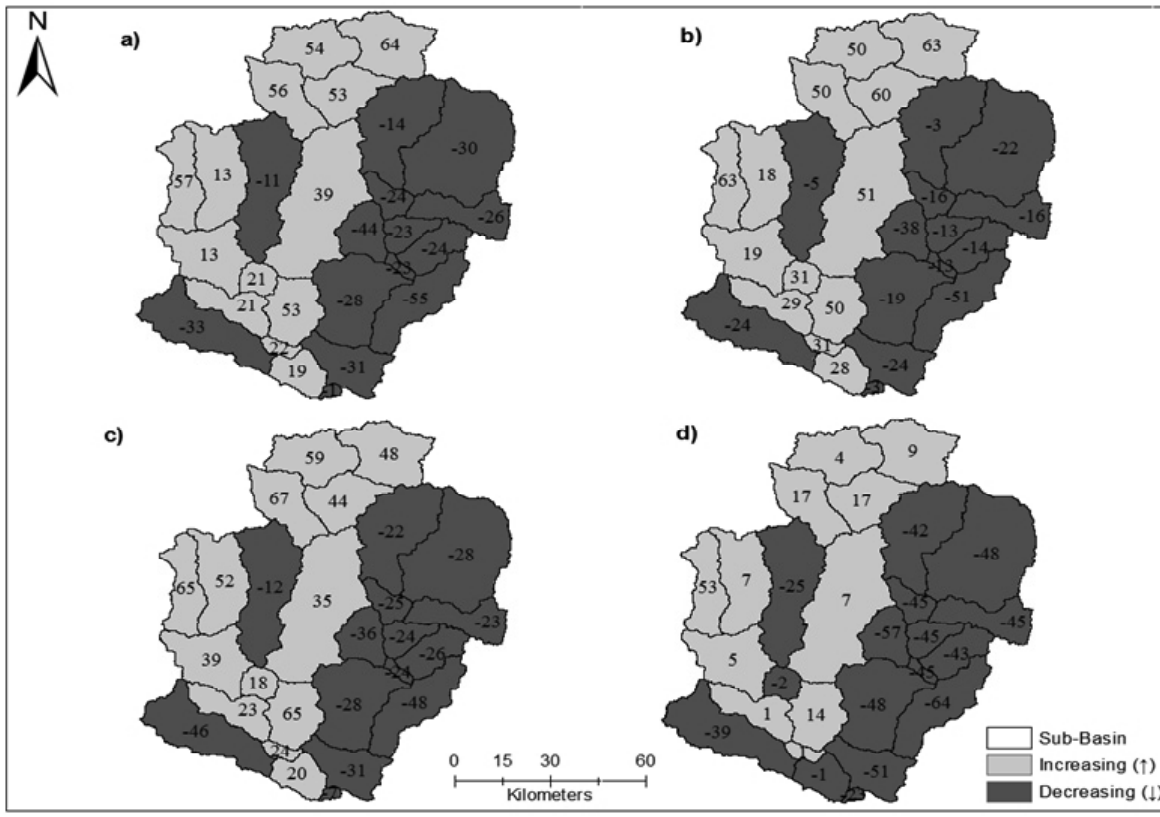

Figure 5: Chang of percentage of average annual average flow for sub-basin for projected period a) 2041-2050-A1B b) 2051-2060-A1B c) 2041-2050-A2 d) 2051-2060-A2

Although, there was less impact on average annual flow at basin's outlet; there was a severe impact on average annual flow at sub-basins scale as shown in figure 5. In addition, climate change has significant impact in changing average seasonal flow at outlet. For example, average seasonal flow was increased incredibly in monsoon season as compare to baseline while the flow was decreased significantly in pre-monsoon, post monsoon season and winter season.

Table 4: Percentage Change of average annual flow at outlet (Khurkot) in response to climate change scenarios (A1B & A2)

Year	Scenario	Average Annual Flow (m3/s)	Flow Change	% Change	Average % Change
1990-2009		510			
2041-2050	A1B	477	-33	-6	
2051-2060	A1B	521	11	2	-2
2041-2050	A2	485	-25	-5	
2051-2060	A2	385	-125	-25	-15

4.3 Change in water balance components

SWAT includes precipitation, actual evapotranspiration (ET), and total water yield as major water balance components. The mean annual precipitation simulated by SWAT of whole basin for historic period 1990 – 2009 was 1665mm. The mean seasonal precipitation was 81mm, 327mm, 35mm and 16mm for pre-monsoon, monsoon, post-monsoon and winter season respectively. The maximum and minimum precipitation simulated was in July (410mm) and December (8mm) respectively. The comparison of simulated average monthly precipitation is illustrated in figure 6.

The simulated mean annual precipitation by SWAT for the period 2041 – 2050 and 2051 – 2060 under A1B scenarios was 1862mm and 2020mm. Under A2 scenarios, this was 2030mm and 1924mm for the period 2041 – 2050 and 2051 – 2060 respectively. The overall mean seasonal precipitation for the projected period 2041 – 2060 under A1B in pre-monsoon, monsoon, post-monsoon and winter was increased by 2%, 15%, 36% and 18% respectively while under A2 ,scenario this was decreased by 6% in pre-monsoon and increased by 13%, 26% and 24% in monsoon, post-monsoon and winter season respectively.

The actual ET is governed by amount of precipitation and land use pattern of the area. The mean annual actual ET of whole basin was 633mm for the period 1990 – 2009. Average monthly actual ET is depicted in figure 6, in which predicted ET is leading in contrast to historic ET. The simulated average annual ET in 2040s and in 2050s under A1B was slightly decreased. Under A2 scenarios, average annual ET in 2040s and 2050s was increased by 22% and 45% respectively. This is because of increased temperature and also the majority of the Sunkoshi basin is covered by forest (40%) and barren land (39%). The actual ET is one of the major water balance component which plays vital role to affect future water yield capacity of the basin.

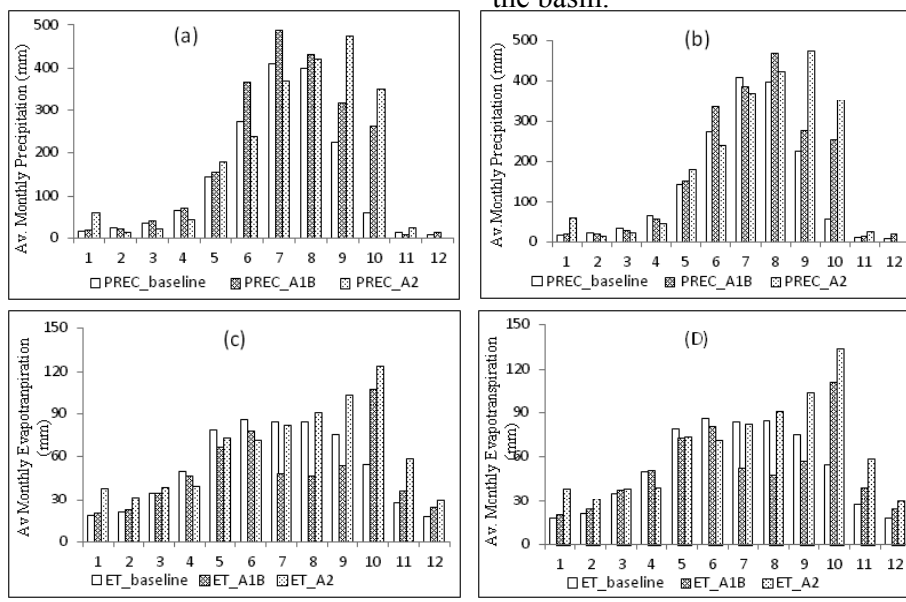

Figure 6: Simulated historic vs future water balance component a) precipitation for 2041-2050 b) precipitation for 2051-2060 c) evapotranspiration for 2041-2050 d) evapotranspiration for 2051-2060

Net water yield (WYLD) is sum of snow melt, runoff from rain, base flow and lateral flow. Although rainfall is major component affecting water yield, soil properties and land cover should also be considered. The simulated average annual water yield of basin for the historic period was 1003mm. The highest water yield was found in middle mountain region (Sub-basin 13 and 14 in Figure 7) than lower region of the basin. The predicted average annual water yield in 2040s and 2050s under A1B scenario was increased by 24% and 36% while under A2 scenario, this was simulated to increase by 27% in 2040s and no any significant change in 2050s.

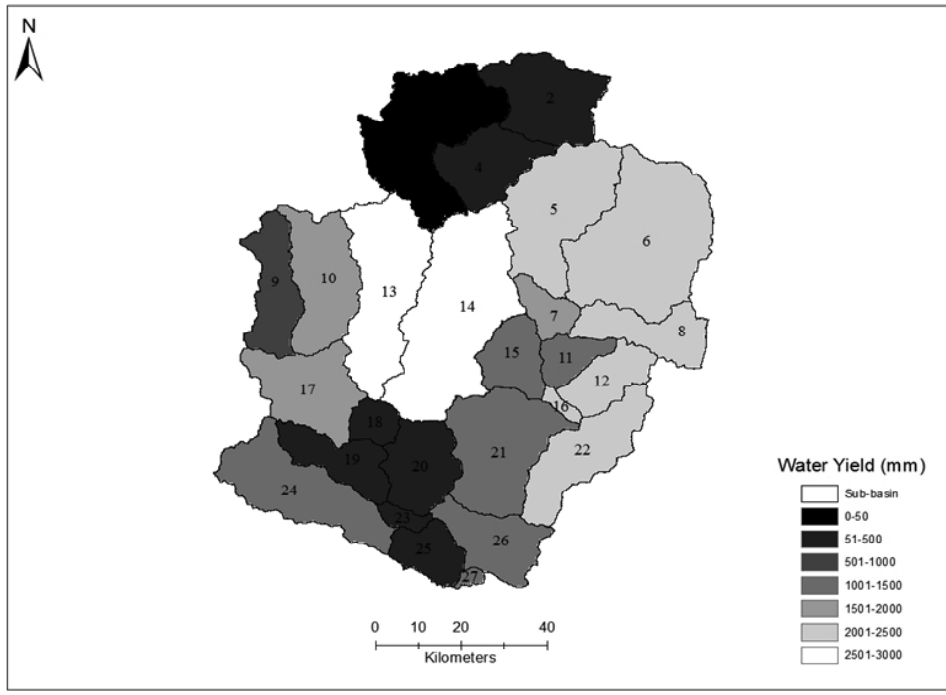

Figure 7: Net water yield by sub-basin for the period 1990 – 2009

Considering historic climatic conditions, mean annual maximum temperature for whole basin was ranged from 5.3° to 27.6°, whereas mean annual minimum temperature was between -8.4° to 13.8° respectively. Under climate change condition, mean annual maximum temperature was ranged from 3.6° to 29.0°, whereas mean annual minimum temperature is from-7.8° to 13.7° under A1B scenario. While, mean annual maximum temperature was varied from 3.0° to 28.7°, and mean annual minimum temperature was ranged from -7.3° to 15.1°. This observation shows that both maximum and minimum temperature was increasing in trend compared to historic climatic conditions. The water balance components; precipitation, evapotranspiration and water yield were predicted to be increased in Sunkoshi river basin. The study by Gosain et al., (2010) in Eastern Himalayas under A2 and B2 scenarios also found significant increase in water balance components; precipitation, snowmelt, surface runoff, actual and potential evapotranspiration. Bharati et al., (2014) also concluded overall increase in water balance components in most parts of Koshi river basin.

5. Conclusion

The hydrologic response due to change in climatic pattern in Sunkoshi river basin was evaluated using SWAT model. SWAT model setup was done using land cover, soil types and meteorological data. Model performance statistics, R^2 and NSCE were calculated as 0.71 and 0.70 for calibration (2000-2004) and 0.78 and 0.79 for validation period (2005-2009) respectively. Hence, SWAT model was considered as strong predictive tool for impact analysis in this study. Application of SWAT demonstrated an efficient method to assess climate change impact analysis for the Sunkoshi river basin and could be used in other watersheds with similar way.

Bias corrected projected climatic data using power transformation method was delivered in model minimizes over simulation in order to interpret hydrologic response of entire Sunkoshi river basin due to climate change. Average annual flow at basin's outlet (Khurkot gauging station) was found slightly decreased by 2% under A1B emission scenario while it was decreased by 15% under A2 emission scenario for projected period 2041-2060. Although, there was minimal impacts on overall flow at outlet, climate change has remarkable impacts on sub-basin. As a result of climate change, there was severe impact on seasonal water availability. The projected water balance component's values were found increased in comparison to baseline value. In historic time period, many natural catastrophes have been observed in peak runoff season (monsoon) and remains drought for rest of the seasons. Also, it is more likely to occur those kinds of unexpected natural disasters due to climate change in future. So, proper planning and development activities should be initiated considering climate change impacts. This study emphasized the need of monitoring station to be established to record climatic data and streamflow at outlet of sub-basin for in-depth calibration and validation of SWAT model to estimate climate change impact properly in future.

Acknowledgement

The authors would like to acknowledge Resources Himalayan Foundation (RHF) for partial financial support and Department of Hydrology and Meteorology (DHM), International Centre for Integrated Mountain Development (ICIMOD), Nepal Development Research Institute (NDRI) and International Water Management Institute (IWMI) for technical support.

Reference

Agarwal, A., Babel, M.S. & Maskey, S. (2014). Analysis of future precipitation in the Koshi River Basin, Nepal. *J. Hydrol. 513*, 422–434.

Agrawala, S., Raksakulthai, V., Aalst, M., Larsen, P., Smith, J. & Reynolds, J. (2003). Development and Climate Change in Nepal: Focus on water resources and hydropower. *Organization for Economic Cooperation and Development (OECD),* Paris, pp. 64.

Akhtar, M., Ahmad, N. & Booij, M.J. (2008). The impact of climate change on the water resources of Hindukush-Karakorum-Himalaya region under different glacier coverage scenarios. *J. Hydrol. 355*, 148–163.

Arnold, J. G., Moriasi, D. N., Gassman, P. W., Abbaspour, K. C., White, M. J.,

Srinivasan, R.,Santhi, C., Harmel, R.D., van Griensven, A., Van Liew, M.W., Kanan, N. & Jha, M.K. (2012). SWAT: model use, calibration and validation. *American Society of Agriculture and Biological Engineers, 55*(4), 1491-1508.

Arnold, J. G., Srinivasan, R., Muttiah, R. S., & Williams, J. R. (1998). Large are hydrologic modelling and assessment-part 1: model development. *American Water Resources Association,* 34(1), 73-89.

Babel, M.S., Bhusal, S.P., Wahid, M.S. & Agarwal, A. (2014). Climate change and water resources in the Bagmati River Basin, Nepal. *Theor. Appl. Climatol. 115*, 639–654.

Balascio, C. C., Palmeri, D. J., & Gao, H. (1998). Use of genetic algorithm and multi-objective programming for calibration of a hydrologic model. *Trans. ASAE*, 41(3), 615-619.

Bang, H. Q., Quan, N. H., & Phu, V. L. (2013). Impacts of climate change on catchment flows and assessing its impacts on hydropower in Vietnam's central highland region. *Global Perspectives on Geography (GPG), 1*(1), 1-8.

Bharati, L., Gurung, P., Jayakody, P., Smakhtin, V., & Bhattarai, U. (2014). The projected impact of climate change on water availability and development in the Koahi basin, Nepal. *Mountain Research and Development, 34*(2), 118-130.

Bharati, L., Lacombe, G., Gurung, P., Jayakody, P., Hoanh, C.T. & Smakhtin, V. (2011). The impacts of water infrastructure and climate change on the hydrology of the Upper Ganges river basin. Colombo, Sri Lanka: International Water Management Institute. 36pp. (IWMI Research Report 142). doi: 10.5337/2011.210.

Chaulagain, N.P. (2003). Change in precipitation parameters and its impacts on micro hydropower development: A case study at Jiri. In: Conference papers of international conference on Renewable Energy Technology for Rural Development 12-14 October 2003, Kathmandu, Nepal, 186-189.

Chaulagain, N.P. (2006). Impacts of Climate Change on Water Resources of Nepal: The Physical and Socioeconomic Dimensions. Thesis for the Degree of Doctor Engineer, University of Flensburg, Germany, 2006.

Christensen, J. H., Boberg, F., Christensen, O. B., & Lucas-Picher, P. (2008). On the need for

bias correction of regional climate change projections of temperature and precipitation.

Geography Research Letters, 35, L20709, 1-6. doi: doi:10.1029/2008GL035694.

Devkota, L.P. & Gyawali, D.R. (2015). Impacts of climate change on hydrological regime and water resources management of the Koshi river basin, Nepal. *Journal of Hydrology; Regional Studies,* 4, 502 -515.

DHM (2007). Climate Change Scenarios for Nepal based on Regional Climate Model RegCM3. Department of Hydrology and Meteorology (DHM), Kathmandu, Nepal.

Dixit, A., Upadhya, M., Dixit, K., Pokhrel, A., & Rai, D. R. (2009). Living with water stress in the hills of the Koshi basin, Nepal. *International Centre for Integrated Mountain Development (ICIMOD)*.

Doherty, J. (2004). PEST: Model-Independent Parameter Estimation User Manual. *Trans. ASAE*, 51(5), 1925-1936.

Dutta, D. & Herath, A. (2005). Trend of Floods in Asia and Flood Risk Management with Integrated River Basin Approach, Human Security and Climate Change, An International Workshop, Asker, near Oslo.

Eckhardt, K., & Arhold, J. G. (2001).Automatic calibration of a distributed catchment model. *Journal of Hydrology*. 251(1-2), 103-109.

Elguindi, N., Bi, X.Q. & Giorgi, F. (2011). Regional climatic model RegCM user manual version 4.1. The Abdus Salam International Centre for Theoretical Physics Strada Costiera, Trieste.

Fontaine, T. A., Cruickshank, T. S., Arnold, J. G., & Hotchkiss, R. H. (2002).Development of a snowfall-snowmelt routine for mountainous terrain for the soil water assessment tool (SWAT). *Journal of Hydrology*, 262(1-4), 209-223.

Gordon, C., Cooper, C., Senior, C. A., Banks, H., Gregory, J. M., Johns, T. C., Wood, R. A. (2000). The simulation of SST, sea ice extents and ocean heat transports in a version of the Hadle Centre coupled model without flux adjustments. *Clim. Dyn*., 16, 147-168.

Gosain, A.K., Shrestha, A.B. & Rao, S. (2010). Modelling climate change impact on the hydrology of the Eastern Himalayas; Climate change impact and vulnerability in the Eastern Himalayas – Technical report 4. Kathmandu: ICIMOD.

Govender, M. & Everson, C.S. (2005). Modelling streamflow from two small South African experimental catchments using the SWAT model. *Hydrological Processes,* 19(3), 683-692.

Graiprab, P., Pongput, K., Tangtham, N., & Gassman, P. W. (2010). Hydrologic evaluation and effect of climate change on the At Samat watershed, Northeastern Region, Thailand. *International Agriculture Engineering Journal,* 19(2), 12-22.

Huntington, T.G. (2006). Evidence of intensification of the global water cycle: review and synthesis. *Journal of Hydrology*, 319(1-4), 83-95.

Immerzeel, W.W., Pellicciotti, F. & Bierkens, M.F.P. (2013). Rising river flows throughout the twenty-first century in two Himalayan glacierized watersheds. Nat. Geosci. 6, 742–745.

Immerzeel, W.W., van Beek, L.P.H., Konz, M., Shrestha, A.B. & Bierkens, M.F.P., (2012). Hydrological response to climate change in a glacierized catchment in the Himalayas. *Clim. Change,* 110 (3–4), 721–736.

ISET-N, (2009). Vulnerability through the Eyes of Vulnerable: Climate Change Induced Uncertainties and Nepal's

Development Predicaments. Institute of for Social and Environmental Transition – Nepal (ISET-N), Kathmandu, Nepal.

Jones, R.G., Noguer, M., Hassell, D.C., Hudson, D., Wilson, S.S., Jenkins, G.J. and Mitchell, J.F.B. (2004).Generating high resolution climate change scenarios using PRECIS, Met Office Hadley Centre, Exeter, UK, 40pp.

Karmacharya, J., Shrestha, A., Rajbhandari, R. & Shrestha, M.L. (2007). Climate change scenarios for Nepal based on regional climate model RegCM3. Department of hydrology and Meteorology, Kathmandu, Nepal.

Kulkarni, A., Patwardhank, S., Kumar, K., Ashok, K., & Krishnan, R. (2013). Projected climate change in the Hindu Kush-Himalaya region by using the High-resolution regional climate model PRECIS. *Mountain Research and Development, 33*(2), 142-151.

Kumar, K.K., Patwardhan, S.K., Kulkarni, A., Kamala, K., Rao, K.K. & Jones, R. (2011). Simulated projections for summer monsoon climate over India by a high-resolution regional climate model (PRECIS). *Curr. Sci. 101 (3),* 312–326.

Leander, R., & Buishand, T. A. (2007). Resampling of regional climate model output for the simulation of extreme river flows. *Journal of Hydrology, 332*, 487-496.

Lenderink, G., Buishand, A., & van Deursen, W. (2007). Estimates of future discharges of the river Rhine using two scenario methodologies: direct versus delta approach. *Hydrol. Earth. Sci.,* 11(3), 1145-1159.

Liu, X. & Chen, B. (2000). Climatic warming in the Tibetan Plateau during recent decades. *Int. J. Climatol.* 20, 1729–1742.

Lutz, A.F., Immerzeel, W.W., Shrestha, A.B. & Bierkens, M.F.P. (2014). Consistent increase in High Asia's runoff due to increasing glacier melt and precipitation. Nat. *Clim. Change*, doi:10.1038/nclimate2237.

MoE (2010). National Adaptation Programme of Action to Climate Change. Kathmandu, Nepal. Ministry of Environment.

Mohammed, Y. (2009). Climate change impact assessment on soil water availability and crop yield in Anjeni watershed Blue Nile basin. Master of Science, Arba Minch University, Ethopia.

MoPE. (2004). Nepal National Action Program on land Degradation and Desertification in the context of UNCCD. Ministry of Population and Environment, Kathmandu, Nepal.

NCVST. (2009). Vulnerability through the Eyes of the Vulnerable: climate change induced uncertainties and Nepal's development predicaments, Kathmandu, Nepal. Institute for social and environmental transition, Nepal climate vulnerability study team.

NDRI. (2013). Disaster risk reduction and climate change adaptation in Koshi river basin, Nepal. Consultation workshop report. Nepal Development Research Institute.

Neitsch, S.L., Arnold, J.G., Kiniry, J.R., Williams J.R. (2005). Soil and Water Assessment Tool-Theoretical Documentation-Version 2005.Grassland, Soil and Water Research Laboratory, Agricultural Research Service and Blackland Research Center, Texas Agriculture Experiment Station, Temple, Texas.

Nepal, S. (2016). Impacts of climate change on the hydrological regime of the Koshi river basin in the Himalayan region. *Journal of Hydro-environment Research,* 10, 76-89.

Nepal, S., Flügel, W.-A. & Shrestha, A.B. (2014). Upstream-downstream linkages of hydrological processes in the Himalayan region. *Ecol. Process,* 3 (19), 1–16.

Pal, J.S., Giorgi, F., Bi, X. & Elguindi, N. (2007). Regional climate modelling for the developing world: the ICTP RegCM3 and RegCNET. *Bull Am Meteorol Soc.* 88: 1395-1409.

Refsgaard, J. C. (1997). Parameterization, calibration and validation of distributed hydrologic models. *Journal of Hydrology, 198*, 69-97.

Refsgaard, J. C., & Knudsen, J. (1996). Operational validation and intercomparison of different types of hydrologic models. *Water Resources and Research, 32*(7), 2189-2202.

Santhi, C., Arnold, J. G., Williams, J. R., Dugas, W. A., Srinivasan, R., & Hauck, L. M. (2001). Validation of the SWAT model on a large river basin with point and nonpoint sources. *Journal of American Water Resource Association, 37*(5), 1169-1188.

Senarath, S. U. S., Ogden, F. L., Downer, C. W., & Sharif, H. O. (2000). On the calibration and verification of two-dimensional, distributed, hortonian, continuous watershed models. *Water Resources and Research, 36*(6), 1495-1510.

Shabalova, M. V., van Deursen, W. P., & Buishand, T. A. (2003). Assessing future discharge of the river Rhine using regional climate model integrations and a hydrological model. *Climate Research, 23*(3), 233-246. doi: doi:10.3354/cr023233.

Sharma, K. P., Moore, B., & Vorosmarty, C. J. (2000). Anthropogenic, climatic and hydrologic trends in the Koshi basin, Himalaya. *Climate Change, 47*(1-2), 141-165.

Shrestha, A. B., Wake, C. P., Mayewski, P. A., & Dibb, J. E. (1999). Maximum temperature trends in the Himalaya and its vicinity: an analysis based on temperature records from

Nepal for the period 1971-94. *Journal of Climate, 12*, 2775-2786.

Shrestha, R. R., Dibike, Y. B., & Prowse, T. D. (2011). Modelling of climate-induced hydrologic changes in the Lake Winnipeg watershed. *Journal of Great Lakes Research*, 1-12. doi: 10.1016/j.jglr.2011.02.004

Soncini, A., Bocchiola, D., Confortola, G., Minora, U., Vuillermoz, E., Salerno, F., Viviano, G., Shrestha, D., Senese, A., Smiraglia, C. & Diolaiuti, G. (2016).

Future hydrological regimes and glacier cover in the Everest region: The case study of the upper Dudh Koshi basin. *Science of The Total Environment, 565*, 1084 – 1101.

Teng, J., Potter, N.J., Chiew, F.H.S., Zhang, L., Vaze, J. & Evans, J.P. (2014). How does bias correction of RCM precipitation affect modelled runoff? *Hydrol. Earth Sci Discuss, 11*, 10683 – 10724. doi:10.5194/hessd-11-10683-2014.

Terink, W., Hurkmans, R. T. W. L., Torfs, P. J. J. F., & Uijlenhoet, R. (2010). Evaluation of a bias correction method applied to downscaled precipitation and temperature reanalysis data for the Rhine basin. *Hydrol. Earth Syst. Sci. Discuss, 14*, 687-703.

Teutschbein, C., & Seibert, J. (2010). Regional climate models for hydrological impact studies at the catchment scale: A review of recent modeling strategies. *Geography compass, 4*(7), 834-860. doi: doi: 10.1111/j.1749-8198.2010.00357.x

Teutschbein, C., & Seibert, J. (2012). Bias correction of regional climate model simulations for hydrological climate-change impact studies: Review and evaluation of different methods. *Journal of Hydrology, 456-457*, 12-29. doi:10.1016/j.jhydrol.2012.05.052

Varis, O., Kajander, T., & Lemmela, R. (2004). Climate and water: from climate models to water resources management and vice versa. *Climate Change, 66*(3), 321-344. doi: doi:10.1023/B:CLIM.0000044622.42657.d4

WECS. (2011). Water Resources of Nepal in the Context of Climate Change. Water and Energy Commission Secretariat, Kathmandu, Nepal.

Winchell, M., Srinivasan, R., Luzio, M.D., Arnold, J. (2013).ArcSWAT Interface for SWAT2012, User's Guide. Blackland Research and Extention Center, Texas Agrilife Research, Grassland, Soil and Water Research Laboratory, USDA Agricultural Research Service, Temple, Texas.

World Bank. (2009). Nepal: Priorities for Agriculture and Rural Development. Washington, DC: World Bank. http://go.worldbank.org/ D9M3ORHVL0; accessed on 2 July 2009.

SOHAM-NEPAL Membership Fee

Membership Type	Nepali (NRs)	SAARC (US$ or equiv NRs.)	Non-SAARC (US$ or equiv NRs.)
General	1000	10	20
Life	4000	120	240
Institutional	5000	300	600
Associate	350	5	10

Please write to info@soham.org.np for membership application form.

Computer Layout : Rishikesh Lamichhane | Mob. 9841366747

JOURNAL OF HYDROLOGY AND METEOROLOGY

CONTENTS

Volume 10, Number 1 **2016**

Harshana Shrestha, Utsav Bhattarai, Khada Nanda Dulal, Shrijwal Adhikari, Suresh Marahatta, Laxmi Prasad Devkota	1	Impact of Climate Change in the Karnali Basin, Nepal
Hemu Kharel Kafle	20	Drought Analysis in Western, Central and Eastern Development Regions of Nepal using Reconnaissance Drought Index
Shobha Kumari Yadav	30	Spatial and Temporal Variation in Rainfall in Panchase Mountain Ecological Region of Nepal
Rajendra Man Dongol	43	Water balance of Nepal and climatic classification based on moisture regimes
Binu Maharjan, Tirtha Raj Adhikari, Laxmi Devi Maharjan	57	Climate Change Impact on Water Availability; A Case Study of West Seti, Gopaghat of Karnali Basin Using SWAT Model
SudeepThakuri, Franco Salerno	70	Recent Evolution of Glacial Lakes in Sagarmatha National Park, Nepal
Mohan Rana Magar, Tirtha Raj Adhikari, Dhiraj Gyawali	80	Modeling the impacts of climate change on hydrology of Sunkoshi river basin, Nepal

Journal of Hydrology and Meteorology is a publication of the Society of Hydrologists and Meteorologists-Nepal (SOHAM-Nepal)
The journal is registered at the District Administration Office, Kathmandu (Regd. No. 88/060/06)

ISSN (Print) 1818-2518
ISSN (Online) 2542-2537